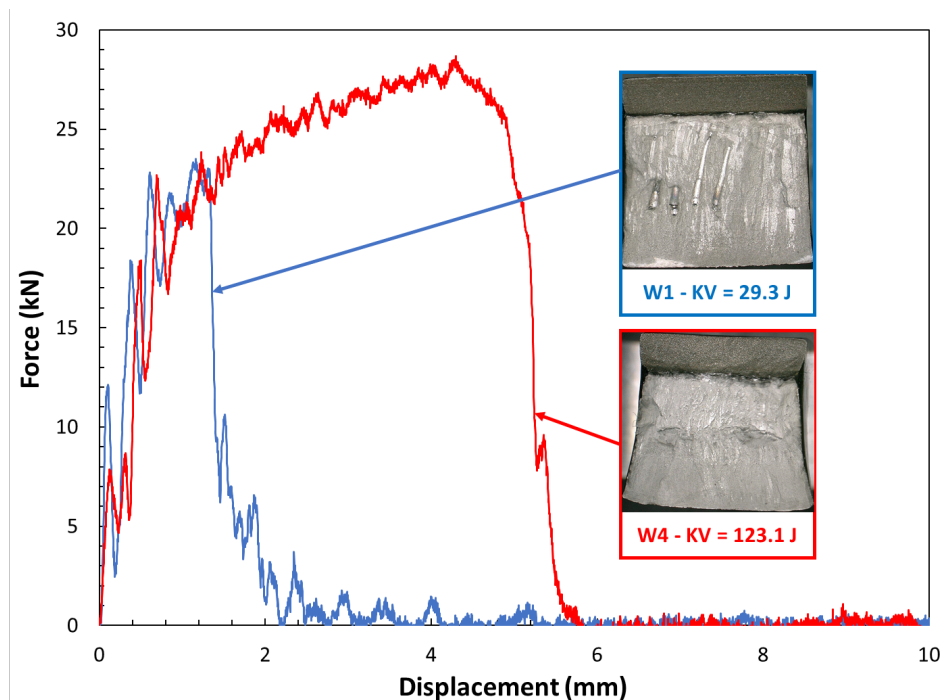


Instrumented Charpy Tests at 77 K on 316L Stainless Steel Welded Plates



Enrico Lucon
Jake Benzing

This publication is available free of charge from:
<https://doi.org/10.6028/NIST.TN.2196>

NIST Technical Note 2196

Instrumented Charpy Tests at 77 K on 316L Stainless Steel Welded Plates

Enrico Lucon

Jake Benzing

*Applied Chemicals and Materials Division
Material Measurement Laboratory*

This publication is available free of charge from:
<https://doi.org/10.6028/NIST.TN.2196>

December 2021



U.S. Department of Commerce
Gina M. Raimondo, Secretary

National Institute of Standards and Technology
*James K. Olthoff, Performing the Non-Exclusive Functions and Duties of the Under Secretary of Commerce
for Standards and Technology & Director, National Institute of Standards and Technology*

Certain commercial entities, equipment, or materials may be identified in this document in order to describe an experimental procedure or concept adequately. Such identification is not intended to imply recommendation or endorsement by the National Institute of Standards and Technology, nor is it intended to imply that the entities, materials, or equipment are necessarily the best available for the purpose.

**National Institute of Standards and Technology Technical Note 2196
Natl. Inst. Stand. Technol. Tech. Note 2196, 73 pages (December 2021)
CODEN: NTNOEF**

**This publication is available free of charge from:
<https://doi.org/10.6028/NIST.TN.2196>**

Abstract

In the framework of a collaborative project between ASME, NASA, and NIST, instrumented Charpy tests have been performed at liquid nitrogen temperature (77 K, or -196 °C) on weld specimens extracted from the centers of four 316L welded stainless steel plates, each produced by a different vendor. Although the plates were produced in accordance with the same specifications from the same material (316L), clear differences in impact toughness have been observed, with the toughest welded plate exhibiting more than twice the absorbed energy of the least tough. Besides impact toughness, the availability of instrumented Charpy data has also allowed deriving estimates of dynamic yield strength and shear fracture appearance. Additional tensile and fracture toughness tests at 77 K and 4 K (liquid helium temperature) will be performed in this project.

Key words

316L stainless steel, impact toughness, instrumented Charpy tests, liquid nitrogen, welded plates.

Table of Contents

Abstract	1
Key words	1
1. Introduction	4
2. Material and Experimental Procedures	5
3. Test Results	7
3.1. Non-Instrumented Data	7
3.2. Instrumented Data	9
3.2.1. Estimates of Dynamic Yield Strengths	11
3.2.2. Estimates of Shear Fracture Appearance and Comparison with Measured Values	12
3.2.3. Correlations with Other Tensile Properties	15
3.3. SEM investigations.....	16
4. Conclusions	20
Acknowledgements	20
References	20
Appendix A: Technical Drawing of the Charpy V-Notch Specimens	23
Appendix B: Dimensional measurements on the Charpy V-Notch Specimens	24
Appendix C: Digital pictures of the fracture surfaces of Charpy specimens	32
Appendix D: Instrumented force/deflection curves of the Charpy specimens	45
Appendix E: SEM images and additional EDS spectra and spot analyses	55

List of Tables

Table 1 - Non-instrumented test results at 77 K for the 316L welded plates.....	7
Table 2 - Instrumented Charpy results for the four welded plates.	10
Table 3 - Estimated dynamic yield strengths calculated for the four welded plates.....	11
Table 4 - Measured and estimated values of Shear Fracture Appearance for the four welded plates.	13

List of Figures

Figure 1 – (a) Possible orientations of Charpy specimens extracted from welded plates [19], and (b) photograph of some as-received Charpy specimens, clearly showing the weld. The specimens tested in this study correspond to orientation "NQ", where the first letter (N) is the direction normal to the crack plane, and the second (Q) is the expected direction of crack propagation (N = normal to weld direction; Q = weld thickness direction).	6
--	---

Figure 2 - Average values of absorbed energy at 77 K for the four welded plates..... 8

Figure 3 - Average values of lateral expansion at 77 K for the four welded plates..... 8

Figure 4 - Average values of shear fracture appearance (measured) at 77 K for the four welded plates..... 9

Figure 5 - Illustrative instrumented test record showing general yield (F_{gy}), maximum force (F_m), unstable fracture (F_{bf}), and crack arrest (F_a) [20]. 10

Figure 6 - Estimated dynamic yield strengths for the four welded plates..... 12

Figure 7 - Estimated values of *SFA* for the four welded plates. 13

Figure 8 - Correlations between estimated/measured shear fracture appearance and absorbed energy for the four welded plates..... 14

Figure 9 - Correlations between estimated/measured shear fracture appearance and lateral expansion for the four welded plates. 14

Figure 10 – Correlation between estimated and measured shear fracture appearance for the four welded plates. Dashed lines correspond to $\pm 20\%$ 15

Figure 11 - Average values of maximum force for the four welded plates. 16

Figure 12 - Average values of displacement at test end for the four welded plates. 16

Figure 13 - SEM images of characteristic features observed on the fracture surfaces of Charpy specimens. Charpy impact direction is parallel to the vertical axis, and the V-notch (not shown in any image) would be found at the extreme top of a given field of view. 18

Figure 14 - EDS analysis of remnant features found in large defects on the fracture surface, where no microvoid coalescence was observed..... 19

1. Introduction

Currently, ASME Boiler and Pressure Vessel Code (BPVC) Section VIII [1] and ASME Piping Code B31.12 Hydrogen Piping and Pipelines [2] both require performing Charpy impact tests at Liquid Nitrogen (LN2) temperature, *i.e.*, 77 K (-196 °C), to assess the fracture performance of austenitic stainless steels at Liquid Helium (LHe) temperature, *i.e.*, 4 K (-277 °C). The same procedure was also proposed for ASME Piping Code B31.3 Process Piping [3].

However, the technical basis of such an approach has often been questioned, as insufficient technical justification is available.

Ample evidence is available in the literature that Charpy testing below 77 K is not technically feasible, due to both temperature rise during the transfer of the specimens from the cooling medium to the impact position and adiabatic heating. While temperature rise during transfer can be minimized by appropriately modifying the test setup, adiabatic heating at elevated strain rates is unavoidable. Adiabatic heating occurs when the energy generated during plastic deformation is converted into heat, but cannot dissipate fast enough to the surrounding environment, causing the temperature of the material to increase. The temperature rise can also be affected by a strain-induced phase transformation, which also releases heat and can thus affect the microstructural evolution [4]. The thermomechanical behavior of austenitic stainless steels at intermediate and high strain rates is the object of ongoing research, particularly to quantify the effects of adiabatic heating on the response of the material [5].

Various means to avoid temperature increase due to specimen transfer have been proposed [6], including:

- boating (specimens glued to the bottom of a paper boat) [7-9];
- boxing (specimens insulated by means of grooved polystyrene foam, with liquid helium continuously flowing from a storage dewar) [10];
- encapsulation (specimens wrapped in a pipe-like casing of grooved polystyrene foam with LHe inlet and outlet, placed on the Charpy anvils) [11,12];
- use of a double-walled vacuum-insulated glass dewar (also placed on the anvils, and filled with helium) [13-15].

In older literature references [8,16], some authors even resorted to encapsulating impact test machines, as well as specimens.

Regardless of the approach taken to keep Charpy specimens fully immersed in liquid helium at the time of impact, all methods required a correction factor to account for the influence of fracturing the container on the energy spent to break the specimens. Those correction factors ranged from 0.27 J for a paper boat to 20 J – 35 J for a glass dewar [6].

While the problem of temperature increase during specimen transfer can be eliminated by one of the methods mentioned above, the heat generated within the specimen during high strain rate deformation and fracture cannot be avoided. Temperatures at impact as high as 150 K (-123 °C) were calculated for AISI 304 by thermal analysis based on the conversion of plastic work to heat [17].

Due to adiabatic heating, the general consensus is that impact tests are of questionable value and little significance at extreme cryogenic temperatures, *i.e.*, below 77 K. However,

the use of 77 K Charpy test results to assess material properties at 4 K, currently advocated by some voluntary consensus standards [1,2], requires additional research efforts.

This is one of the objectives of a collaborative project between the American Society of Mechanical Engineers (ASME), the National Aeronautics and Space Administration (NASA), and the National Institute for Standards and Technology (NIST). The project investigates the feasibility of performing mechanical tests on austenitic stainless steels (AISI 316L) at 77 K as a means of validating steels for use at 4 K in liquid hydrogen and liquid helium piping and pressure vessels. Correlation between results of fracture toughness test (to be performed at both 4 K and 77 K) and Charpy test (only performed at 77 K) will be performed to determine whether testing at 77 K is statistically justifiable for 4 K operation.

The present report provides results from instrumented impact tests performed at NIST in Boulder, Colorado, at 77 K on Charpy specimens from four AISI 316L welded plates in the as-welded condition.

2. Material and Experimental Procedures

Charpy V-notch specimens were extracted from welds in four welded 316L stainless steel plate samples provided by ASME/Jacob ESSCA Group, identified as W1, W2, W3, and W4. The samples were all in the as-welded condition, and had the following approximate dimensions: 254 mm × 610 mm, thickness = 16 mm. The plates were welded by four different vendors in accordance with ASME Boiler and Pressure Vessel Code requirements, but using 316L plate and weld material individually procured by each vendor, and following each vendor's standard in-house welding procedure specification.

The technical drawing of the Charpy specimens, compliant with Fig. 1 of ASTM E23-18 [18], is reproduced in Appendix A, while the results of the dimensional measurements are collected in Appendix B¹. The Charpy specimens were extracted from the plates at the same time as tensile and fracture toughness specimens. All specimens were centered on the weld seams. The specimen orientation with respect to the plate thickness and the weld geometry corresponds to orientation “NQ” in Figure 1, which is taken from ISO 15653:2018 [19]. As seen in the figure, the crack grows from the narrower side of the weld (root) to the wider side (cap), which makes it more likely for crack propagation to occur fully within the weld material.

Instrumented impact tests were performed at LN₂ temperature (77 K) on 20 Charpy specimens (5 tests on each welded plate). A large capacity (953 J) Charpy machine, equipped with an instrumented striker with an 8 mm radius striking edge, was employed. The hammer velocity at the moment of impact was 5.47 m/s, and all tests were conducted in accordance with the current versions of ASTM E23 [18], ASTM E2298 [20], ISO 148-1 [21], and ISO 14556 [22].

Before being tested, the specimens were kept immersed in liquid nitrogen for at least 10 minutes² after their temperature had stabilized. During soaking, the temperature was

¹ Even though some of the measurements in Appendix B are outside the specifications of ASTM E23-18, those variations are not considered important and their influence on the results reported herein is deemed negligible.

² Both ASTM E23-18 and ISO 148-1 (2016) prescribe a minimum soaking time of 5 minutes for specimen conditioning using a liquid medium. In view of the low specific heat of stainless steel, this minimum time was doubled.

measured by means of a dummy steel sample with a type K thermocouple embedded. The transfer time between removal of the specimens from the cooling medium and impact was 3 seconds or less³.

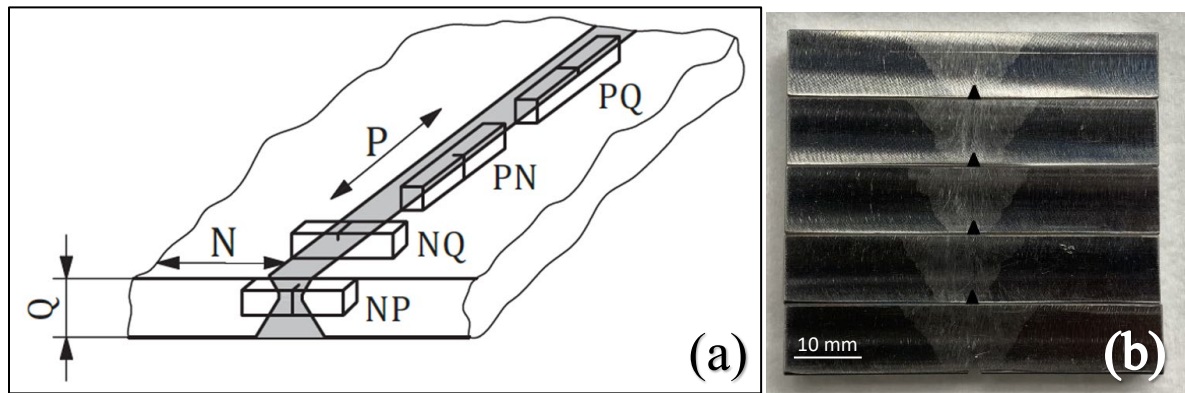


Figure 1 – (a) Possible orientations of Charpy specimens extracted from welded plates [19], and (b) photograph of some as-received Charpy specimens, clearly showing the weld. The specimens tested in this study correspond to orientation "NQ", where the first letter (N) is the direction normal to the crack plane, and the second (Q) is the expected direction of crack propagation (N = normal to weld direction; Q = weld thickness direction).

For every test performed, the following parameters were measured: *KV* (absorbed energy, in J), *LE* (lateral expansion, in mm), and *SFA* (shear fracture appearance, in %). Specifically:

- *KV* was returned by the digital encoder of the impact machine.
- *LE* was measured on the broken specimens by means of a calibrated caliper, as the difference between the thickness of the specimen in the notched cross section before and after the test.
- *SFA* was estimated by means of the following two approaches:
 - (a) Quantifying the proportion of brittle and ductile fracture surface by optically analyzing digital pictures of the fracture surfaces (*SFA_{meas}*).
 - (b) Using characteristic values of force obtained from the analysis of the instrumented test record (*SFA_{est}*, see 3.2.2).

Following Charpy testing, fracture surfaces of selected Charpy specimens were examined using scanning electron microscopy (SEM) to characterize unique features that were previously observed in optical microscopy. When collecting secondary electron (SE) images and energy dispersive spectroscopy (EDS) measurements, the following parameters were used: 60 μm aperture, high current mode, and 25 kV accelerating voltage.

³ For both ASTM E23 and ISO 148-1 (2016), the maximum allowable transfer time is 5 seconds.

3. Test Results

3.1. Non-Instrumented Data

Values of absorbed energy, lateral expansion, and shear fracture appearance (measured from digital pictures of the fracture surfaces – method (a) above) are reported in Table 1, with average values and standard deviations for each welded plate.

Average values of KV , LE , and SFA_{meas} (with error bars corresponding to ± 1 standard deviation) for the four welded plates are compared in Figure 2, Figure 3, and Figure 4, respectively.

Digital pictures of the fracture surfaces for all specimens tested are reproduced in Appendix C.

Table 1 - Non-instrumented test results at 77 K for the 316L welded plates.

Welded plate	Specimen id	KV (J)	LE (mm)	SFA_{meas} (%)
1	W1-C1	52.10	0.47	55
	W1-C2	49.08	0.49	52
	W1-C3	50.59	0.55	52
	W1-C4	29.26	0.39	22
	W1-C5	33.98	0.53	29
Average values		43.00	0.49	42
Standard deviations		10.58	0.06	15.3
2	W2-C1	88.09	1.04	36
	W2-C2	87.14	0.96	75
	W2-C3	79.10	0.94	42
	W2-C4	88.25	0.99	57
	W2-C5	73.94	0.96	58
Average values		83.31	0.98	54
Standard deviations		6.47	0.04	15.3
3	W3-C1	59.42	0.69	29
	W3-C2	62.03	0.78	37
	W3-C3	62.03	0.76	65
	W3-C4	55.90	0.77	47
	W3-C5	62.95	0.63	48
Average values		60.47	0.73	45
Standard deviations		2.87	0.06	13.5
4	W4-C1	81.93	0.97	57
	W4-C2	85.87	0.93	57
	W4-C3	91.74	1.21	62
	W4-C4	78.95	1.00	68
	W4-C5	123.08	1.32	59
Average values		92.31	1.09	61
Standard deviations		17.85	0.17	4.6

W4 exhibited the highest impact toughness in terms of all three parameters, followed by W2. W4 is also the plate that showed the largest scatter for both KV and LE . The least tough welded plate was W1, and its average absorbed energy was less than half of the average value for W4.

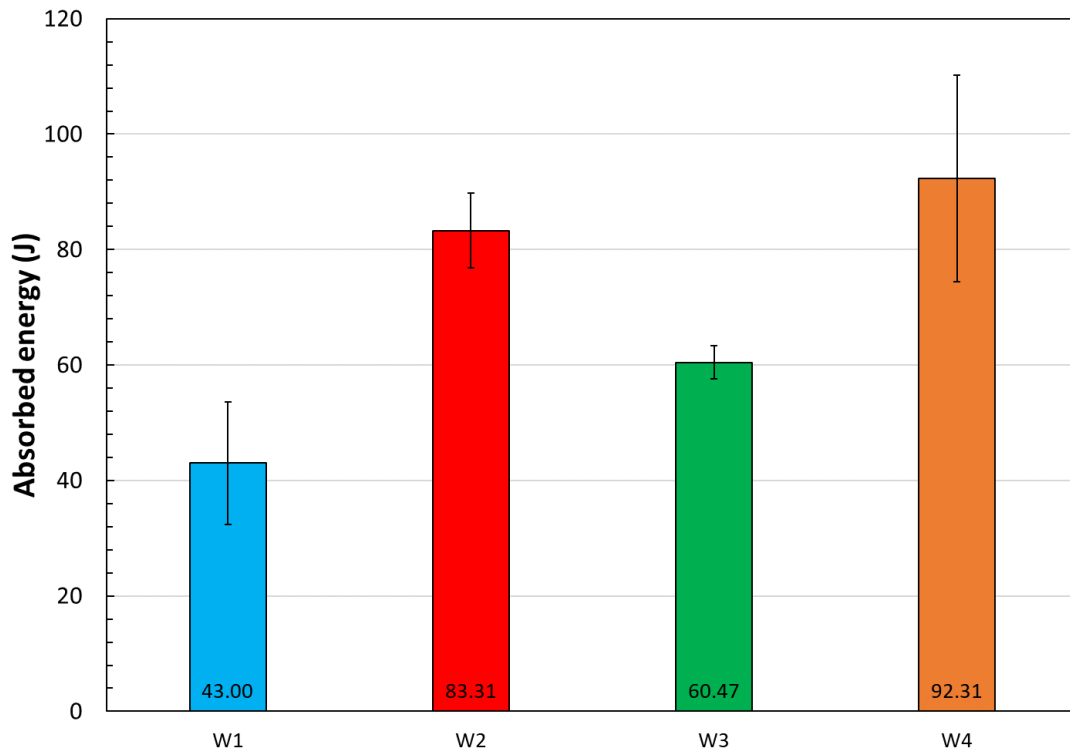


Figure 2 - Average values of absorbed energy at 77 K for the four welded plates. Error bars correspond to ± 1 standard deviation.

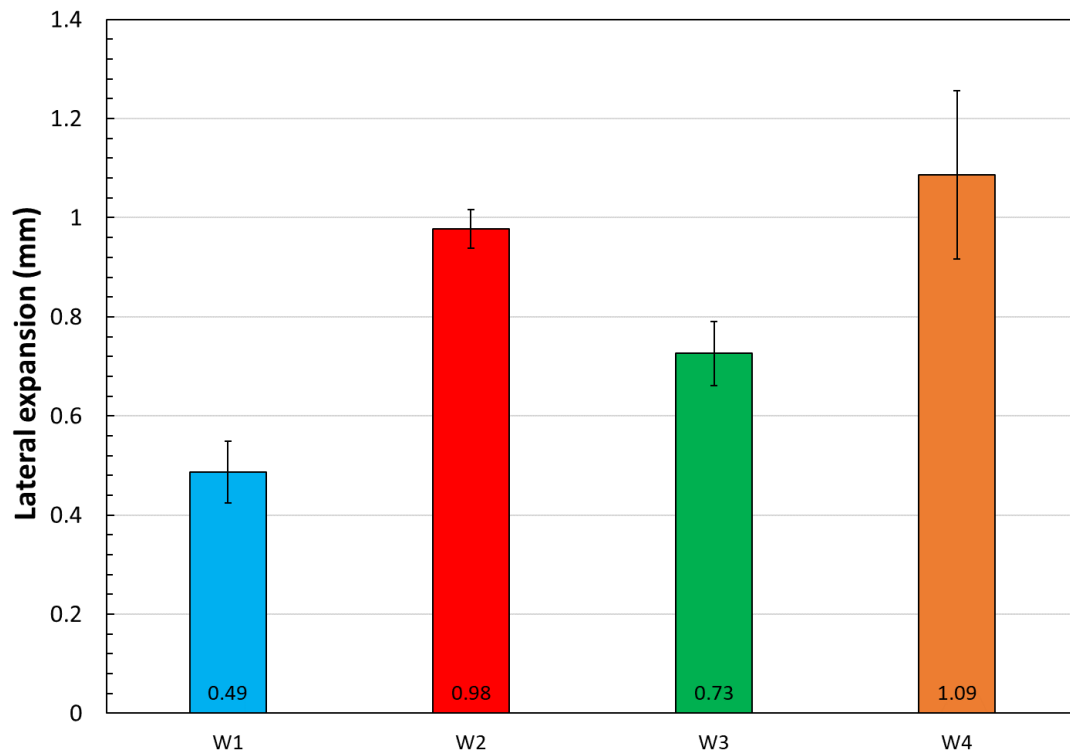


Figure 3 - Average values of lateral expansion at 77 K for the four welded plates. Error bars correspond to ± 1 standard deviation.

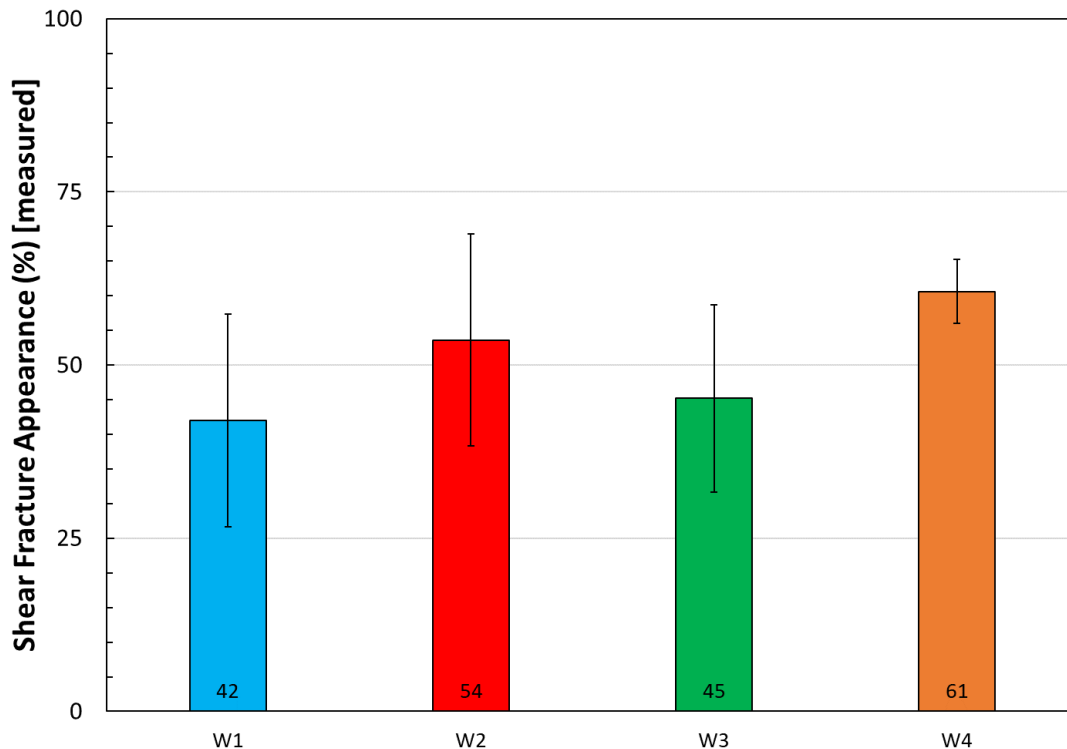


Figure 4 - Average values of shear fracture appearance (measured) at 77 K for the four welded plates. Error bars correspond to ± 1 standard deviation.

3.2. Instrumented Data

For every Charpy test performed on an impact machine equipped with an instrumented striker, a full record of the force applied to the specimen during the test is available, in the form of electrical signal from the striker strain-gages. Strain-gage signals are converted into force by the use of a conversion factor or calibration function, which has previously been established through a static calibration of the striker. By double integration of force and velocity data over time, specimen deflection is calculated. The force/deflection test record is analyzed to establish characteristic instrumented values of force, deflection, and absorbed energy⁴ corresponding to the following events that may have occurred during the test:

- general yield, when plastic deformation spreads through the remaining ligament;
- maximum force sustained by the specimen during the test;
- onset of unstable (brittle) fracture, if applicable;
- arrest of unstable (brittle) fracture, if applicable.

Referencing the illustrative curve reproduced in Figure 5 [20], the subscripts used for the events listed above are “gy”, “m”, “bf”, and “a”. The symbols for instrumented force, deflection, and absorbed energy are F , s , and W . In addition, s_t and W_t are deflection and absorbed energy corresponding to test termination.

⁴ Absorbed energy for an instrumented Charpy test is calculated by integrating force as a function of deflection.

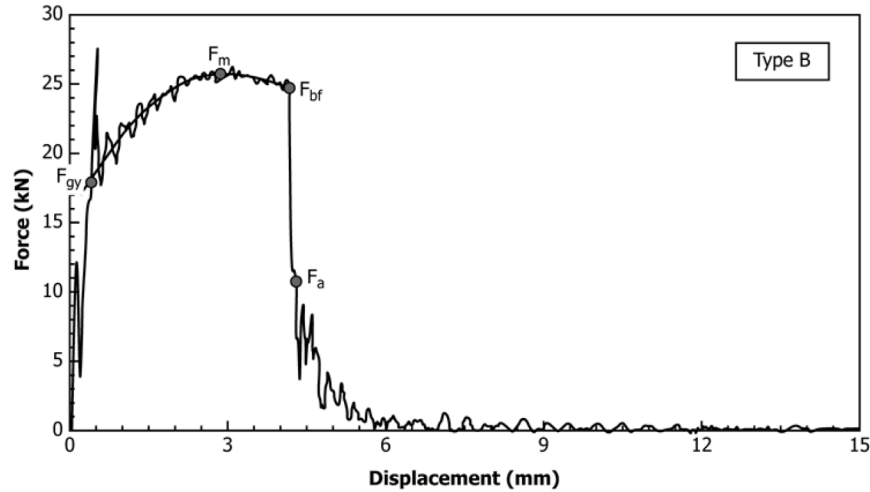


Figure 5 - Illustrative instrumented test record showing general yield (F_{gy}), maximum force (F_m), unstable fracture (F_{bf}), and crack arrest (F_a) [20].

Characteristic values for the 20 tests performed are summarized in Table 2, with average values and standard deviations (SD) for each plate.

Table 2 - Instrumented Charpy results for the four welded plates.

Specimen id	C_{el} (mm/kN)	F_{gy} (kN)	F_m (kN)	F_{bf} (kN)	F_a (kN)	s_{gy} (mm)	s_m (mm)	s_{bf} (mm)	s_a (mm)	s_t (mm)	W_{gy} (J)	W_m (J)	W_{bf} (J)	W_a (J)	W_t (J)	KV (J)	W_t -KV (%)
W1-C1	0.02492	18.69	25.39	21.67	3.41	0.58	2.23	2.31	2.55	10.70	5.99	44.27	46.08	48.84	50.70	52.10	-2.7%
W1-C2	0.02472	19.39	25.68	23.09	2.93	0.58	2.19	2.30	2.60	10.52	6.35	44.29	47.14	50.54	52.49	49.08	7.0%
W1-C3	0.02089	18.82	25.68	22.70	4.00	0.52	2.08	2.25	2.35	10.43	5.30	40.64	44.65	45.87	48.34	50.59	-4.4%
W1-C4	0.02310	18.80	22.98	22.63	9.00	0.57	1.34	1.34	1.43	10.70	5.94	22.28	22.28	23.48	28.67	29.26	-2.0%
W1-C5	0.02221	19.12	24.25	23.76	4.28	0.56	1.64	1.64	1.73	10.68	5.57	28.99	28.99	30.09	33.62	33.98	-1.1%
Mean	0.02317	18.96	24.80	22.77	4.72	0.56	1.90	1.97	2.13	10.61	5.83	36.09	37.83	39.76	42.76	43.00	-0.7%
SD	0.00170	0.29	1.17	0.76	2.45	0.02	0.39	0.45	0.52	0.12	0.41	9.95	11.41	12.19	10.85	10.58	4.4%
W2-C1	0.01626	20.99	26.78	23.00	7.94	0.70	2.50	2.68	2.78	11.73	6.28	50.62	55.61	58.04	87.56	88.09	-0.6%
W2-C2	0.00685	18.10	26.89	23.30	21.21	0.80	2.21	2.79	2.91	22.43	6.55	40.54	55.96	58.55	87.31	87.14	0.2%
W2-C3	0.02047	18.63	26.05	21.60	20.28	0.52	1.97	2.57	2.66	10.05	5.32	39.86	55.03	56.95	78.17	79.10	-1.2%
W2-C4	0.01874	18.42	25.99	24.76	23.94	0.48	2.36	2.65	2.70	15.52	4.90	48.97	56.61	57.84	88.72	88.25	0.5%
W2-C5	0.01866	19.79	25.08	25.00	23.79	0.50	1.94	2.01	2.13	9.87	5.26	38.66	40.52	43.24	72.88	73.94	-1.4%
Mean	0.01620	19.19	26.16	23.67	22.31	0.60	2.20	2.54	2.64	13.92	5.66	43.73	52.75	54.92	82.93	83.31	-0.5%
SD	0.00544	1.19	0.73	1.57	1.84	0.14	0.24	0.31	0.30	5.27	0.71	5.61	6.86	6.56	7.03	6.47	0.9%
W3-C1	0.02566	16.73	23.07	23.00	7.94	0.55	2.19	2.19	2.97	9.58	4.82	39.22	39.22	51.32	58.47	59.42	-1.6%
W3-C2	0.04584	17.75	23.57	22.48	5.62	0.60	2.01	2.37	3.26	21.01	5.74	35.17	43.63	56.53	62.54	62.03	0.8%
W3-C3	0.02270	16.71	23.97	23.96	9.08	0.55	2.19	2.19	2.47	21.01	4.79	39.78	39.78	45.15	63.64	62.03	2.6%
W3-C4	0.01993	15.83	22.23	22.24	7.49	0.53	1.94	1.94	2.84	21.14	3.69	31.86	31.86	46.67	57.34	55.90	2.6%
W3-C5	0.02560	15.78	23.24	21.14	7.43	0.56	2.11	2.11	3.18	21.01	4.82	37.18	37.18	54.95	62.38	62.95	-0.9%
Mean	0.02795	16.56	23.22	22.56	7.51	0.56	2.09	2.16	2.94	18.75	4.77	36.64	38.33	50.92	60.87	60.47	0.7%
SD	0.01028	0.81	0.65	1.03	1.25	0.03	0.11	0.16	0.31	5.13	0.73	3.23	4.31	4.98	2.78	2.87	1.9%
W4-C1	0.02394	17.82	26.44	19.65	3.29	0.55	2.51	3.61	3.73	3.97	5.13	51.54	78.87	80.69	81.67	81.93	-0.3%
W4-C2	0.02276	17.72	26.33	22.51	2.37	0.54	2.71	3.74	4.01	20.66	5.15	56.39	82.59	85.23	87.52	85.87	1.9%
W4-C3	0.02437	18.34	26.35	23.03	10.56	0.63	2.76	3.83	4.09	5.98	5.75	56.06	83.55	87.41	90.58	91.74	-1.3%
W4-C4	0.02322	17.72	25.27	21.25	2.47	0.56	2.51	3.54	3.83	20.75	5.08	49.32	74.42	77.68	79.25	78.95	0.4%
W4-C5	0.02270	19.96	27.32	18.73	8.80	0.67	4.04	5.20	5.26	5.78	6.26	89.44	119.40	120.27	122.25	123.08	-0.7%
Mean	0.02340	18.31	26.34	21.03	5.50	0.59	2.91	3.98	4.18	11.43	5.47	60.55	87.77	90.26	92.25	92.31	0.0%
SD	0.00074	0.96	0.73	1.83	3.88	0.06	0.64	0.69	0.62	8.50	0.52	16.43	18.05	17.20	17.36	17.85	1.2%

Additional information presented in Table 2 is:

- Elastic compliance C_{el} (mm/kN), obtained by linearly fitting the initial elastic portion of the test record.
- Relative difference between absorbed energy calculated under the instrumented curve (W_t) and measured by the machine encoder (KV). For all plates, the average difference was found to be within $\pm 1\%$, which indicates that the static calibration of the instrumented striker used can be considered reliable [23].

Instrumented force/deflection records for all specimens tested are collected in Appendix D.

3.2.1. Estimates of Dynamic Yield Strengths

Forces at general yield, F_{gy} , have been successfully correlated to values of dynamic yield strength, σ_{yd} , using the following relationship [24]:

$$\sigma_{yd} = \frac{\eta_{gy} F_{gy} W}{B(W-a)^2} \quad , \quad (1)$$

where: $\eta_{gy} = 2.793$ is a dimensionless parameter that accounts for the ratio between shear and tensile stress and the constraint conditions at general yield;
 $W = 10$ mm is the nominal Charpy specimen width;
 $B = 10$ mm is the nominal Charpy specimen thickness;
 $a = 2$ mm is the nominal depth of the machines notch.

Substituting the values above into Eq. (1), one obtains:

$$\sigma_{yd} = 43.65 F_{gy} \quad , \quad (2)$$

with σ_{yd} in MPa and F_{gy} in kN. Eqs. (1) and (2) provide estimates of the dynamic yield strength of a material at a strain rate corresponding to the loading rate of the instrumented Charpy test [25,26].

Using the values of F_{gy} reported in Table 2, the estimated dynamic yield strengths presented in Table 3 and plotted in Figure 6 were obtained.

Table 3 - Estimated dynamic yield strengths calculated for the four welded plates.

Specimen id	σ_{gy} (MPa)
W1-C1	815.82
W1-C2	846.37
W1-C3	821.49
W1-C4	820.62
W1-C5	834.59
Mean	827.78
SD	12.51
W2-C1	916.21
W2-C2	790.07
W2-C3	813.20
W2-C4	804.03
W2-C5	863.83
Mean	837.47
SD	52.08
W3-C1	730.26
W3-C2	774.79
W3-C3	729.39
W3-C4	690.98
W3-C5	688.80
Mean	722.84
SD	35.25
W4-C1	777.84
W4-C2	773.48
W4-C3	800.54
W4-C4	773.48
W4-C5	871.25
Mean	799.32
SD	41.75

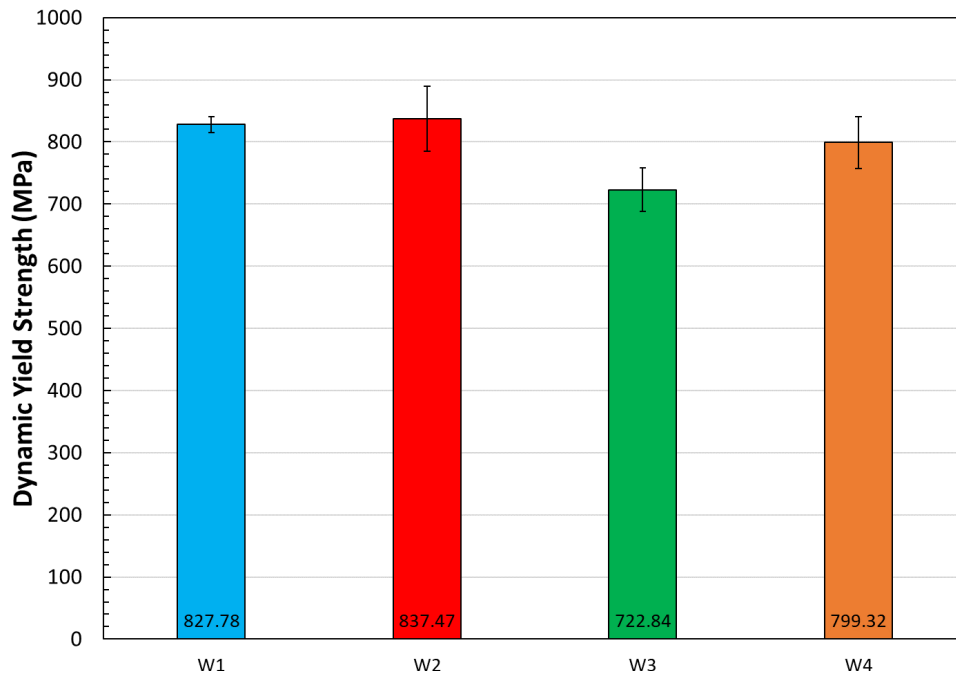


Figure 6 - Estimated dynamic yield strengths for the four welded plates. Error bars correspond to ± 1 standard deviation.

Plate W2 exhibited the highest estimated dynamic yield strength, coupled with the largest standard deviation. Plate W3 had the lowest values of σ_{yd} , while the lowest scatter corresponded to W1.

Once tensile test results at 77 K and 4 K are available for the welded plates, it will be interesting to compare them to the values of σ_{yd} obtained from the instrumented Charpy tests.

3.2.2. Estimates of Shear Fracture Appearance and Comparison with Measured Values

Both ASTM E2298-18 [20] and ISO 14556:2015 [22] include four empirical correlations, which allow obtaining estimates of Shear Fracture Appearance (SFA_{est}) based on characteristic values of force extracted from the analysis of the instrumented Charpy traces (F_{gy} , F_m , F_{bf} , and F_a). The general principles for all correlations are the following:

- If no step drop of force occurs, this should indicate that the ductile proportion of the fracture surface amounts to 100 %, *i.e.*, $SFA_{est} = 100$ %.
- If no evidence of general yield can be observed, this should indicate that the ductile proportion of the fracture surface amounts to 0 %, *i.e.*, $SFA_{est} = 0$ %.
- If a steep force drop occurs, the magnitude of the drop ($F_{bf} - F_a$) in relation to other characteristic forces (F_{gy} , F_m) allows an estimated value SFA to be calculated.

According to both standards, these formulae allow estimating the proportion of ductile fracture surface within ± 20 % with respect to optically measured values.

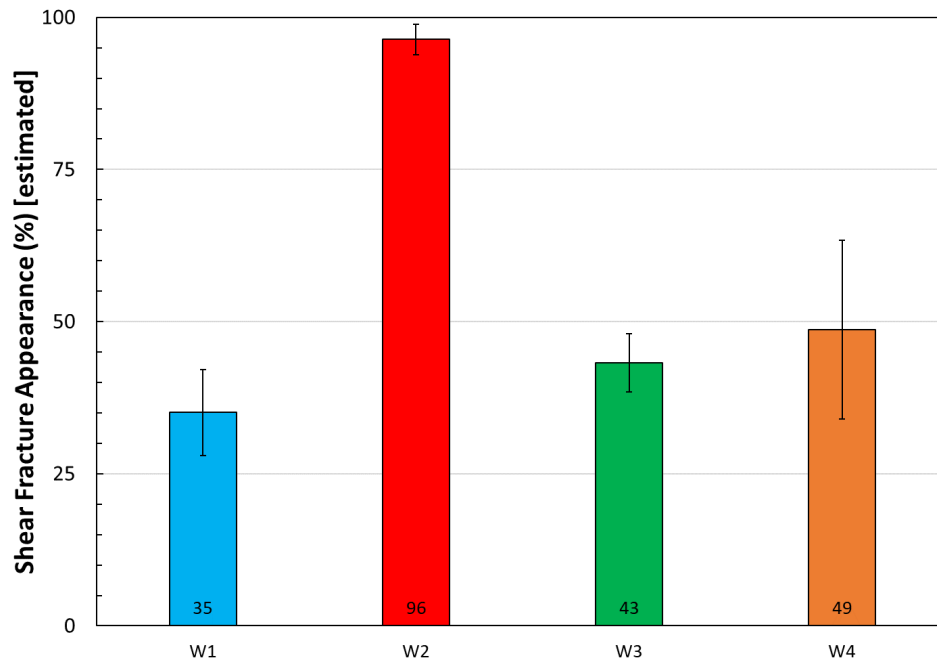
Of the four correlations, the following [27] has proven to be the most reliable according to the authors' experience and has been used to estimate shear fracture appearance in this project:

$$SFA_{est} = \left[1 - \frac{F_{bf} - F_a}{F_m + 0.5(F_m - F_{gy})} \right] \times 100 \quad (3)$$

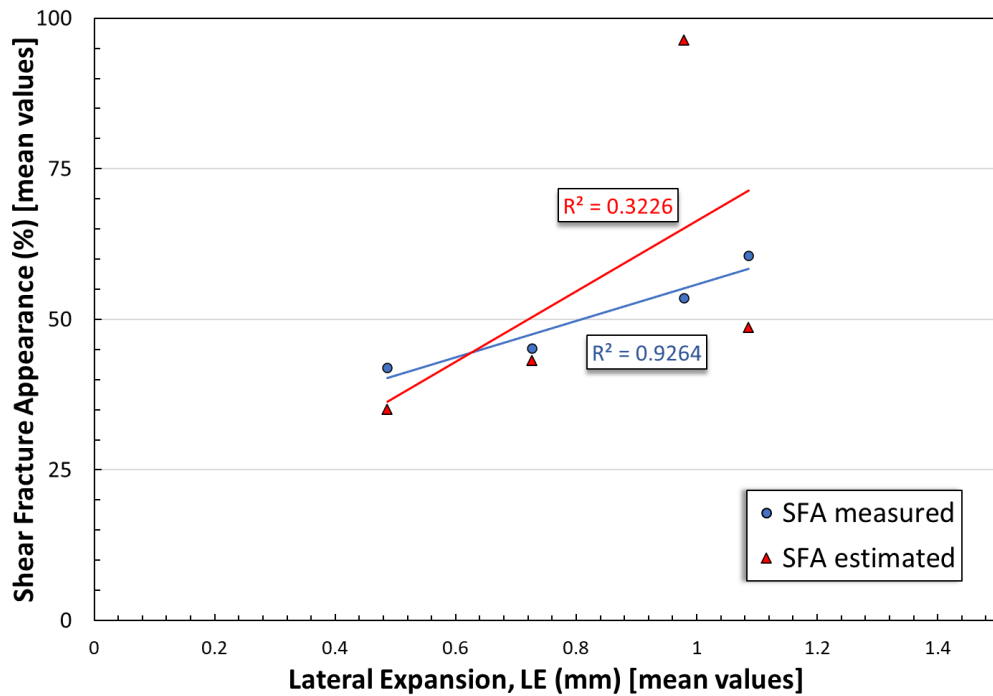
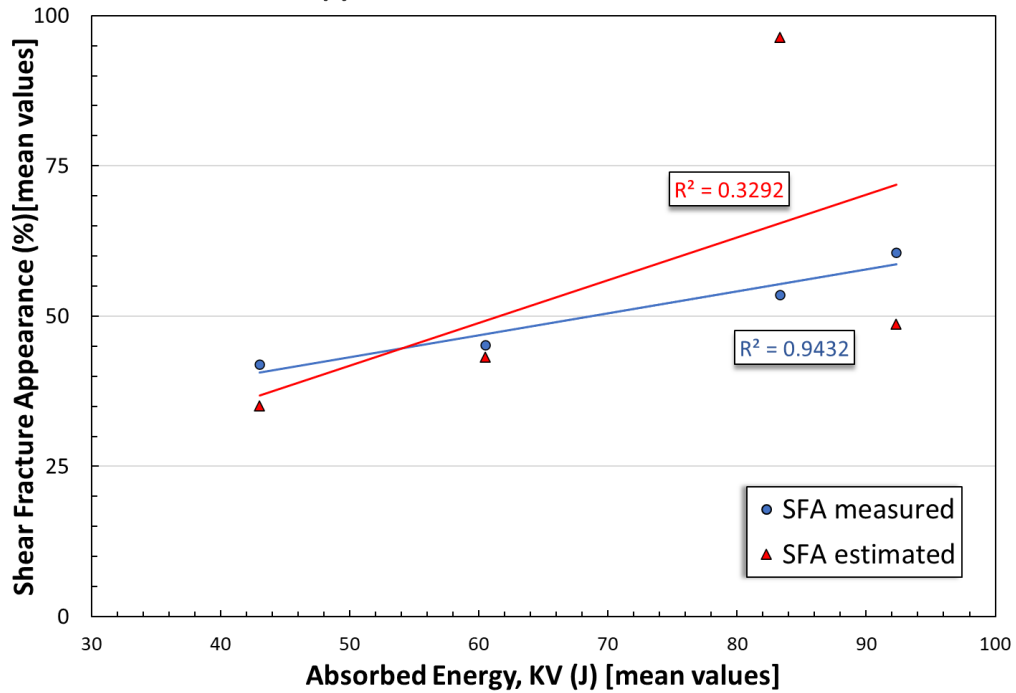
The values estimated by means of Eq. (3) are presented in Table 4 (along with measured values) and Figure 7.

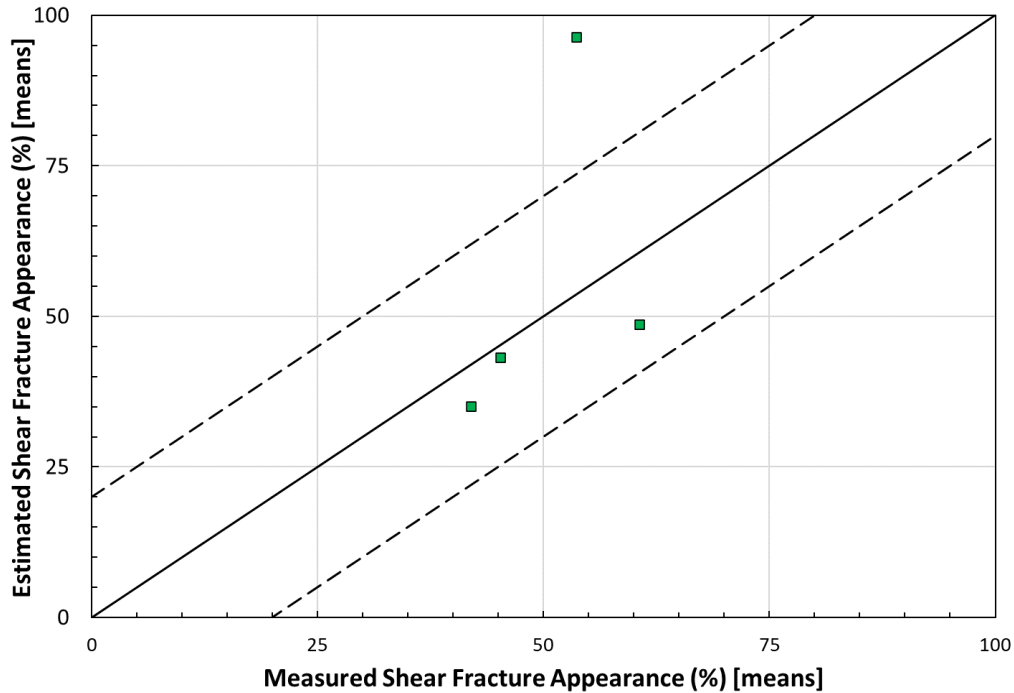
Table 4 - Measured and estimated values of Shear Fracture Appearance for the four welded plates.

Specimen id	SFA _{meas} (%)	SFA _{est} (%)
W1-C1	55	36
W1-C2	52	30
W1-C3	52	36
W1-C4	22	46
W1-C5	29	27
Mean	42	35
SD	15.3	7.0
W2-C1	36	100
W2-C2	75	93
W2-C3	42	96
W2-C4	57	97
W2-C5	58	96
Mean	54	96
SD	15.3	2.5
W3-C1	29	43
W3-C2	37	36
W3-C3	65	46
W3-C4	47	42
W3-C5	48	49
Mean	45	43
SD	13.5	4.8
W4-C1	57	47
W4-C2	57	34
W4-C3	62	59
W4-C4	68	35
W4-C5	59	68
Mean	61	49
SD	4.6	14.7



The extremely high average value of SFA_{est} obtained for W2 (96 %) appears suspicious, as it doesn't correlate with either absorbed energy (Figure 8), lateral expansion (Figure 9), or measured shear fracture appearance (Figure 10).





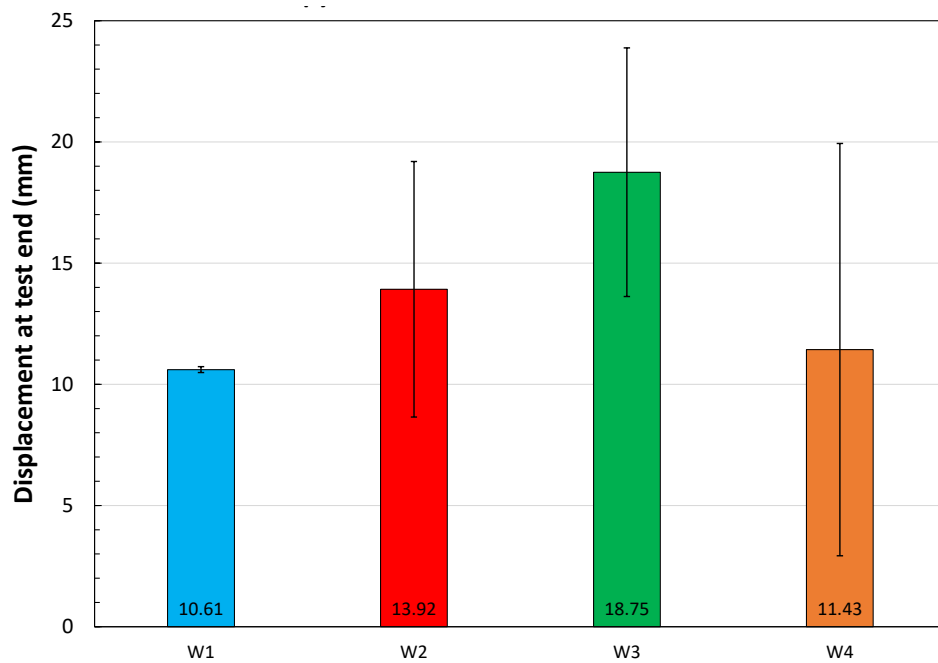
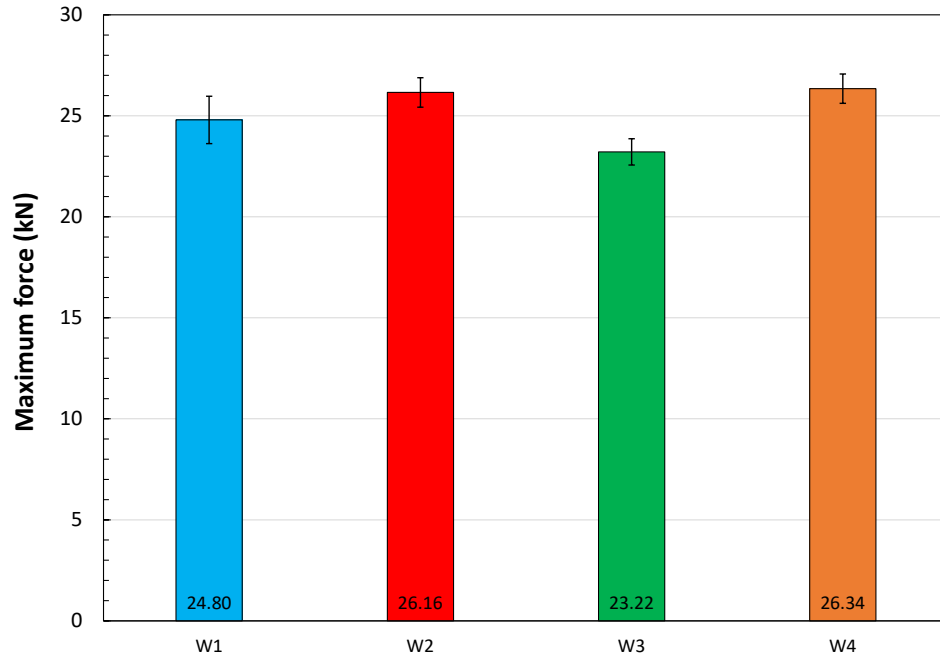
Conversely, SFA_{meas} was found to be strongly correlated (correlation coefficient $R > 0.96$) with both absorbed energy (Figure 8) and lateral expansion (Figure 9).

Further inspection of the instrumented curves for W2 specimens revealed that some apparent force drops probably corresponded to dynamic oscillations, and therefore contributed to the overestimated SFA_{est} values. For the remaining plates, however, the agreement between average values of measured and estimated SFA was well within $\pm 20\%$ (Figure 10).

3.2.3. Correlations with Other Tensile Properties

Although specific analytical relationships have not been published, maximum forces (F_m) and displacements at test end (s_t) can be correlated with dynamic tensile strength ($\sigma_{TS,d}$) and total elongation (ε_t), respectively. Average values and standard deviations for the four welded plates are shown in Figure 11 (F_m) and Figure 12 (s_t).

Plate W3 appeared to exhibit the lowest tensile strength and the highest ductility. Once again, it will be interesting to compare these observations with the results of the forthcoming tensile tests.



3.3. Optical and SEM investigations

While optical microscopy was used to measure lateral expansion (as previously shown), the digital images of the fracture surfaces also reveal differences in the amount of plastic deformation and size of plastic zones between specimens and weld types. Generally, more

tortuous macroscopic crack pathways (as opposed to flat features) and larger plastic zones below the Charpy V-notch tended to correlate with greater amounts of absorbed energy.

Following observations made with optical microscopy, SEM was used to characterize features observed on fracture surfaces of specimens that represent a range of behaviors.

At low magnification (Figure 13, a₁ and b₁), large defects were observed with parallel alignment (Figure 13, a₁) and perpendicular to (Figure 13, b₁) the direction of impact during Charpy testing. Upon closer inspection, multiple types of defects/features were observed:

- elongated cavities consistent with characteristics of wormhole porosity (Figure 13, a₁),
- inclusions, nodules, and cracked bands of surface oxides (Figure 13, a₂),
- microvoid coalescence (Figure 13, a₃),
- cracks with a morphology akin to lack-of-fusion defects commonly found in welds (Figure 13, b₂), and
- smooth spherical pockets that are characteristic of remnant gas porosity, also commonly found in welds (Figure 13, b₃).

Weld 1 contained by far the greatest number of lack-of-fusion defects, gas porosity, inclusions, and large cavities (wormhole porosity) aligned with the impact direction. All fracture surfaces from each weld type (1-4) showed evidence of microvoid coalescence. Lack-of-fusion and gas porosity were observed on fracture surfaces of specimens originating from Welds 2 and 3, but no evidence of large cavities (wormhole porosity) was detected. All fracture surfaces from each weld type (1-4) showed evidence of microvoid coalescence, lack-of-fusion, and gas porosity. In Weld 1, the number of large cavities and the reduction of microvoid coalescence (per area) along the pathway of a crack propagating through the material during impact testing were both consistent with the results from Charpy tests, in that Weld 1 exhibited the lowest absorbed energy and lateral expansion.

To understand what type of inclusions remained inside large cavities after impact testing, EDS analysis was conducted on the fracture surface of specimen W1-C4 (Figure 14, a and b). EDS mapping and EDS line scans revealed that remnants of inclusions and cracked surface oxides are depleted in Fe, Cr, and Ni, and enriched with Mn, Ti, Si, and P. Depending on the area measured, trace amounts of S and O were measured, thus indicating that remnant oxides and sulfides remained on the inner surfaces of the large cavities (no microvoid coalescence was observed in these regions). All SEM images and additional EDS spectra and spot analyses can be found in Appendix E.

Additional detailed microstructural analysis and hardness mapping of the weld metal and base metal will be conducted on remnants of the welded plates that were left over after specimens were removed.

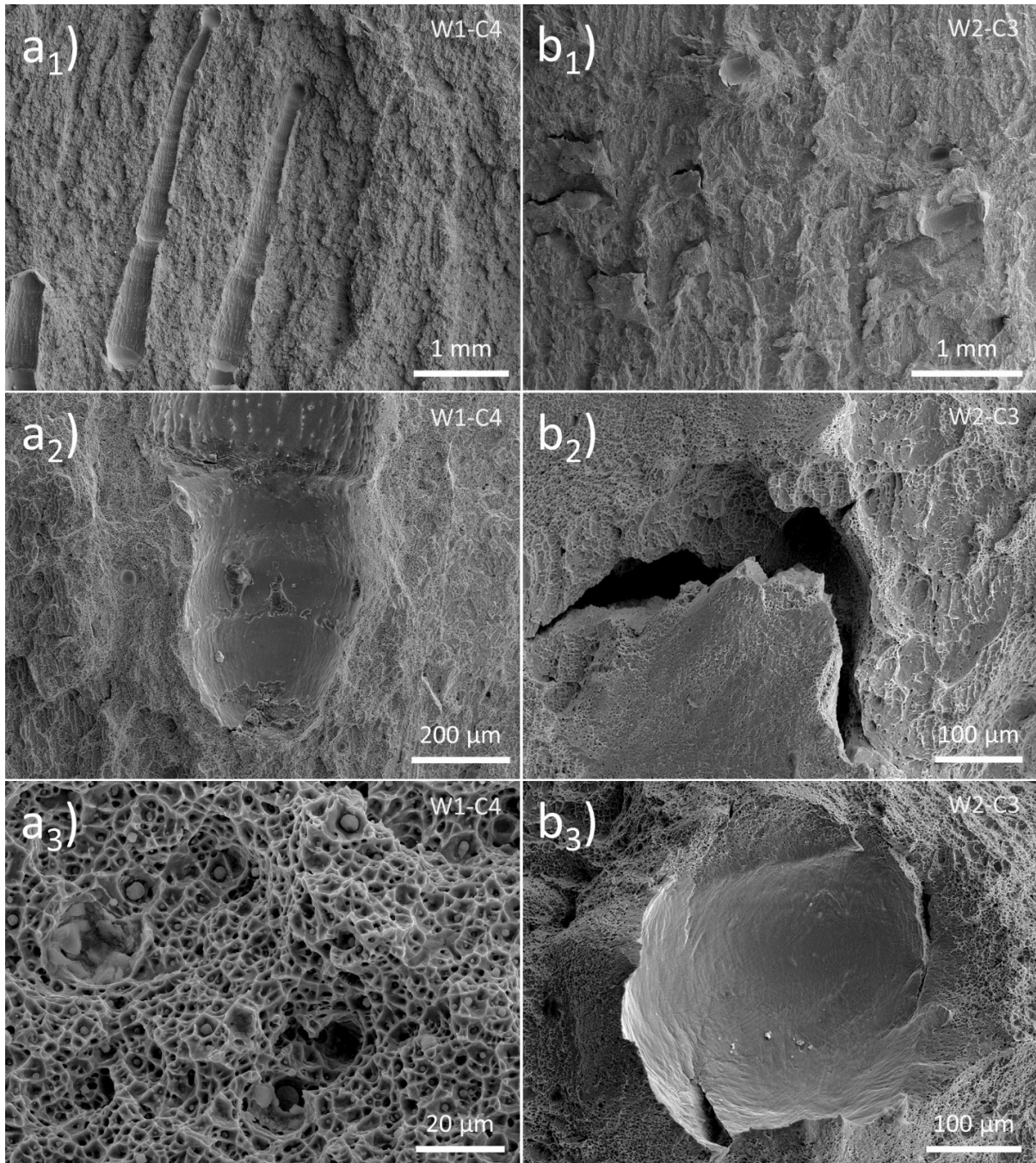


Figure 13 - SEM images of characteristic features observed on the fracture surfaces of Charpy specimens. Charpy impact direction is parallel to the vertical axis, and the V-notch (not shown in any image) would be found at the extreme top of a given field of view.

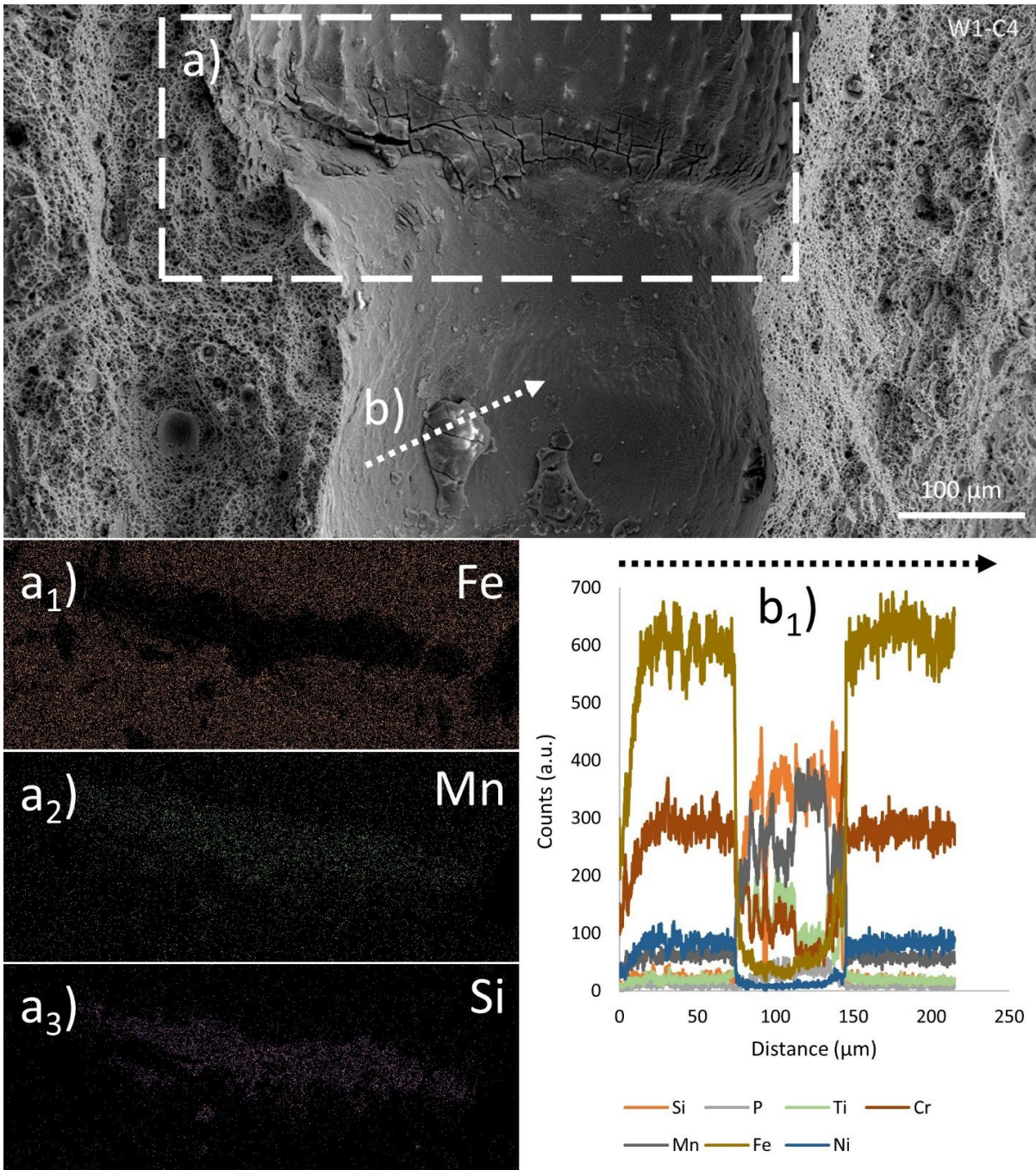


Figure 14 - EDS analysis of remnant features found in large defects on the fracture surface, where no microvoid coalescence was observed.

4. Conclusions

Even though all four welded plates were manufactured by different vendors in accordance with the same overarching welding requirements and using nominally the same material (316L stainless steel), the results of instrumented Charpy tests performed at NIST at liquid nitrogen temperature (77 K) show clear differences in the mechanical properties of the plates.

Specifically, plate W4 was found to be the toughest in terms of both absorbed energy and lateral expansion, followed closely by W2. The least tough was W1, with less than half the average absorbed energy of W4. This is likely due to the variation in plastic zone size as well as to the size, shape, orientation, and frequency of large cavities (wormhole porosity) observed on the fracture surfaces in most of the W1 specimens, which were not observed in specimens extracted from other welds. Data scatter was also found to be significantly different among the plates.

Tensile and fracture toughness properties will be characterized at both liquid nitrogen and liquid helium temperatures in the framework of this same collaborative project between ASME, NASA, and NIST, and the results will be compared to the Charpy measurements presented in this report.

Acknowledgements

The collaboration of Ross Rentz in preparing the technical drawing for the Charpy specimens (Appendix A) is gratefully acknowledged.

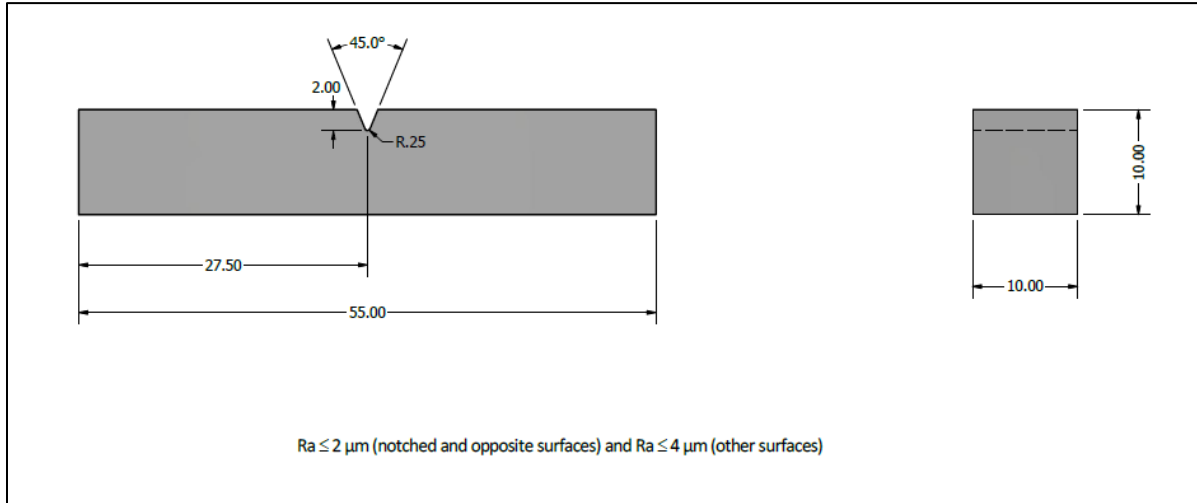
References

- [1] The American Society of Mechanical Engineers (2021) Boiler and Pressure Vessel Code, BPVC Section VIII-Rules for Construction of Pressure Vessels, Division 1, BVPC-VIII-1, ASME.
- [2] The American Society of Mechanical Engineers (2019), Hydrogen Piping and Pipelines, B31.12, ASME.
- [3] The American Society of Mechanical Engineers (2020) Process Piping, ASME Code for Pressure Piping, B31, ASME.
- [4] Talonen J, Nenonen P, Pape G, Hänninen H (2005) Effect of Strain Rate on the Strain-Induced $\gamma \rightarrow \alpha'$ -Martensite Transformation and Mechanical Properties of Austenitic Stainless Steels. *Metallurgical and Materials Transactions A*, 36A.
<http://dx.doi.org/10.1007/s11661-005-0313-y>
- [5] Vazquez-Fernandez NI, Soares GC, Smith JL, Seidt JD, Isakov M, Gilat A, Kuokkala VT, Hokka M (2019) Adiabatic Heating of Austenitic Stainless Steels at Different Strain Rates. *Journal of Dynamic Behavior of Materials* 5, pp. 221-229.
<http://dx.doi.org/10.1007/s40870-019-00204-z>
- [6] Tobler RL, Reed RP, Hwang IS, Morra MM, Ballinger RG, Nakajima H, Shimamoto S (1991) Charpy Impact Tests Near Absolute Zero. *Journal of Testing and Evaluation* 19(1), pp. 34-40. <https://doi.org/10.1520/JTE12527J>
- [7] Zambrow JL, Fontana MG (1949) Mechanical Properties, Including Fatigue, of Aircraft Alloys at Very Low Temperatures. *Transaction of ASM* 41, pp. 480-518.

- [8] Kiefer TF, Keys RD, Schwartzberg FR (1965) Charpy Impact Testing at 20 K. *Advances in Cryogenic Engineering* (10), pp. 56-62.
http://dx.doi.org/10.1007/978-1-4684-3108-7_7
- [9] Long HM (1974), Comment in *Advances in Cryogenic Engineering* (19), p. 378.
- [10] Jin S, Horwood WA, Morris JW, Jr., Zackay VF (1974) A Simplified Method for Charpy Impact Testing Below 6 K. *Advances in Cryogenic Engineering* (19), pp. 373-378.
- [11] Ogata T, Hiraga K, Nagai K, Ishikawa K (1982) A Simplified Method for Charpy Impact Testing Near Liquid Helium Temperature. *Cryogenics* (22), pp. 481-482.
[http://dx.doi.org/10.1016/0011-2275\(82\)90135-7](http://dx.doi.org/10.1016/0011-2275(82)90135-7),
- [12] Ogata T, Hiraga K, Nagai K, Ishikawa K (1984) A Simple Method for Charpy Impact Test at Liquid Helium Temperature. *Transactions of the National Research Institute for Metals* (26), pp. 238-242.
- [13] Takahashi Y, Yoshida K, Shimada M, Tada E, Miura R, Shimamoto S (1982) *Advances in Cryogenic Engineering* (28), pp. 73-81.
- [14] Matsumoto T, Satoh H, Wadayama Y, Hataya F (1987) Mechanical Properties of Fully Austenitic Weld Deposits for Cryogenic Structures. *Welding Research Supplement* (66), pp. 120-126s.
- [15] Mori T, Kuroda T (1985) Prediction of Energy Absorbed in Impact for Austenitic Weld Metals at 4.2 K. *Cryogenics* (25), pp. 243-248.
[http://dx.doi.org/10.1016/0011-2275\(85\)90203-6](http://dx.doi.org/10.1016/0011-2275(85)90203-6)
- [16] DeSisto TS (1958) Automatic Impact Testing to 8 K. Technical Report 112/93. Watertown Arsenal Laboratories, Watertown, Massachusetts.
- [17] Dobson WG, Johnson DL (1984) Effect of Strain Rate on Measured Mechanical Properties of Stainless Steel at 4 K. *Advances in Cryogenics Engineering* (30), pp. 185-192.
- [18] ASTM E23 (2018) Standard Test Methods for Notched Bar Impact Testing of Metallic Materials. American Society for Testing and Material International, West Conshohocken, PA.
- [19] ISO 15653 (2018) Metallic materials — Method of test for the determination of quasistatic fracture toughness of welds. International Standards Organization, Geneva (Switzerland).
- [20] ASTM E2298 (2018) Standard Test Method for Instrumented Impact Testing of Metallic Materials. American Society for Testing and Material International, West Conshohocken, PA.
- [21] ISO 148-1 (2016) Metallic materials — Charpy pendulum impact test — Part 1: Test method. International Standards Organization, Geneva (Switzerland).
- [22] ISO 14556 (2015) Metallic materials — Charpy V-notch pendulum impact test — Instrumented test method. International Standards Organization, Geneva (Switzerland).
- [23] Lucon E (2009) On the Effectiveness of the Dynamic Force Adjustment for Reducing the Scatter of Instrumented Charpy Results. *Journal of ASTM International* 6(1).
- [24] Server WL (1978) General Yielding of Charpy V-Notch and Precracked Charpy Specimens. *Journal of Engineering Materials and Technology* 100(2), pp. 183-188.
<http://dx.doi.org/10.1115/1.3443469>

- [25] Irwin GR (1964) Crack-Toughness Testing of Strain-Rate Sensitive Materials. *Journal of Engineering for Power, Transactions of the ASME*, pp. 444-450. <http://dx.doi.org/10.1115/1.3677632>
- [26] Shoemaker, AK (1969) Factors Influencing the Plane-Strain Crack Toughness Values of a Structural Steel. *Transactions of the ASME, Journal of Basic Engineering*, pp. 506-511. <http://dx.doi.org/10.1115/1.3571171>
- [27] van Walle E (1996) *Evaluating Material Properties by Dynamic Testing*. European Structural Integrity Society (ESIS) Publication 20, Mechanical Engineering Publications Limited, Suffolk (UK).

Appendix A: Technical Drawing of the Charpy V-Notch Specimens



NOTES: all dimensions in millimeters. Default tolerances are $\pm 0.1 \text{ mm}$ and $\pm 1^\circ$. Default surface finish, unless specified, is $< 1.6 \mu\text{m}$.

Appendix B: Dimensional measurements on the Charpy V-Notch Specimens

CHARPY LOT DIMENSIONAL MEASUREMENT REPORT

Measurement date: 7/15/2021

Material id: ASME/NASA 316L Weld 1

Measuring instruments: Keyence IM-7030 + Mitutoyo perpendicularity gage (*)

Specimen W1-C1

Dimension	Unit	Measured value	Corrected value	Nominal value	ASTM E23-18 tolerances		Acceptable? (YES/NO)	NOTES
					Min	Max		
Length [L]	mm	55.0303	55.0238	55	52.5	55	NO	
Notch centering	mm	0.0161	0.0161	0	-1	1	YES	
Width [W]	mm	10.0346	10.0286	10	9.925	10.075	YES	
Thickness [B]	mm	10.0367	10.0307	10	9.925	10.075	YES	
Ligament [b]	mm	7.9959	7.9915	8	7.975	8.025	YES	
Notch radius [ρ]	mm	0.2612	0.2612	0.25	0.225	0.275	YES	
Notch angle [α]	°	44.94	44.94	45	44	46	YES	
Angle adj sides 1	°	90.02	90	89.83	90.17	90.17	YES	(*)
Angle adj sides 2	°	89.98	90	89.83	90.17	90.17	YES	(*)
Angle adj sides 3	°	90.11	90	89.83	90.17	90.17	YES	(*)
Angle adj sides 4	°	90.03	90	89.83	90.17	90.17	YES	(*)

Specimen W1-C2

Dimension	Unit	Measured value	Corrected value	Nominal value	ASTM E23-18 tolerances		Acceptable? (Y/N)	NOTES
					Min	Max		
Length [L]	mm	54.974	54.9675	55	52.5	55	YES	
Notch centering	mm	0.0405	0.0405	0	-1	1	YES	
Width [W]	mm	10.0392	10.0332	10	9.925	10.075	YES	
Thickness [B]	mm	10.033	10.027	10	9.925	10.075	YES	
Ligament [b]	mm	7.9755	7.9711	8	7.975	8.025	NO	
Notch radius [ρ]	mm	0.2692	0.2692	0.25	0.225	0.275	YES	
Notch angle [α]	°	44.93	44.93	45	44	46	YES	
Angle adj sides 1	°	89.94	90	89.83	90.17	90.17	YES	(*)
Angle adj sides 2	°	90.05	90	89.83	90.17	90.17	YES	(*)
Angle adj sides 3	°	90.18	90	89.83	90.17	90.17	NO	(*)
Angle adj sides 4	°	90.03	90	89.83	90.17	90.17	YES	(*)

Specimen W1-C3

Dimension	Unit	Measured value	Corrected value	Nominal value	ASTM E23-18 tolerances		Acceptable? (Y/N)	NOTES
					Min	Max		
Length [L]	mm	55.0202	55.0137	55	52.5	55	NO	
Notch centering	mm	0.0174	0.0174	0	-1	1	YES	
Width [W]	mm	10.0405	10.0345	10	9.925	10.075	YES	
Thickness [B]	mm	10.0302	10.0242	10	9.925	10.075	YES	
Ligament [b]	mm	7.998	7.9936	8	7.975	8.025	YES	
Notch radius [ρ]	mm	0.2513	0.2513	0.25	0.225	0.275	YES	
Notch angle [α]	°	44.67	44.67	45	44	46	YES	
Angle adj sides 1	°	89.92	90	89.83	90.17	90.17	YES	(*)
Angle adj sides 2	°	89.98	90	89.83	90.17	90.17	YES	(*)
Angle adj sides 3	°	90.05	90	89.83	90.17	90.17	YES	(*)
Angle adj sides 4	°	90.04	90	89.83	90.17	90.17	YES	(*)

Specimen W1-C4:

Dimension	Unit	Measured value	Corrected value	Nominal value	ASTM E23-18 tolerances		Acceptable? (Y/N)	NOTES
					Min	Max		
Length [L]	mm	54.9987	54.9922	55	52.5	55	YES	
Notch centering	mm	0.004	0.004	0	-1	1	YES	
Width [W]	mm	10.038	10.032	10	9.925	10.075	YES	
Thickness [B]	mm	10.0377	10.0317	10	9.925	10.075	YES	
Ligament [b]	mm	7.997	7.9926	8	7.975	8.025	YES	
Notch radius [ρ]	mm	0.2541	0.2541	0.25	0.225	0.275	YES	
Notch angle [α]	°	44.79	44.79	45	44	46	YES	
Angle adj sides 1	°	90.10	90	90	89.83	90.17	YES	(*)
Angle adj sides 2	°	90.01	90	90	89.83	90.17	YES	(*)
Angle adj sides 3	°	90.02	90	90	89.83	90.17	YES	(*)
Angle adj sides 4	°	90.00	90	90	89.83	90.17	YES	(*)

Specimen W1-C5:

Dimension	Unit	Measured value	Corrected value	Nominal value	ASTM E23-18 tolerances		Acceptable? (Y/N)	NOTES
					Min	Max		
Length [L]	mm	55.0133	55.0068	55	52.5	55	NO	
Notch centering	mm	0.0215	0.0215	0	-1	1	YES	
Width [W]	mm	10.0412	10.0352	10	9.925	10.075	YES	
Thickness [B]	mm	10.031	10.025	10	9.925	10.075	YES	
Ligament [b]	mm	7.9734	7.969	8	7.975	8.025	NO	
Notch radius [ρ]	mm	0.2578	0.2578	0.25	0.225	0.275	YES	
Notch angle [α]	°	44.87	44.87	45	44	46	YES	
Angle adj sides 1	°	90.06	90	90	89.83	90.17	YES	(*)
Angle adj sides 2	°	90.02	90	90	89.83	90.17	YES	(*)
Angle adj sides 3	°	90.08	90	90	89.83	90.17	YES	(*)
Angle adj sides 4	°	89.98	90	90	89.83	90.17	YES	(*)

CHARPY LOT DIMENSIONAL MEASUREMENT REPORT

Measurement date: 7/15/2021

Material id: ASME/NASA 316L Weld 2

Measuring instruments: Keyence IM-7030 + Mitutoyo perpendicularity gage (*)

Specimen W2-C1

Dimension	Unit	Measured value	Corrected value	Nominal value	ASTM E23-18 tolerances		Acceptable? (YES/NO)	NOTES
					Min	Max		
Length [L]	mm	55.0074	55.0009	55	52.5	55	NO	
Notch centering	mm	0.0032	0.0032	0	-1	1	YES	
Width [W]	mm	10.0123	10.0063	10	9.925	10.075	YES	
Thickness [B]	mm	10.0276	10.0216	10	9.925	10.075	YES	
Ligament [b]	mm	7.9989	7.9945	8	7.975	8.025	YES	
Notch radius [ρ]	mm	0.2632	0.2632	0.25	0.225	0.275	YES	
Notch angle [α]	°	44.8	44.8	45	44	46	YES	
Angle adj sides 1	°	90.10		90	89.83	90.17	YES	(*)
Angle adj sides 2	°	90.10		90	89.83	90.17	YES	(*)
Angle adj sides 3	°	90.02		90	89.83	90.17	YES	(*)
Angle adj sides 4	°	89.99		90	89.83	90.17	YES	(*)

Specimen W2-C2

Dimension	Unit	Measured value	Corrected value	Nominal value	ASTM E23-18 tolerances		Acceptable? (Y/N)	NOTES
					Min	Max		
Length [L]	mm	55.024	55.0175	55	52.5	55	NO	
Notch centering	mm	0.0152	0.0152	0	-1	1	YES	
Width [W]	mm	10.0246	10.0186	10	9.925	10.075	YES	
Thickness [B]	mm	10.0361	10.0301	10	9.925	10.075	YES	
Ligament [b]	mm	8.0278	8.0234	8	7.975	8.025	YES	
Notch radius [ρ]	mm	0.2611	0.2611	0.25	0.225	0.275	YES	
Notch angle [α]	°	44.87	44.87	45	44	46	YES	
Angle adj sides 1	°	89.96		90	89.83	90.17	YES	(*)
Angle adj sides 2	°	90.07		90	89.83	90.17	YES	(*)
Angle adj sides 3	°	90.02		90	89.83	90.17	YES	(*)
Angle adj sides 4	°	90.00		90	89.83	90.17	YES	(*)

Specimen W2-C3

Dimension	Unit	Measured value	Corrected value	Nominal value	ASTM E23-18 tolerances		Acceptable? (Y/N)	NOTES
					Min	Max		
Length [L]	mm	54.9859	54.9794	55	52.5	55	YES	
Notch centering	mm	0.0442	0.0442	0	-1	1	YES	
Width [W]	mm	10.0227	10.0167	10	9.925	10.075	YES	
Thickness [B]	mm	10.027	10.021	10	9.925	10.075	YES	
Ligament [b]	mm	8.0106	8.0062	8	7.975	8.025	YES	
Notch radius [ρ]	mm	0.2597	0.2597	0.25	0.225	0.275	YES	
Notch angle [α]	°	44.98	44.98	45	44	46	YES	
Angle adj sides 1	°	89.98		90	89.83	90.17	YES	(*)
Angle adj sides 2	°	89.91		90	89.83	90.17	YES	(*)
Angle adj sides 3	°	89.86		90	89.83	90.17	YES	(*)
Angle adj sides 4	°	90.34		90	89.83	90.17	NO	(*)

Specimen W2-C4:

Dimension	Unit	Measured value	Corrected value	Nominal value	ASTM E23-18 tolerances		Acceptable? (Y/N)	NOTES
					Min	Max		
Length [L]	mm	54.9918	54.9853	55	52.5	55	YES	
Notch centering	mm	0.0337	0.0337	0	-1	1	YES	
Width [W]	mm	10.0312	10.0252	10	9.925	10.075	YES	
Thickness [B]	mm	10.031	10.025	10	9.925	10.075	YES	
Ligament [b]	mm	8.0103	8.0059	8	7.975	8.025	YES	
Notch radius [ρ]	mm	0.2614	0.2614	0.25	0.225	0.275	YES	
Notch angle [α]	°	44.94	44.94	45	44	46	YES	
Angle adj sides 1	°	90.05	90	90	89.83	90.17	YES	(*)
Angle adj sides 2	°	89.99	90	90	89.83	90.17	YES	(*)
Angle adj sides 3	°	90.07	90	90	89.83	90.17	YES	(*)
Angle adj sides 4	°	89.95	90	90	89.83	90.17	YES	(*)

Specimen W2-C5:

Dimension	Unit	Measured value	Corrected value	Nominal value	ASTM E23-18 tolerances		Acceptable? (Y/N)	NOTES
					Min	Max		
Length [L]	mm	55.0143	55.0078	55	52.5	55	NO	
Notch centering	mm	0.0279	0.0279	0	-1	1	YES	
Width [W]	mm	10.0217	10.0157	10	9.925	10.075	YES	
Thickness [B]	mm	10.0341	10.0281	10	9.925	10.075	YES	
Ligament [b]	mm	8.0302	8.0258	8	7.975	8.025	NO	
Notch radius [ρ]	mm	0.2535	0.2535	0.25	0.225	0.275	YES	
Notch angle [α]	°	44.75	44.75	45	44	46	YES	
Angle adj sides 1	°	90.03	90	90	89.83	90.17	YES	(*)
Angle adj sides 2	°	90.00	90	90	89.83	90.17	YES	(*)
Angle adj sides 3	°	90.08	90	90	89.83	90.17	YES	(*)
Angle adj sides 4	°	89.99	90	90	89.83	90.17	YES	(*)

CHARPY LOT DIMENSIONAL MEASUREMENT REPORT

Measurement date: 7/15/2021

Material id: ASME/NASA 316L Weld 3

Measuring instruments: Keyence IM-7030 + Mitutoyo perpendicularity gage (*)

Specimen W3-C1

Dimension	Unit	Measured value	Corrected value	Nominal value	ASTM E23-18 tolerances		Acceptable? (YES/NO)	NOTES
					Min	Max		
Length [L]	mm	54.995	54.9885	55	52.5	55	YES	
Notch centering	mm	0.0087	0.0087	0	-1	1	YES	
Width [W]	mm	10.0196	10.0136	10	9.925	10.075	YES	
Thickness [B]	mm	10.0128	10.0068	10	9.925	10.075	YES	
Ligament [b]	mm	8.0142	8.0098	8	7.975	8.025	YES	
Notch radius [ρ]	mm	0.2647	0.2647	0.25	0.225	0.275	YES	
Notch angle [α]	°	44.76	44.76	45	44	46	YES	
Angle adj sides 1	°		90.15	90	89.83	90.17	YES	(*)
Angle adj sides 2	°		90.07	90	89.83	90.17	YES	(*)
Angle adj sides 3	°		90.00	90	89.83	90.17	YES	(*)
Angle adj sides 4	°		89.98	90	89.83	90.17	YES	(*)

Specimen W3-C2

Dimension	Unit	Measured value	Corrected value	Nominal value	ASTM E23-18 tolerances		Acceptable? (Y/N)	NOTES
					Min	Max		
Length [L]	mm	55.0002	54.9937	55	52.5	55	YES	
Notch centering	mm	0.0229	0.0229	0	-1	1	YES	
Width [W]	mm	10.047	10.041	10	9.925	10.075	YES	
Thickness [B]	mm	10.0167	10.0107	10	9.925	10.075	YES	
Ligament [b]	mm	8.0115	8.0071	8	7.975	8.025	YES	
Notch radius [ρ]	mm	0.2635	0.2635	0.25	0.225	0.275	YES	
Notch angle [α]	°	44.99	44.99	45	44	46	YES	
Angle adj sides 1	°		89.99	90	89.83	90.17	YES	(*)
Angle adj sides 2	°		89.98	90	89.83	90.17	YES	(*)
Angle adj sides 3	°		90.06	90	89.83	90.17	YES	(*)
Angle adj sides 4	°		90.00	90	89.83	90.17	YES	(*)

Specimen W3-C3

Dimension	Unit	Measured value	Corrected value	Nominal value	ASTM E23-18 tolerances		Acceptable? (Y/N)	NOTES
					Min	Max		
Length [L]	mm	55.0182	55.0117	55	52.5	55	NO	
Notch centering	mm	0.0265	0.0265	0	-1	1	YES	
Width [W]	mm	10.0277	10.0217	10	9.925	10.075	YES	
Thickness [B]	mm	10.016	10.01	10	9.925	10.075	YES	
Ligament [b]	mm	8.0095	8.0051	8	7.975	8.025	YES	
Notch radius [ρ]	mm	0.2672	0.2672	0.25	0.225	0.275	YES	
Notch angle [α]	°	45.02	45.02	45	44	46	YES	
Angle adj sides 1	°		90.10	90	89.83	90.17	YES	(*)
Angle adj sides 2	°		90.03	90	89.83	90.17	YES	(*)
Angle adj sides 3	°		89.94	90	89.83	90.17	YES	(*)
Angle adj sides 4	°		90.02	90	89.83	90.17	YES	(*)

Specimen W3-C4:

Dimension	Unit	Measured value	Corrected value	Nominal value	ASTM E23-18 tolerances		Acceptable? (Y/N)	NOTES
					Min	Max		
Length [L]	mm	55.0416	55.0351	55	52.5	55	NO	
Notch centering	mm	0.024	0.024	0	-1	1	YES	
Width [W]	mm	10.0358	10.0298	10	9.925	10.075	YES	
Thickness [B]	mm	10.012	10.006	10	9.925	10.075	YES	
Ligament [b]	mm	8.0205	8.0161	8	7.975	8.025	YES	
Notch radius [ρ]	mm	0.2563	0.2563	0.25	0.225	0.275	YES	
Notch angle [α]	°	45.01	45.01	45	44	46	YES	
Angle adj sides 1	°	90.17	90	90	89.83	90.17	NO	(*)
Angle adj sides 2	°	90.07	90	90	89.83	90.17	YES	(*)
Angle adj sides 3	°	90.06	90	90	89.83	90.17	YES	(*)
Angle adj sides 4	°	89.89	90	90	89.83	90.17	YES	(*)

Specimen W3-C5:

Dimension	Unit	Measured value	Corrected value	Nominal value	ASTM E23-18 tolerances		Acceptable? (Y/N)	NOTES
					Min	Max		
Length [L]	mm	54.9977	54.9912	55	52.5	55	YES	
Notch centering	mm	0.0005	0.0005	0	-1	1	YES	
Width [W]	mm	10.0438	10.0378	10	9.925	10.075	YES	
Thickness [B]	mm	10.0208	10.0148	10	9.925	10.075	YES	
Ligament [b]	mm	8.0327	8.0283	8	7.975	8.025	NO	
Notch radius [ρ]	mm	0.2618	0.2618	0.25	0.225	0.275	YES	
Notch angle [α]	°	44.99	44.99	45	44	46	YES	
Angle adj sides 1	°	90.04	90	90	89.83	90.17	YES	(*)
Angle adj sides 2	°	90.02	90	90	89.83	90.17	YES	(*)
Angle adj sides 3	°	89.95	90	90	89.83	90.17	YES	(*)
Angle adj sides 4	°	90.03	90	90	89.83	90.17	YES	(*)

CHARPY LOT DIMENSIONAL MEASUREMENT REPORT

Measurement date: 7/15/2021

Material id: ASME/NASA 316L Weld 4

Measuring instruments: Keyence IM-7030 + Mitutoyo perpendicularity gage (*)

Specimen W4-C1

Dimension	Unit	Measured value	Corrected value	Nominal value	ASTM E23-18 tolerances		Acceptable? (YES/NO)	NOTES
					Min	Max		
Length [L]	mm	54.9919	54.9854	55	52.5	55	YES	
Notch centering	mm	0.0117	0.0117	0	-1	1	YES	
Width [W]	mm	10.0129	10.0069	10	9.925	10.075	YES	
Thickness [B]	mm	10.0276	10.0216	10	9.925	10.075	YES	
Ligament [b]	mm	7.9706	7.9662	8	7.975	8.025	NO	
Notch radius [ρ]	mm	0.2551	0.2551	0.25	0.225	0.275	YES	
Notch angle [α]	°	44.9	44.9	45	44	46	YES	
Angle adj sides 1	°	89.89		90	89.83	90.17	YES	(*)
Angle adj sides 2	°	89.99		90	89.83	90.17	YES	(*)
Angle adj sides 3	°	89.98		90	89.83	90.17	YES	(*)
Angle adj sides 4	°	90.13		90	89.83	90.17	YES	(*)

Specimen W4-C2

Dimension	Unit	Measured value	Corrected value	Nominal value	ASTM E23-18 tolerances		Acceptable? (Y/N)	NOTES
					Min	Max		
Length [L]	mm	54.9829	54.9764	55	52.5	55	YES	
Notch centering	mm	0.0239	0.0239	0	-1	1	YES	
Width [W]	mm	10.0102	10.0042	10	9.925	10.075	YES	
Thickness [B]	mm	10.0102	10.0042	10	9.925	10.075	YES	
Ligament [b]	mm	7.954	7.9496	8	7.975	8.025	NO	
Notch radius [ρ]	mm	0.2666	0.2666	0.25	0.225	0.275	YES	
Notch angle [α]	°	44.85	44.85	45	44	46	YES	
Angle adj sides 1	°	89.99		90	89.83	90.17	YES	(*)
Angle adj sides 2	°	90.00		90	89.83	90.17	YES	(*)
Angle adj sides 3	°	90.15		90	89.83	90.17	YES	(*)
Angle adj sides 4	°	89.99		90	89.83	90.17	YES	(*)

Specimen W4-C3

Dimension	Unit	Measured value	Corrected value	Nominal value	ASTM E23-18 tolerances		Acceptable? (Y/N)	NOTES
					Min	Max		
Length [L]	mm	54.9737	54.9672	55	52.5	55	YES	
Notch centering	mm	0.0019	0.0019	0	-1	1	YES	
Width [W]	mm	10.0335	10.0275	10	9.925	10.075	YES	
Thickness [B]	mm	10.0364	10.0304	10	9.925	10.075	YES	
Ligament [b]	mm	8.0179	8.0135	8	7.975	8.025	YES	
Notch radius [ρ]	mm	0.2614	0.2614	0.25	0.225	0.275	YES	
Notch angle [α]	°	44.98	44.98	45	44	46	YES	
Angle adj sides 1	°	90.05		90	89.83	90.17	YES	(*)
Angle adj sides 2	°	89.99		90	89.83	90.17	YES	(*)
Angle adj sides 3	°	90.01		90	89.83	90.17	YES	(*)
Angle adj sides 4	°	90.09		90	89.83	90.17	YES	(*)

Specimen W4-C4:

Dimension	Unit	Measured value	Corrected value	Nominal value	ASTM E23-18 tolerances		Acceptable? (Y/N)	NOTES
					Min	Max		
Length [L]	mm	54.9708	54.9643	55	52.5	55	YES	
Notch centering	mm	0.0011	0.0011	0	-1	1	YES	
Width [W]	mm	10.0268	10.0208	10	9.925	10.075	YES	
Thickness [B]	mm	10.0244	10.0184	10	9.925	10.075	YES	
Ligament [b]	mm	7.9635	7.9591	8	7.975	8.025	NO	
Notch radius [ρ]	mm	0.2586	0.2586	0.25	0.225	0.275	YES	
Notch angle [α]	°	45.02	45.02	45	44	46	YES	
Angle adj sides 1	°	89.91		90	89.83	90.17	YES	(*)
Angle adj sides 2	°	89.97		90	89.83	90.17	YES	(*)
Angle adj sides 3	°	90.03		90	89.83	90.17	YES	(*)
Angle adj sides 4	°	90.03		90	89.83	90.17	YES	(*)

Specimen W4-C5:

Dimension	Unit	Measured value	Corrected value	Nominal value	ASTM E23-18 tolerances		Acceptable? (Y/N)	NOTES
					Min	Max		
Length [L]	mm	54.961	54.9545	55	52.5	55	YES	
Notch centering	mm	0.0334	0.0334	0	-1	1	YES	
Width [W]	mm	10.0334	10.0274	10	9.925	10.075	YES	
Thickness [B]	mm	10.0338	10.0278	10	9.925	10.075	YES	
Ligament [b]	mm	7.9709	7.9665	8	7.975	8.025	NO	
Notch radius [ρ]	mm	0.2627	0.2627	0.25	0.225	0.275	YES	
Notch angle [α]	°	44.92	44.92	45	44	46	YES	
Angle adj sides 1	°	89.99		90	89.83	90.17	YES	(*)
Angle adj sides 2	°	90.01		90	89.83	90.17	YES	(*)
Angle adj sides 3	°	90.08		90	89.83	90.17	YES	(*)
Angle adj sides 4	°	90.05		90	89.83	90.17	YES	(*)

Appendix C: Digital pictures of the fracture surfaces of Charpy specimens



Specimen W1-C1



Specimen W1-C2



Specimen W1-C3



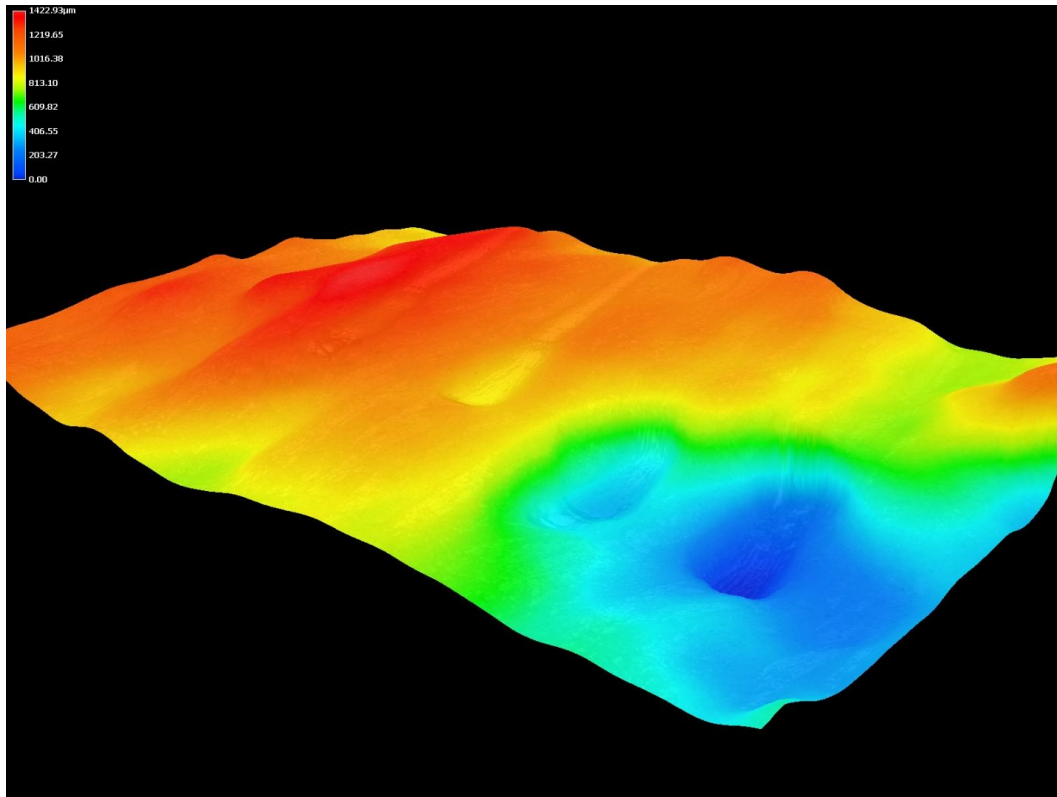
Specimen W1-C4



Specimen W1-C4, left side: detail of the wormhole cavities



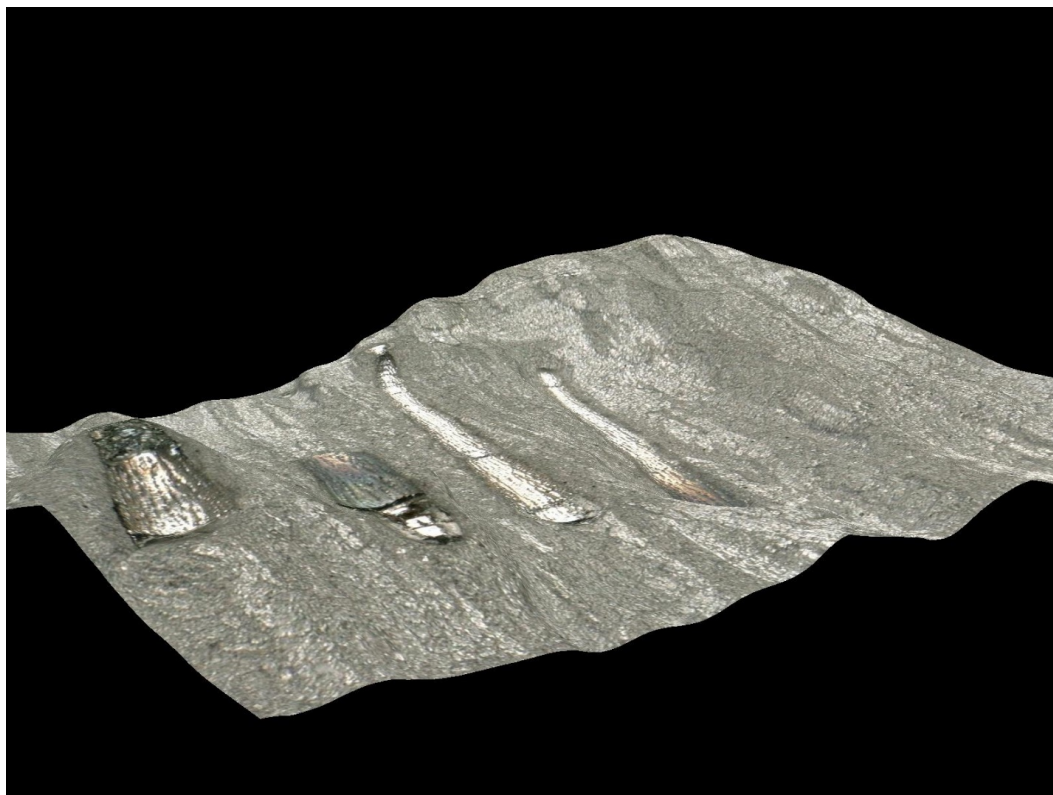
Specimen W1-C4, left side: detail of the wormhole cavities



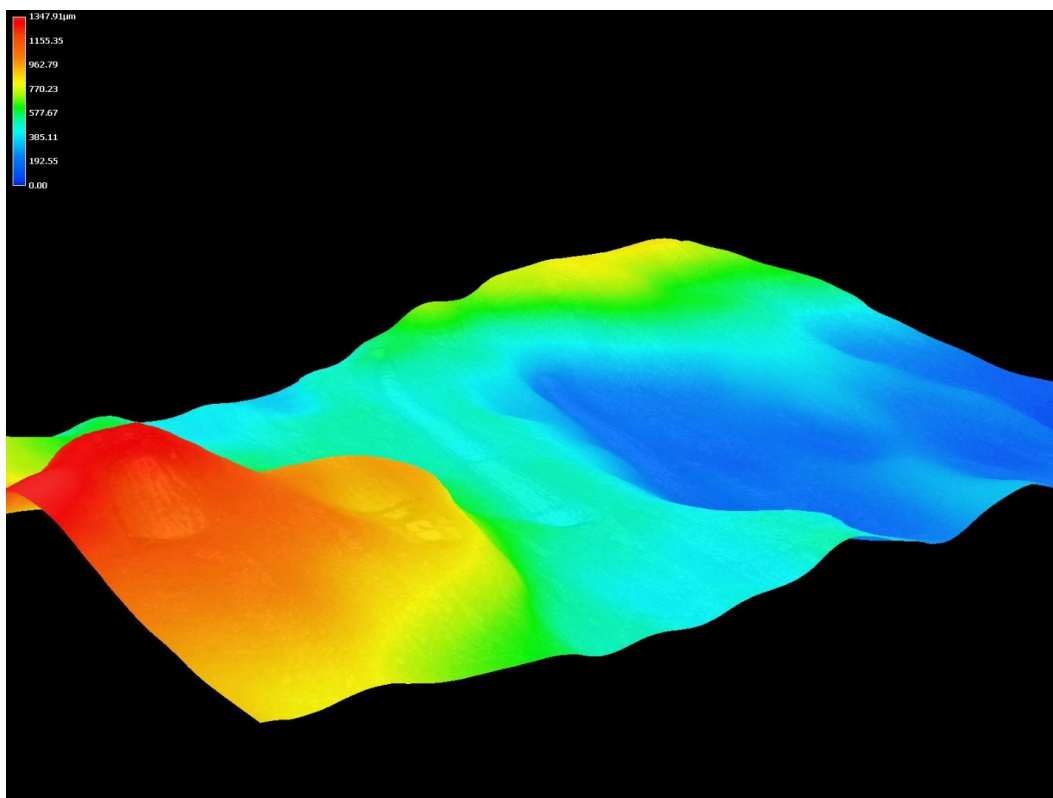
Specimen W1-C4, left side: wormhole cavities



Specimen W1-C4, right side: detail of the wormhole cavities



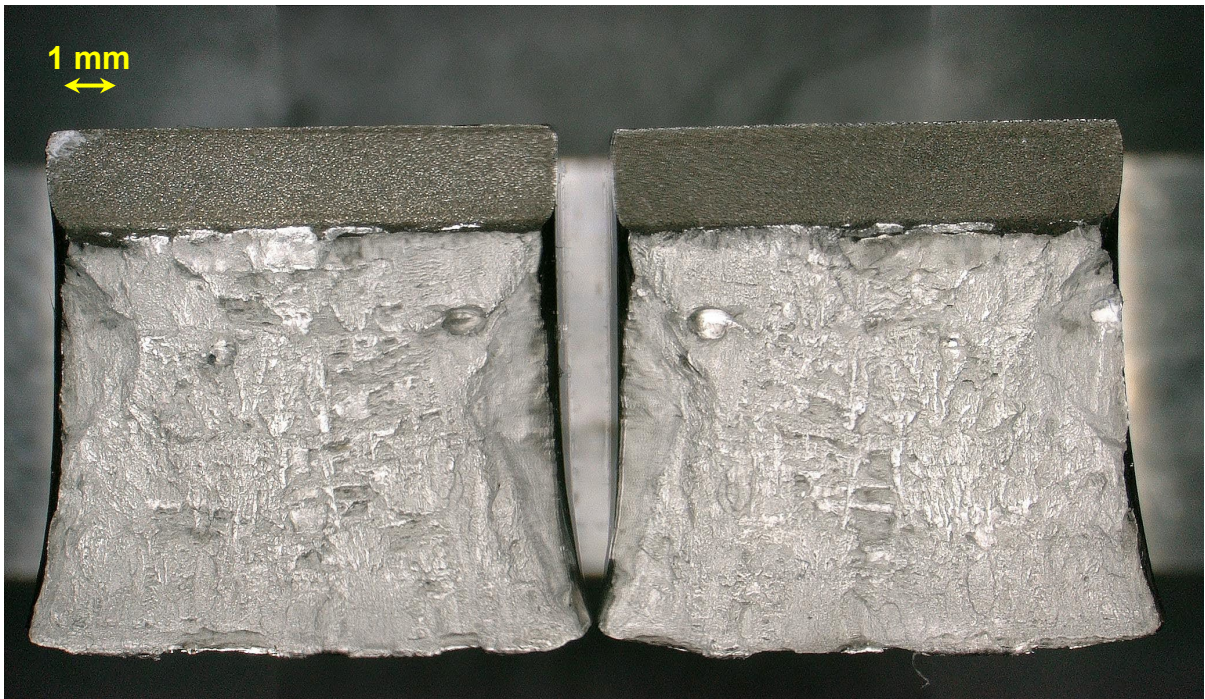
Specimen W1-C4, right side: detail of the wormhole cavities



Specimen W1-C4, right side: wormhole cavities



Specimen W1-C5



Specimen W2-C1



Specimen W2-C2



Specimen W2-C3



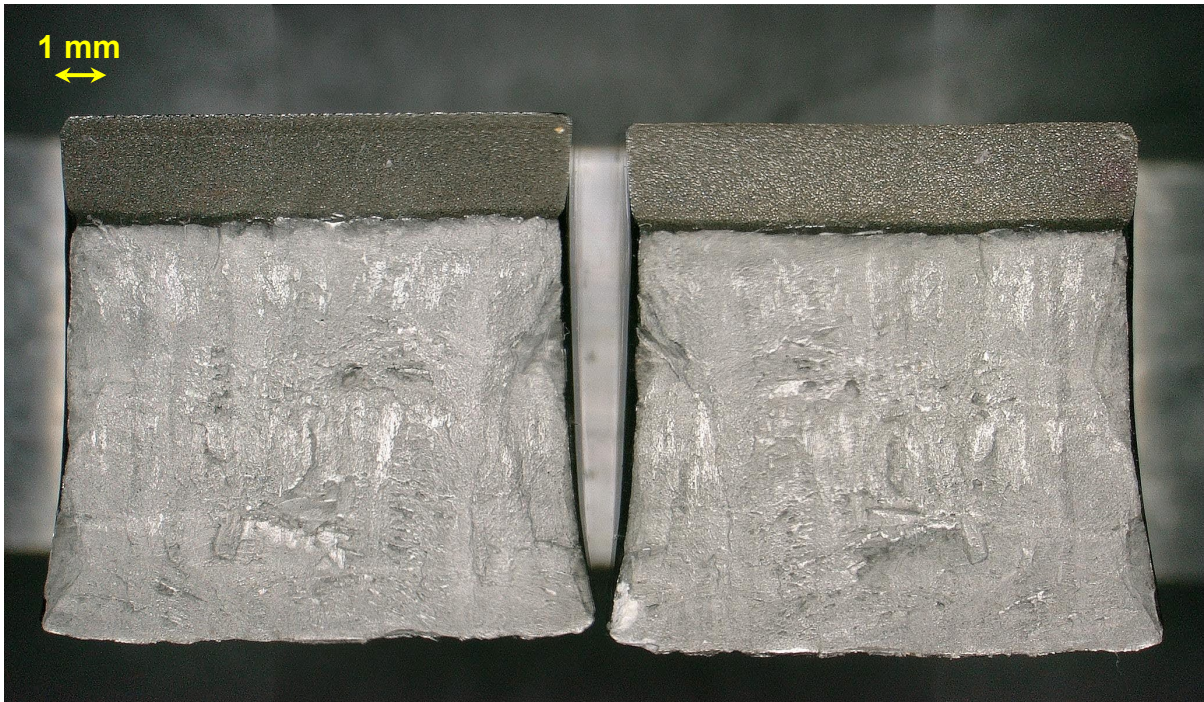
Specimen W2-C4



Specimen W2-C5



Specimen W3-C1



Specimen W3-C2



Specimen W3-C3



Specimen W3-C4



Specimen W3-C5



Specimen W4-C1



Specimen W4-C2



Specimen W4-C3

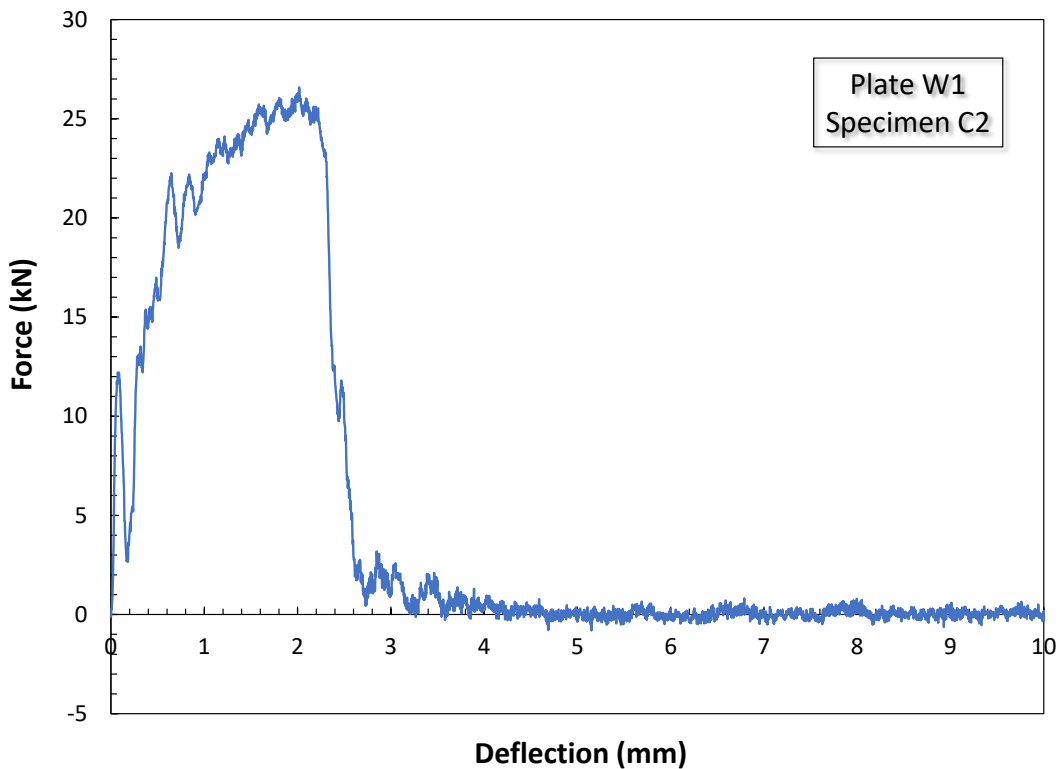
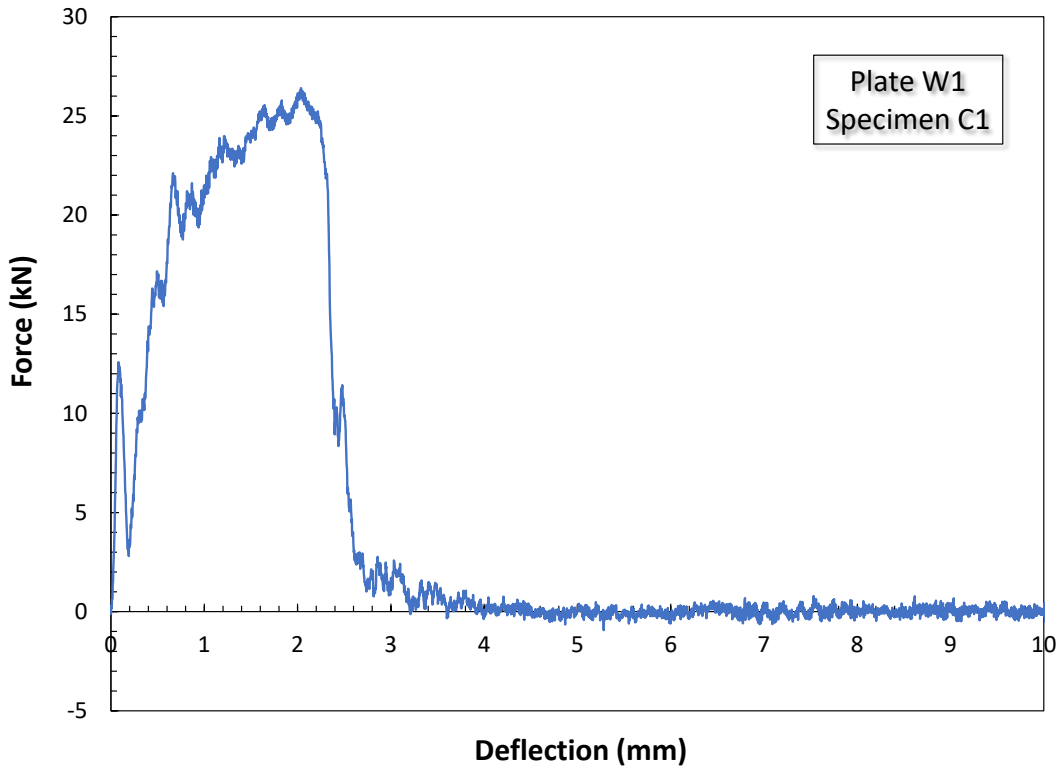


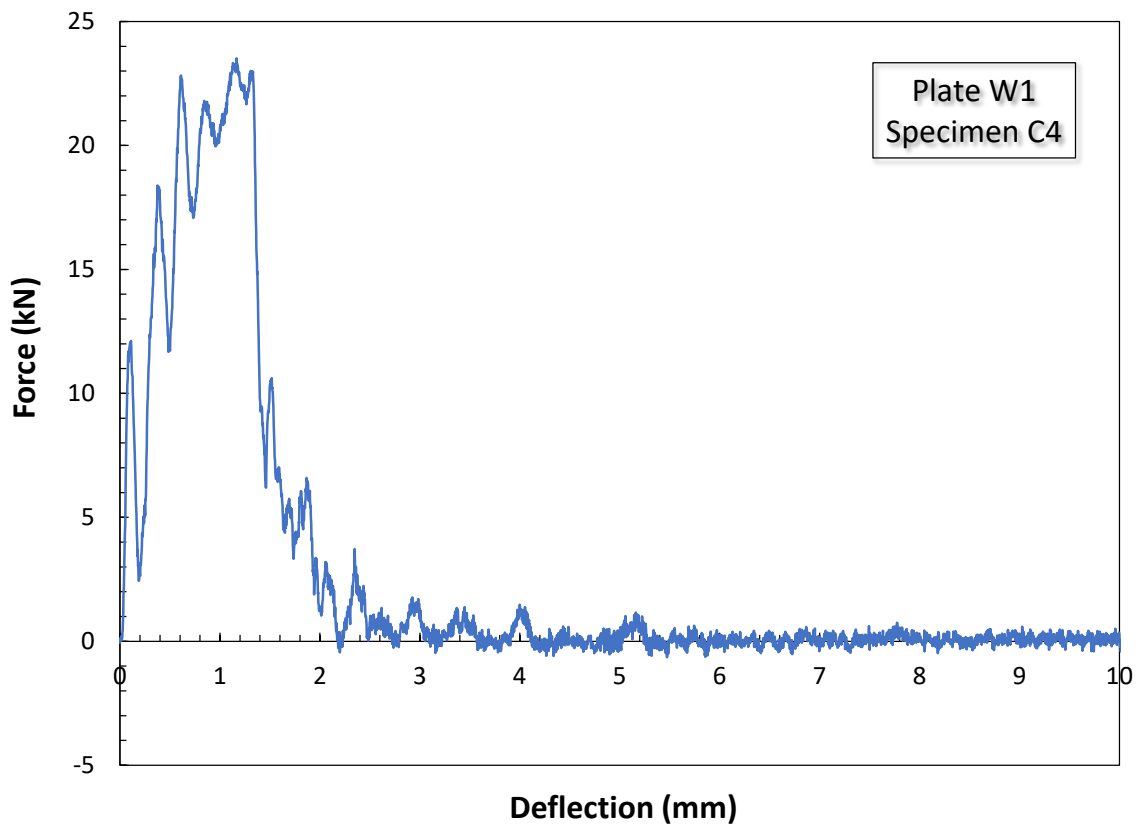
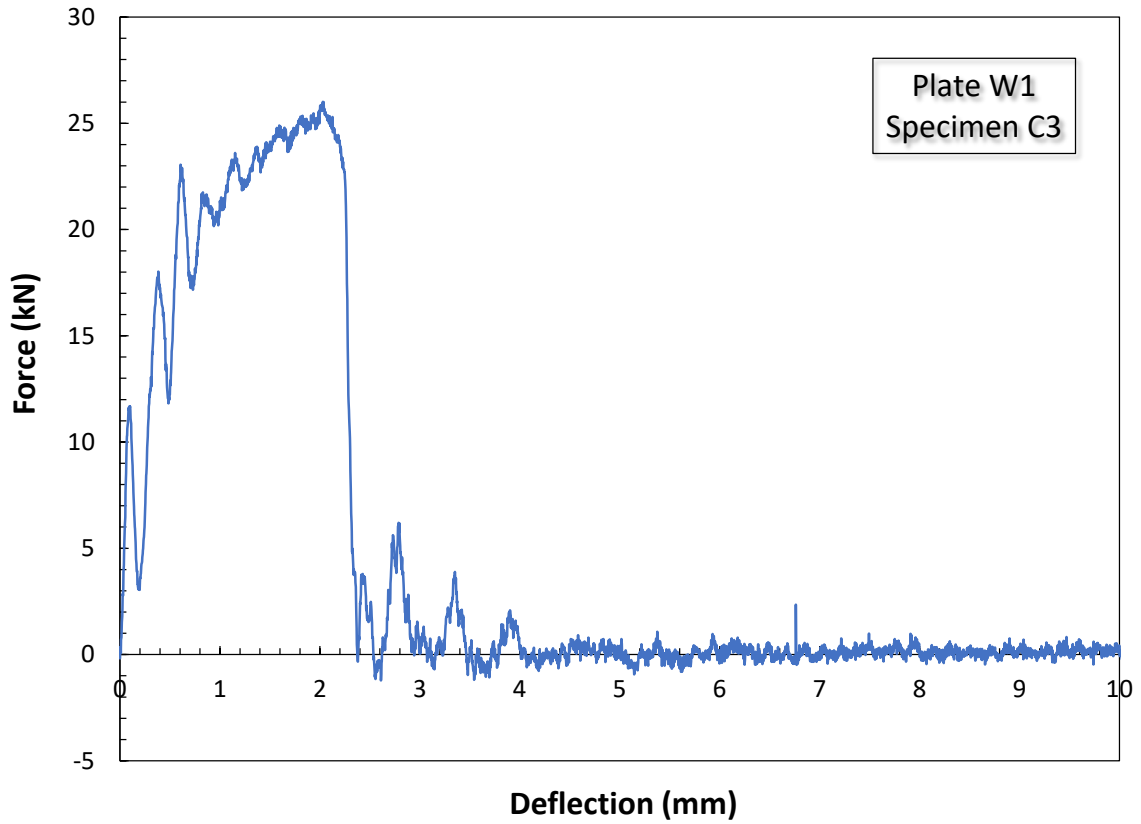
Specimen W4-C4

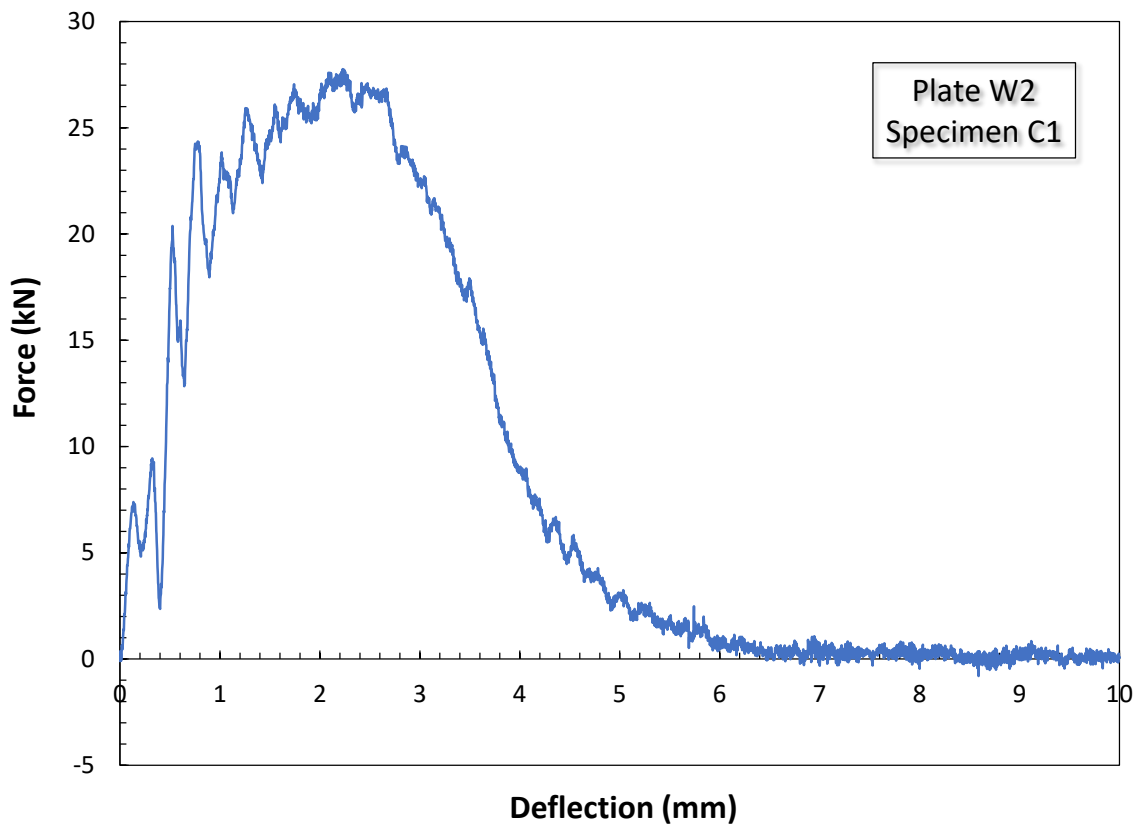
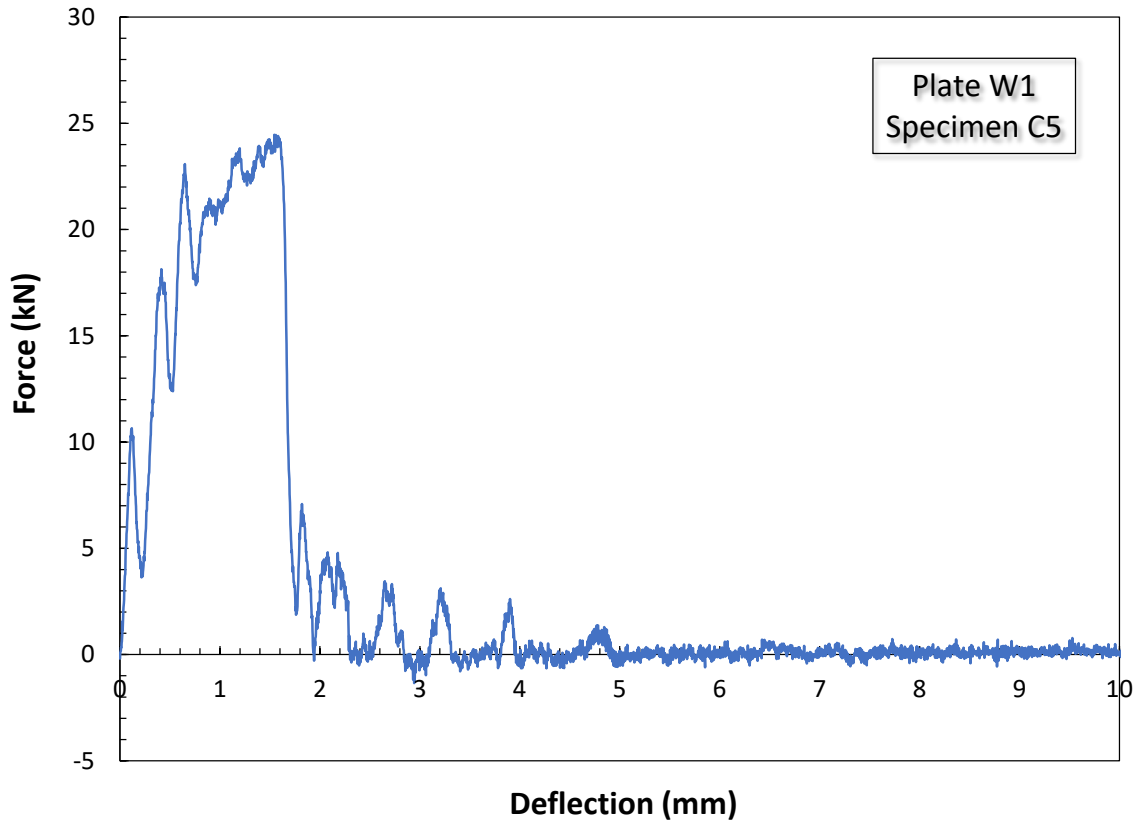


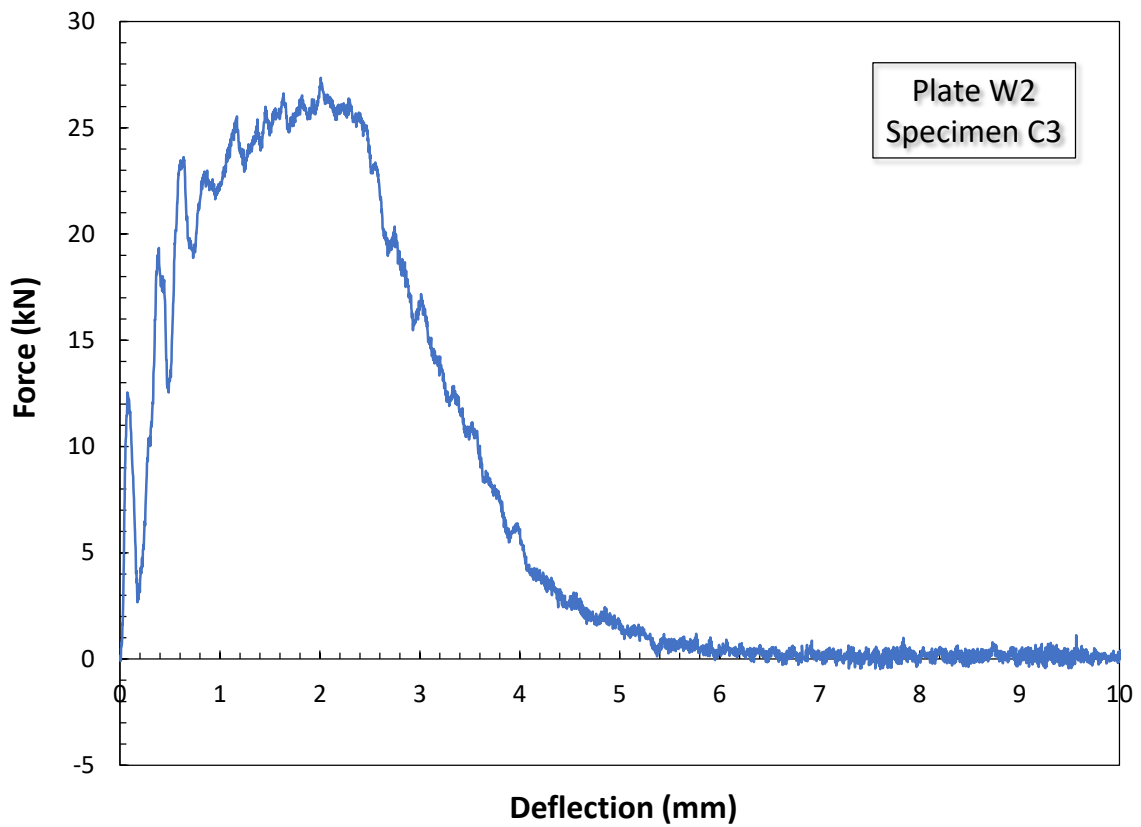
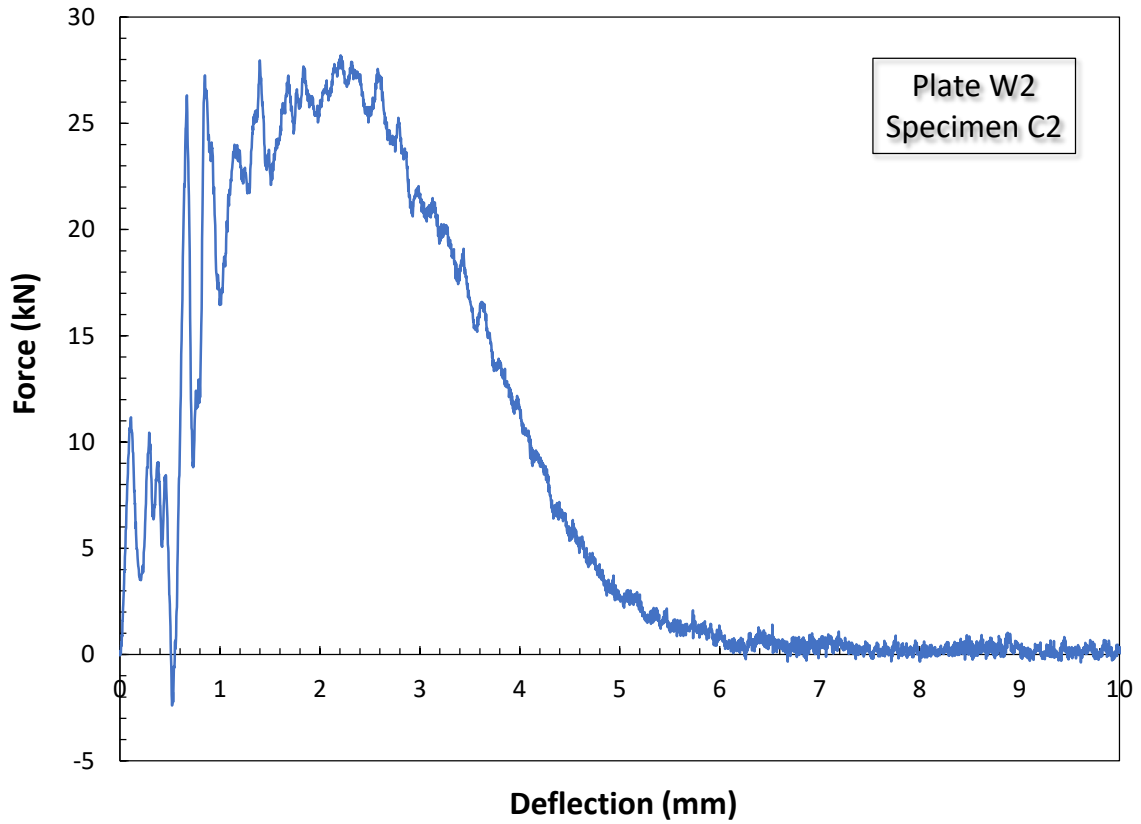
Specimen W4-C5

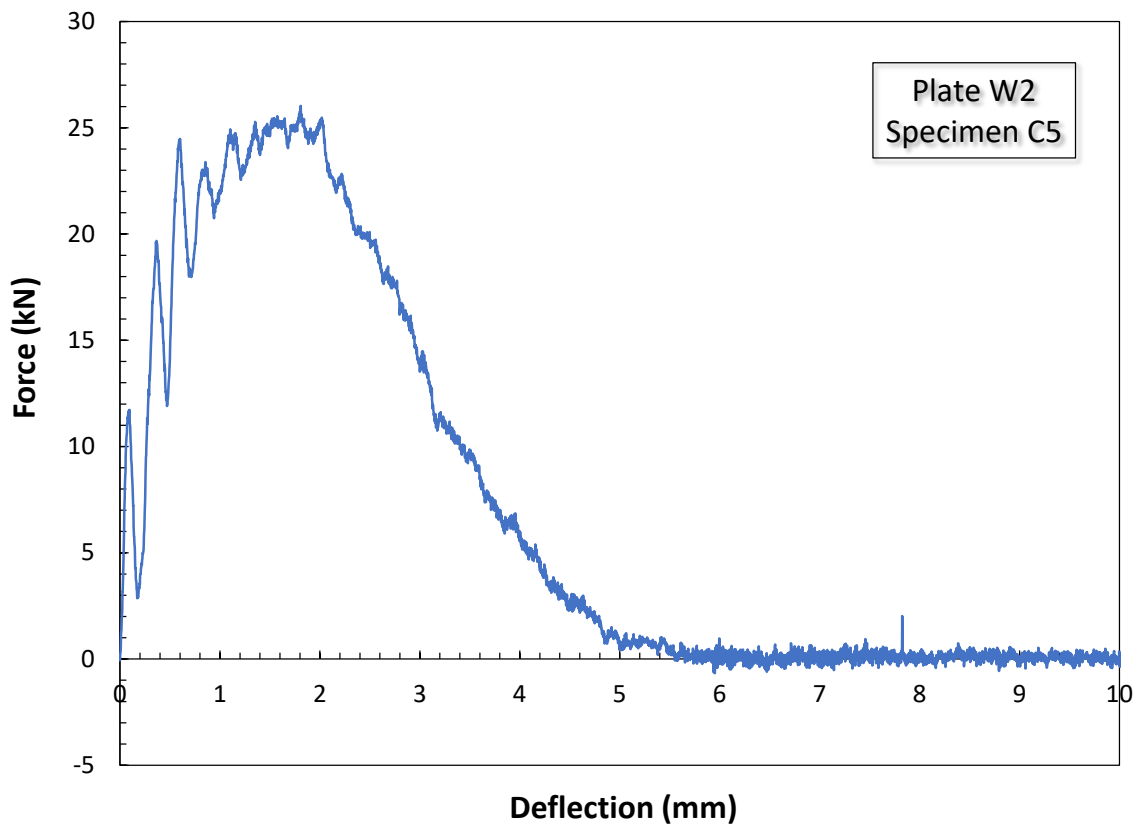
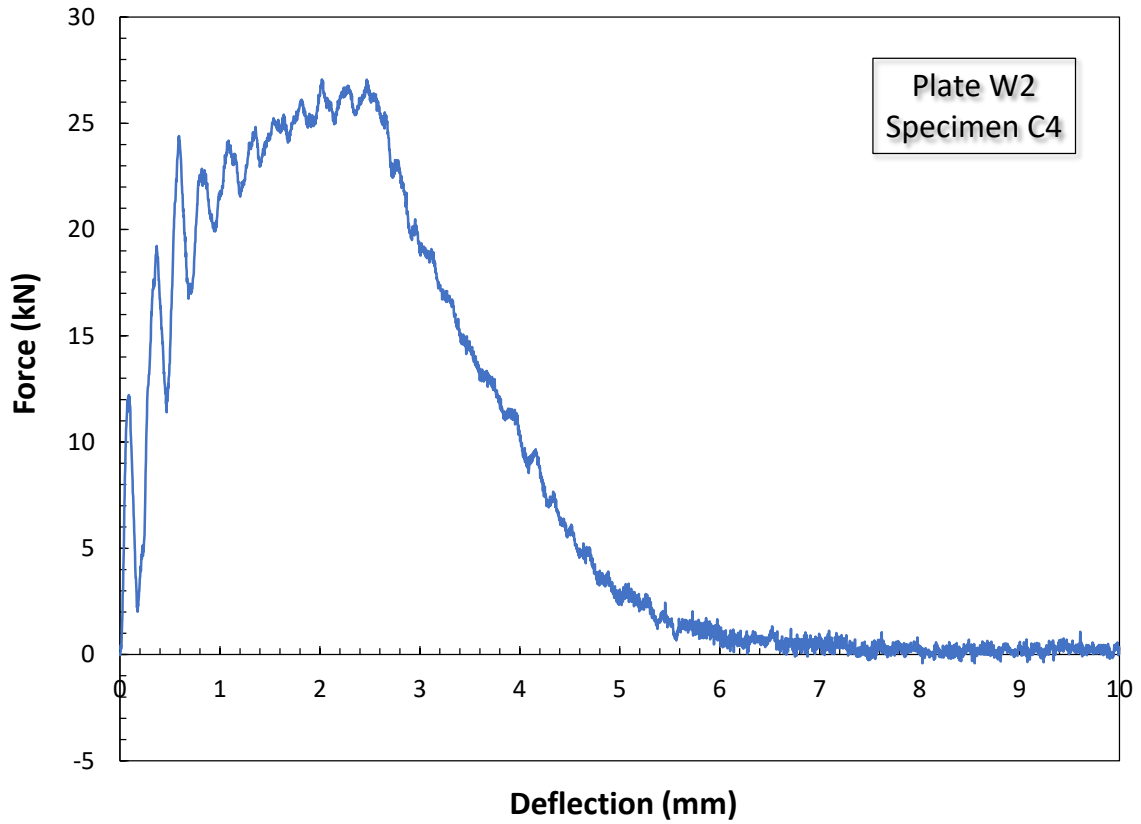
Appendix D: Instrumented force/deflection curves of the Charpy specimens

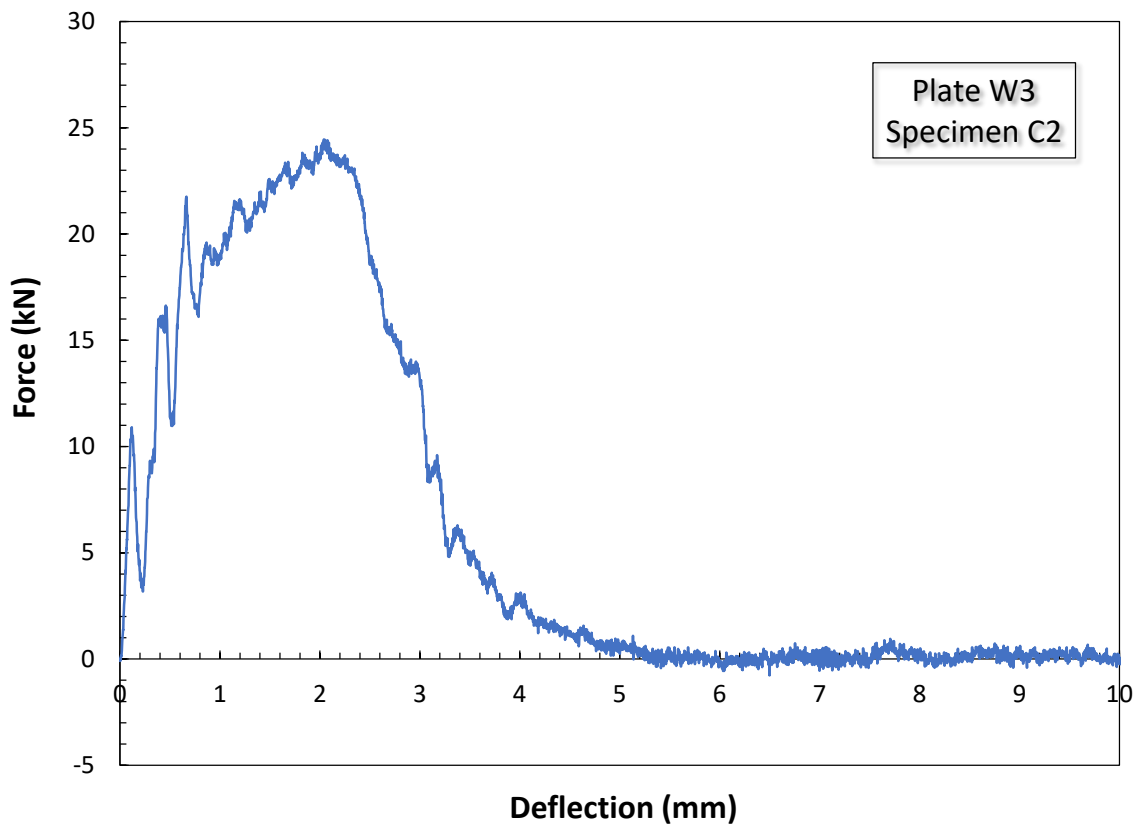
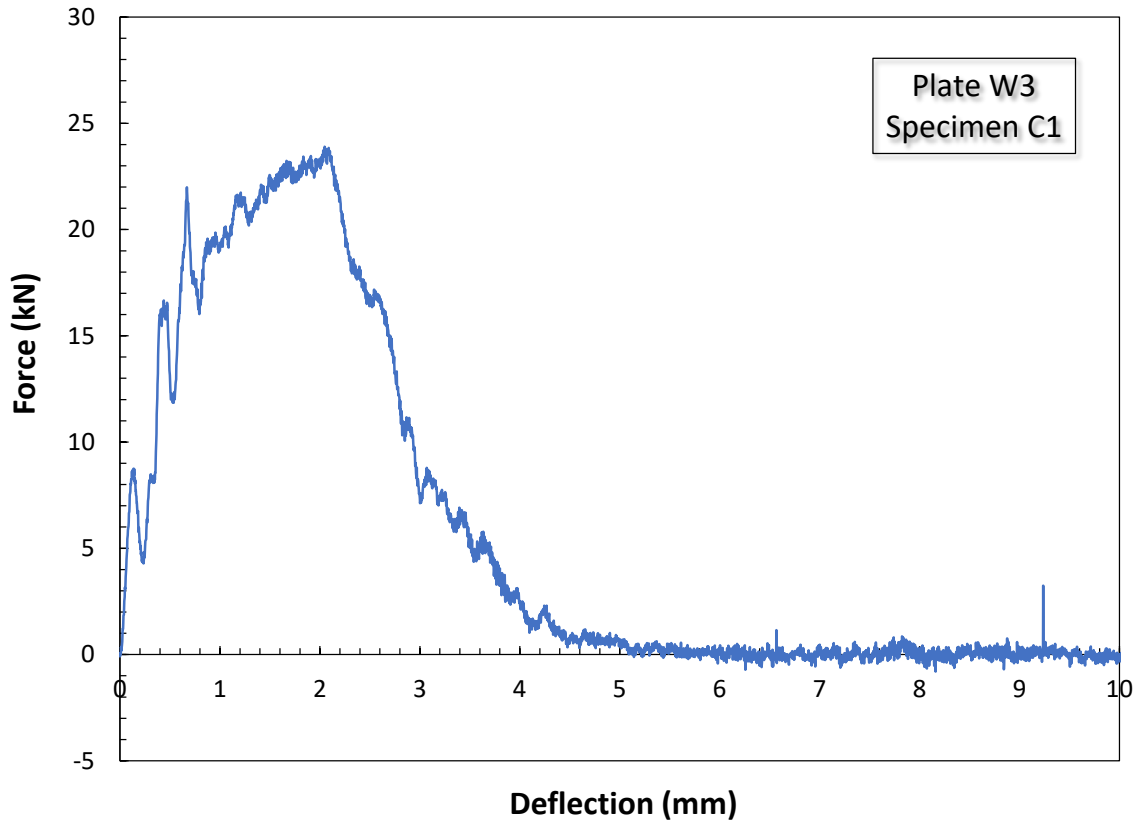


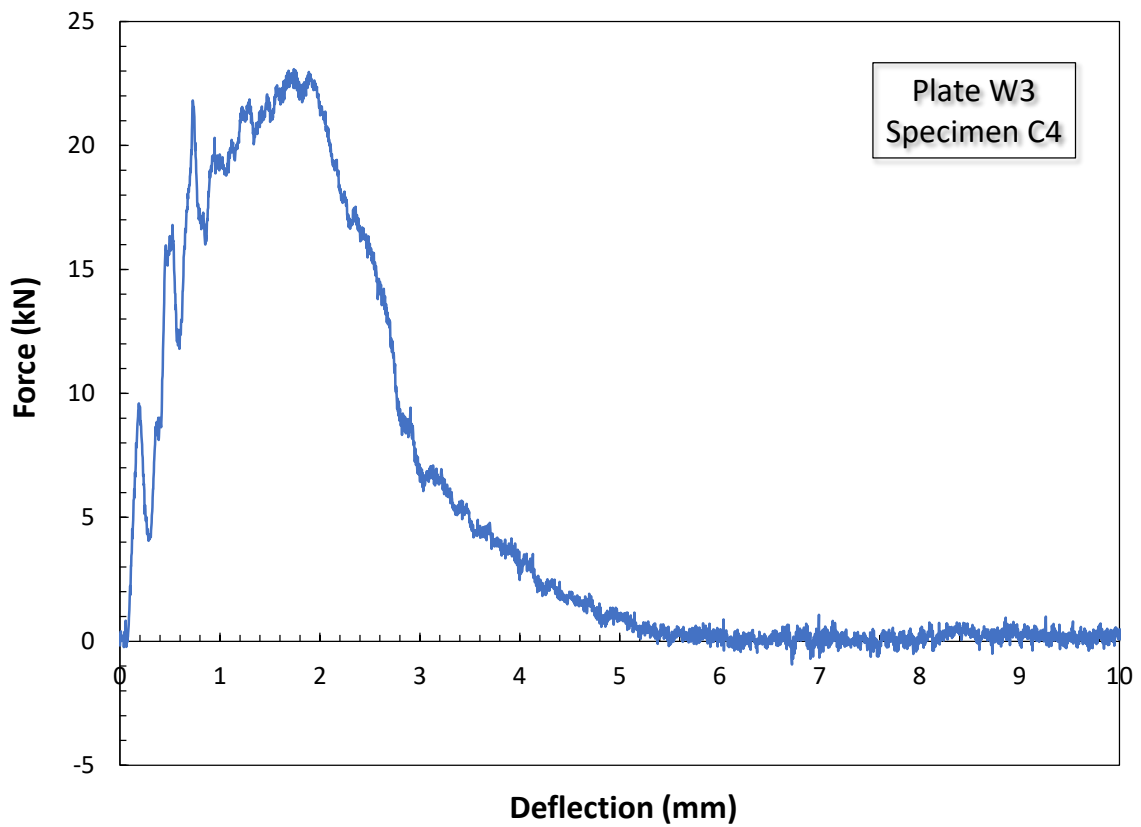
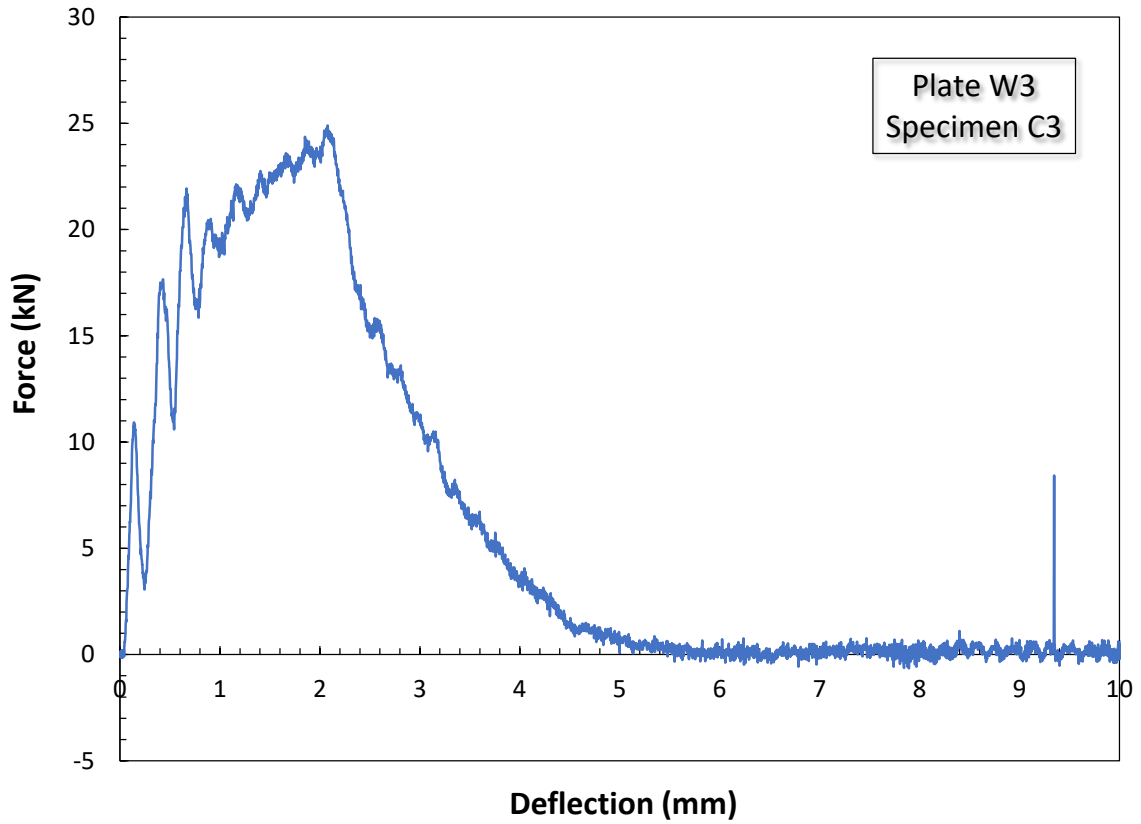


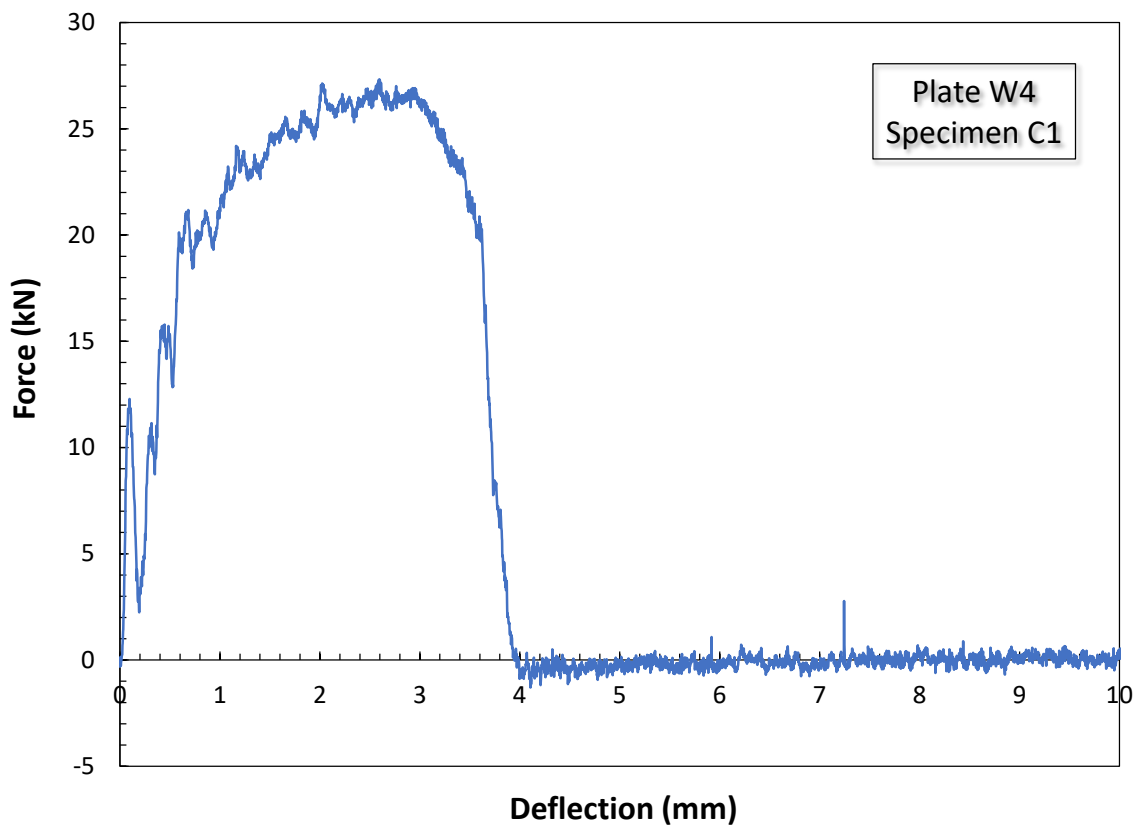
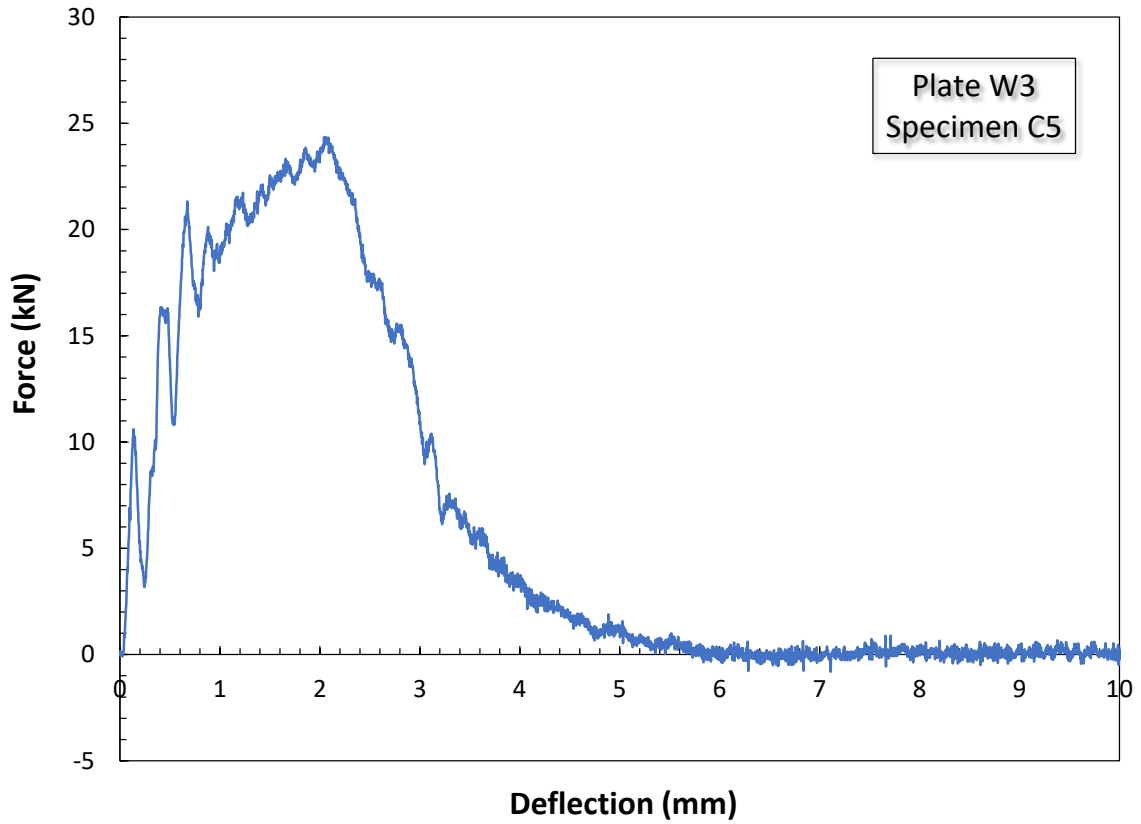


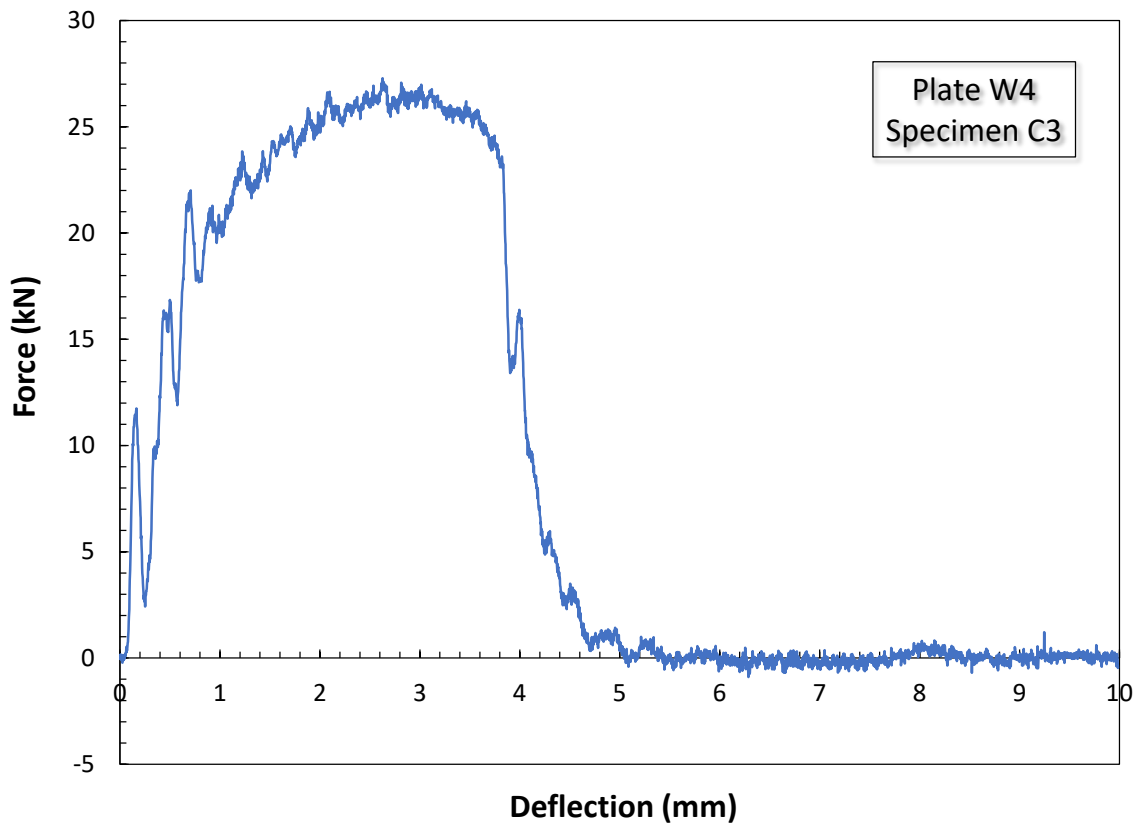
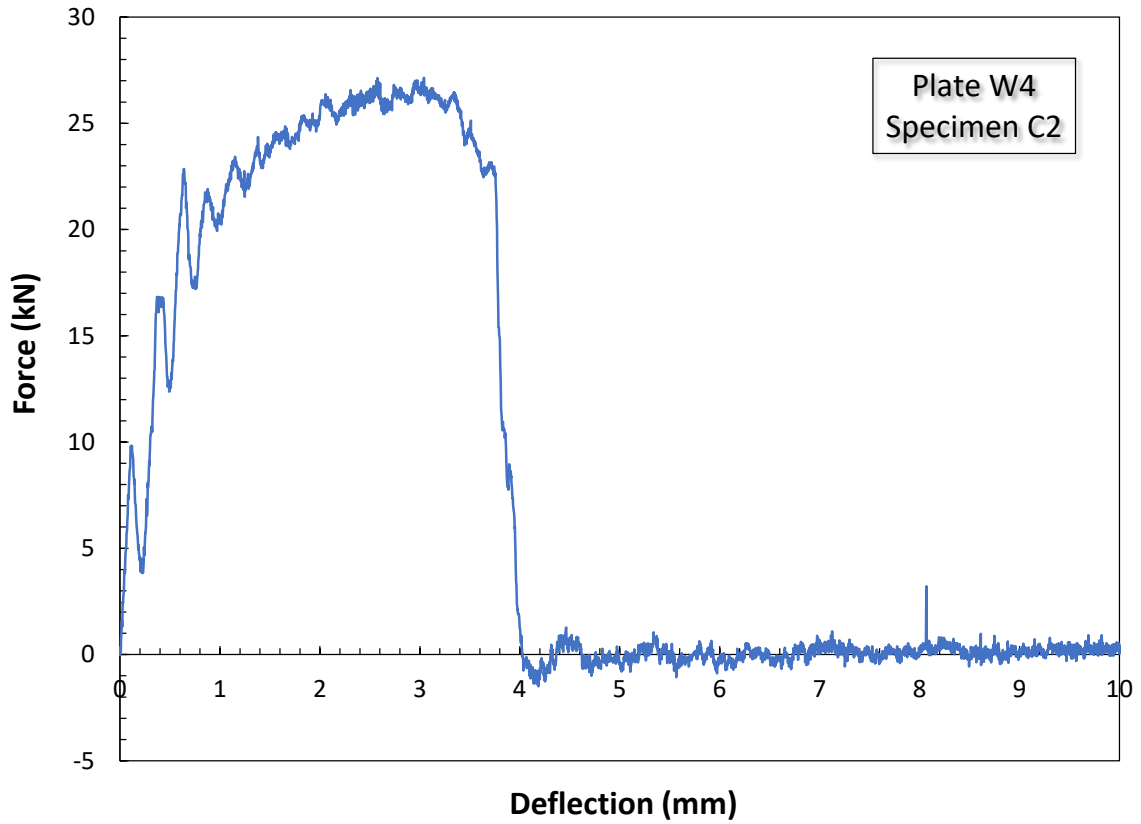


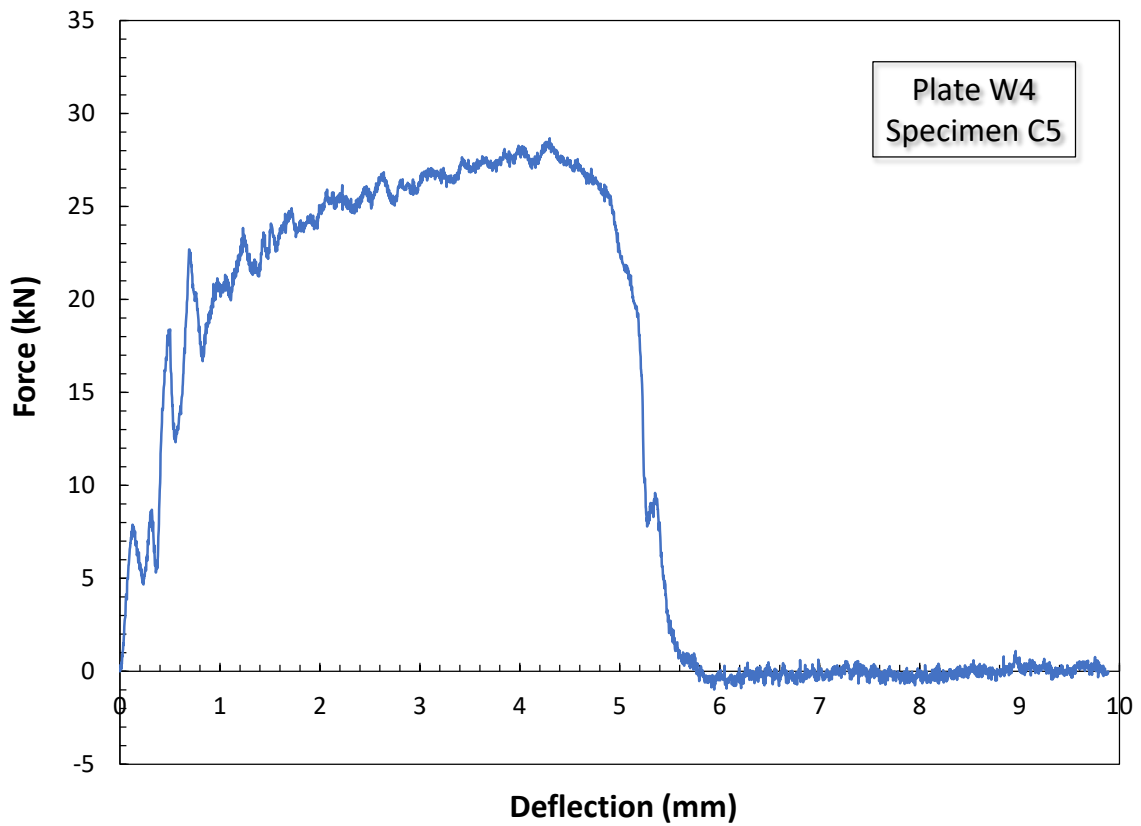
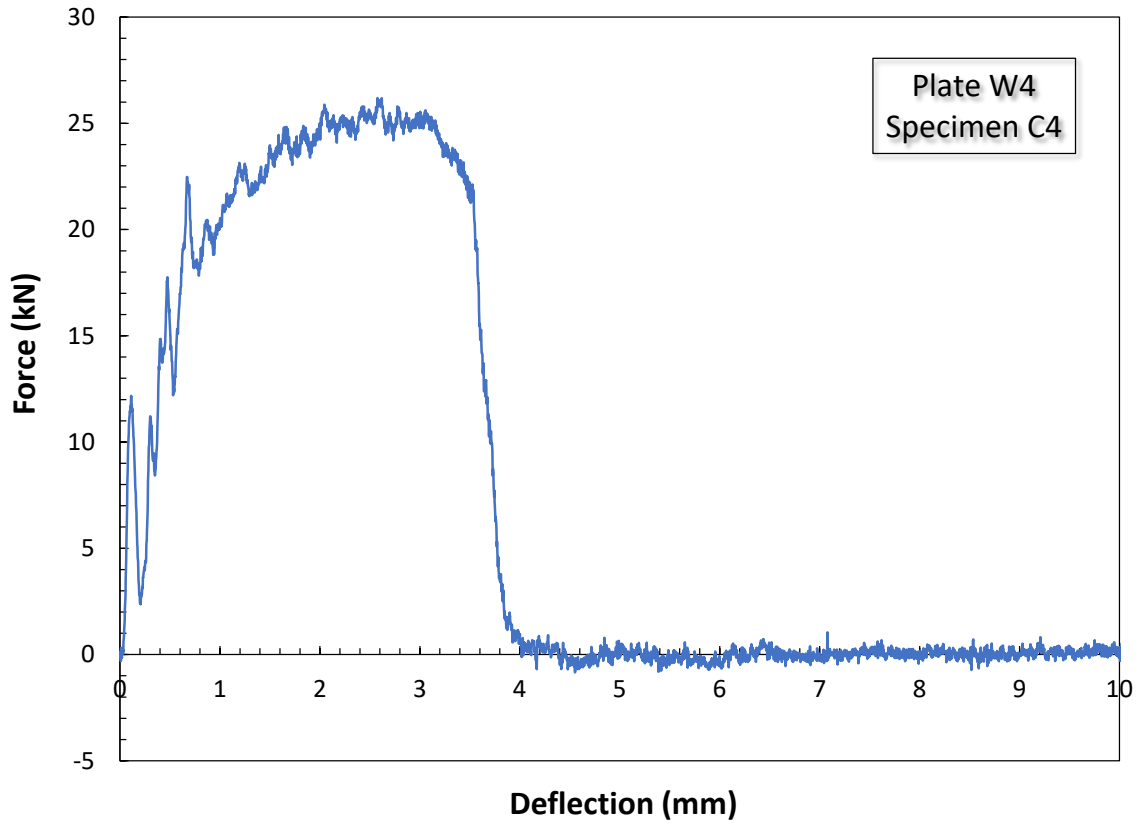




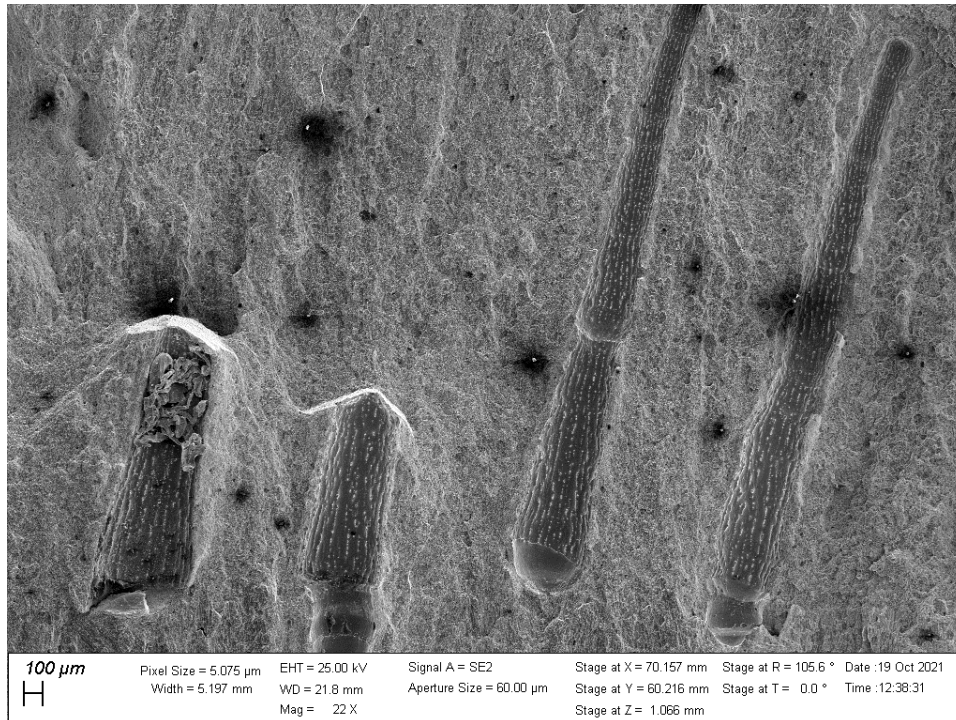




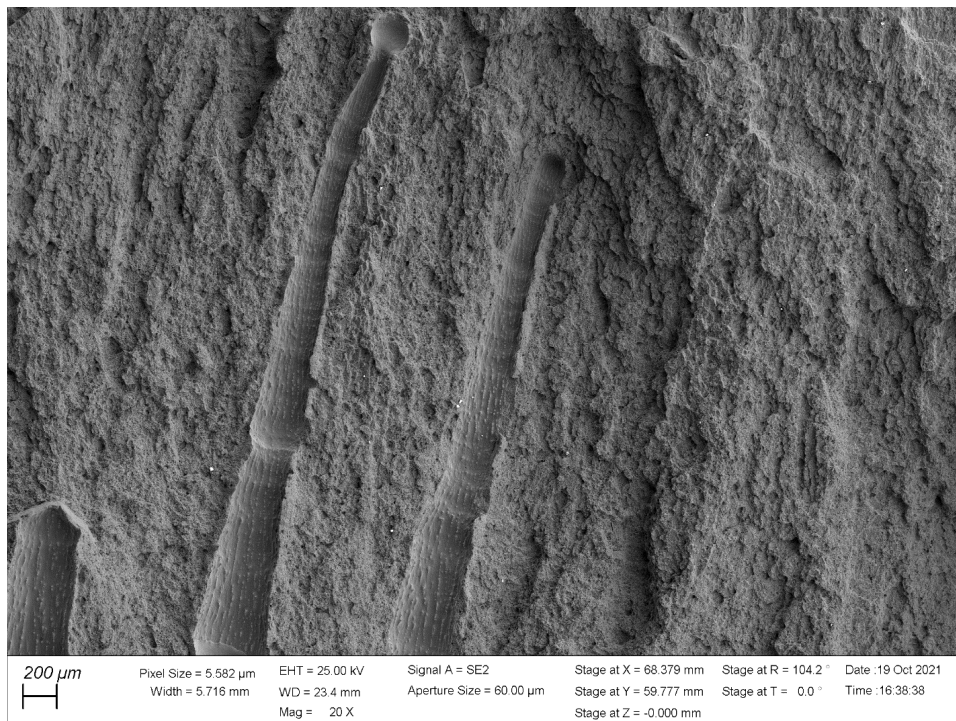




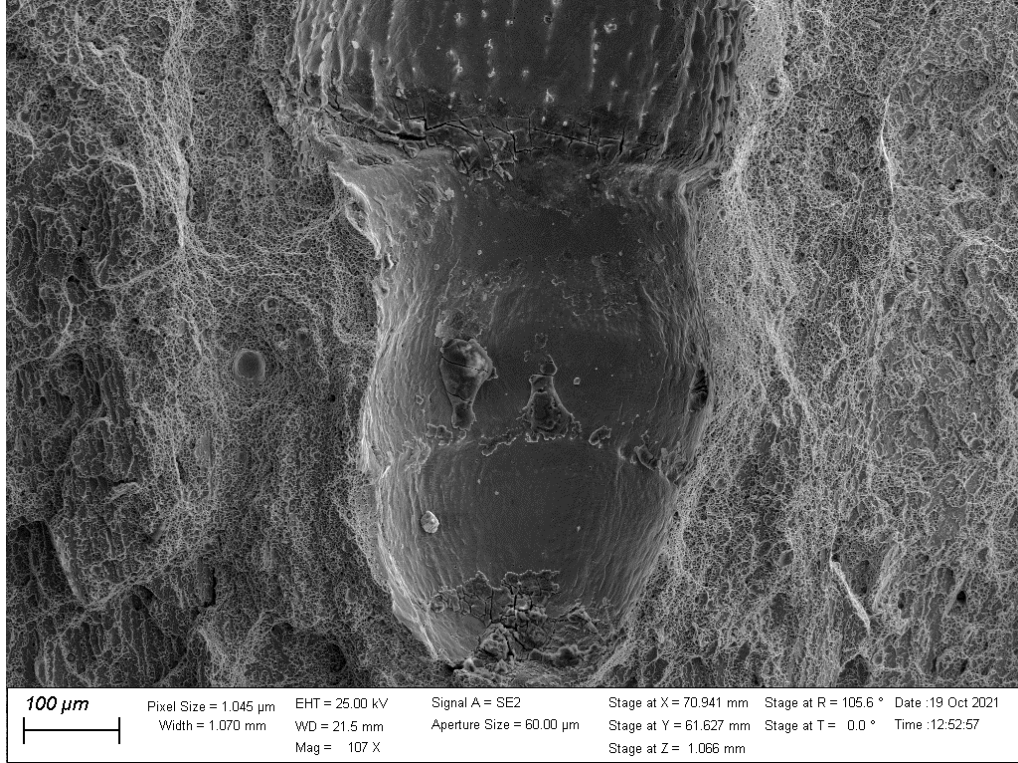
Appendix E: SEM images and additional EDS spectra and spot analyses



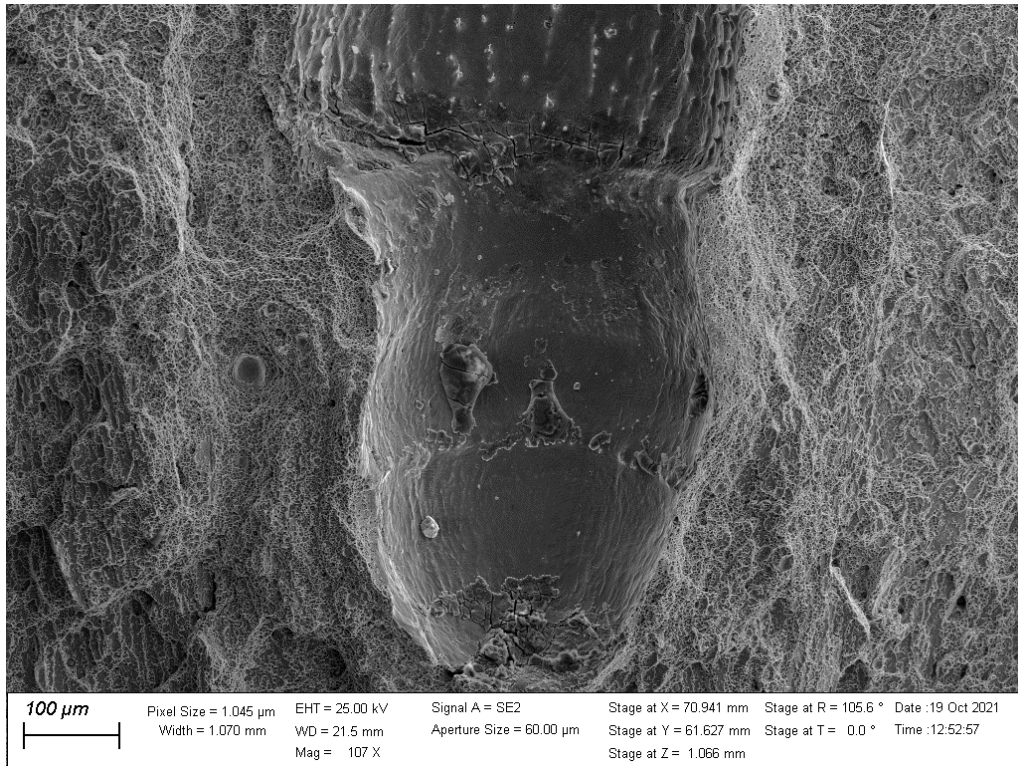
Specimen W1-C4



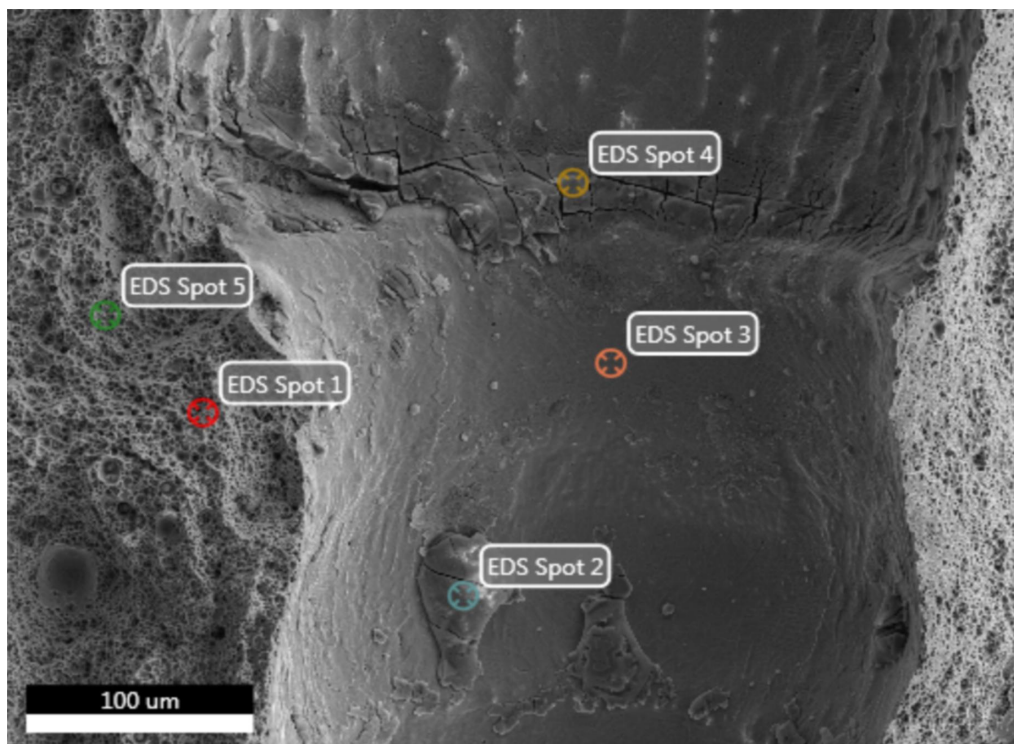
Specimen W1-C4



Specimen W1-C4

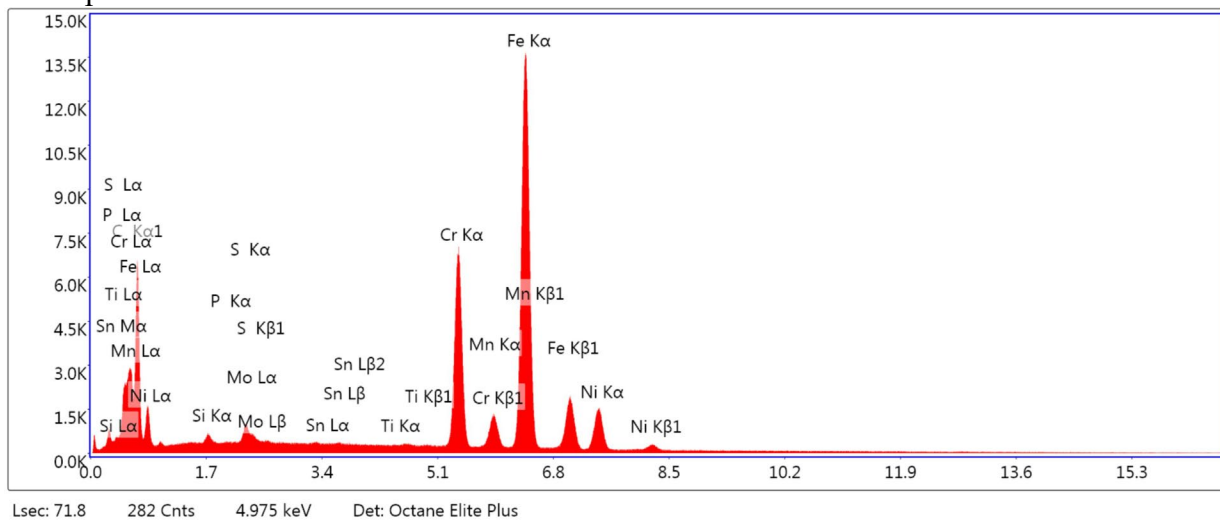


Specimen W1-C4



Specimen W1-C4

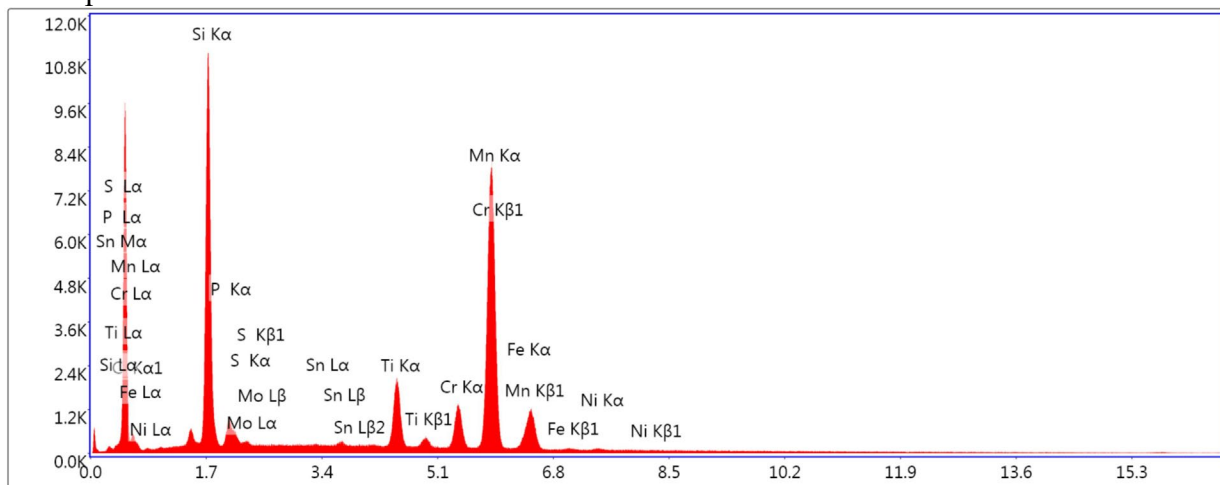
EDS Spot 1 - Det 1



eZAF Smart Quant Results

Element	Weight %	Atomic %	Net Int.	Error %
C K	1.29	5.71	80.19	6.80
SiK	0.26	0.49	51.44	10.69
P K	0.00	0.00	0.01	99.99
MoL	1.69	0.93	160.72	5.24
S K	0.00	0.00	0.01	99.99
SnL	0.81	0.36	55.48	10.62
TiK	0.53	0.59	71.45	6.06
CrK	22.88	23.36	2527.13	1.76
MnK	1.59	1.53	154.41	6.37
FeK	62.43	59.33	5333.05	1.36
NiK	8.52	7.70	598.21	2.68

EDS Spot 2 - Det 1

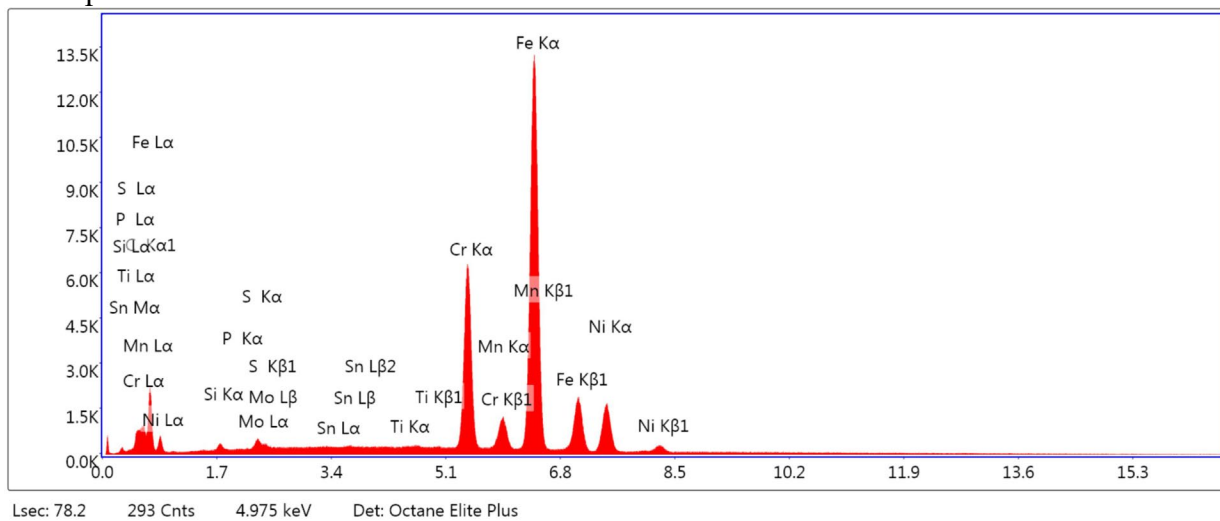


Lsec: 81.9 349 Cnts 4.975 keV Det: Octane Elite Plus

eZAF Smart Quant Results

Element	Weight %	Atomic %	Net Int.	Error %
C K	0.00	0.00	0.01	99.99
SiK	20.02	32.22	2127.96	2.96
P K	1.48	2.16	119.47	5.83
MoL	0.27	0.13	12.03	49.52
S K	0.00	0.00	0.01	99.99
SnL	0.62	0.24	20.26	16.69
TiK	9.17	8.65	580.86	2.12
CrK	7.89	6.86	402.54	2.48
MnK	58.36	48.01	2576.48	1.31
FeK	1.76	1.42	71.80	11.30
NiK	0.42	0.32	14.24	38.49

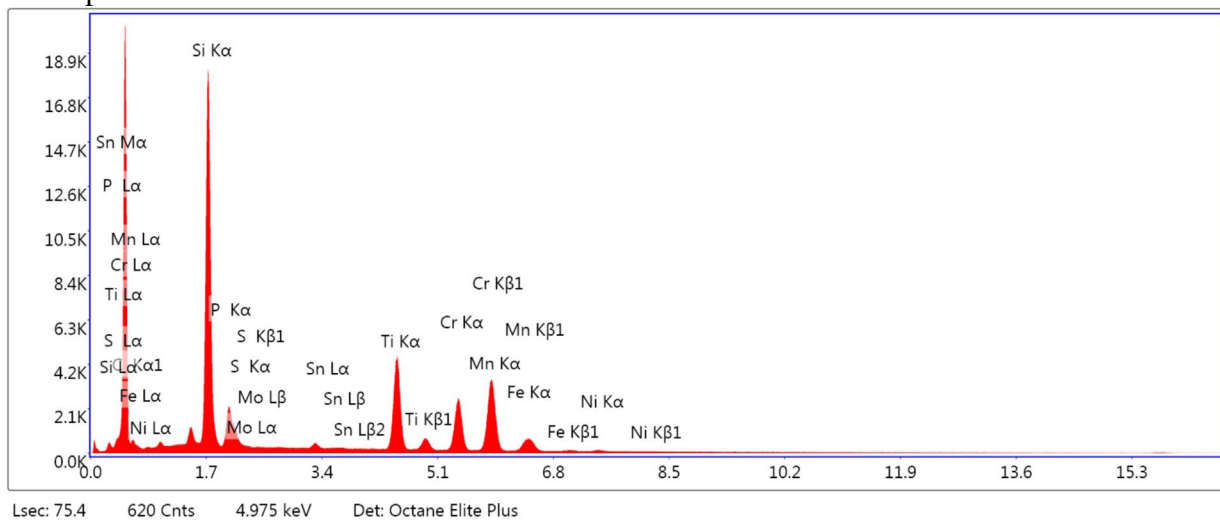
EDS Spot 3 - Det 1



eZAF Smart Quant Results

Element	Weight %	Atomic %	Net Int.	Error %
C K	0.00	0.00	0.01	99.99
SiK	0.00	0.01	0.43	99.99
P K	0.00	0.00	0.00	99.99
MoL	0.11	0.06	8.80	56.19
S K	0.20	0.35	32.77	14.21
SnL	0.30	0.14	17.84	18.52
TiK	0.64	0.74	74.87	5.62
CrK	22.31	23.67	2131.57	1.78
MnK	2.15	2.16	180.99	4.62
FeK	64.21	63.41	4734.52	1.33
NiK	10.07	9.46	607.71	2.47

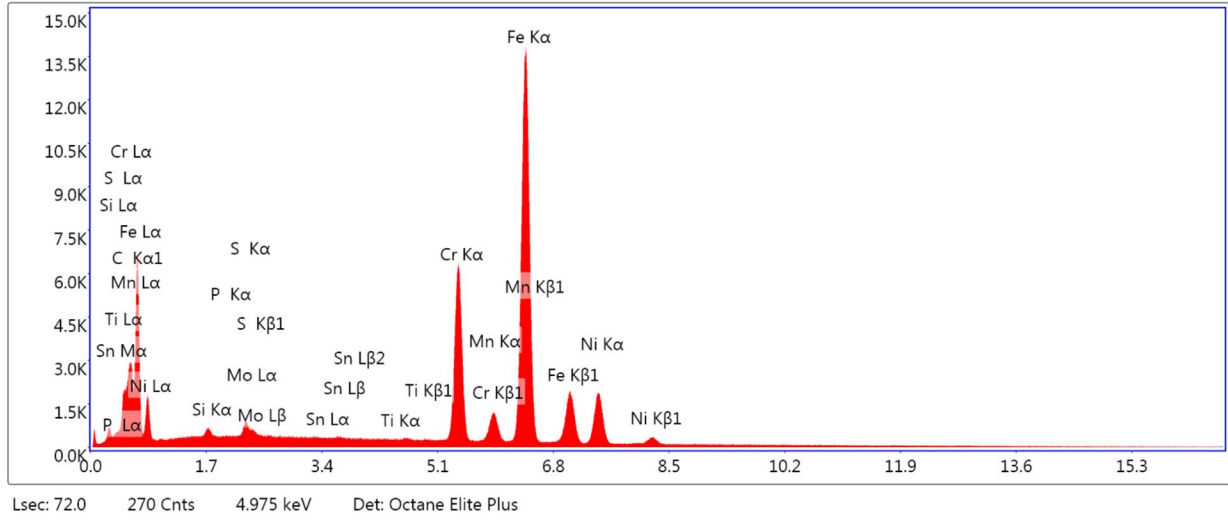
EDS Spot 4 - Det 1



eZAF Smart Quant Results

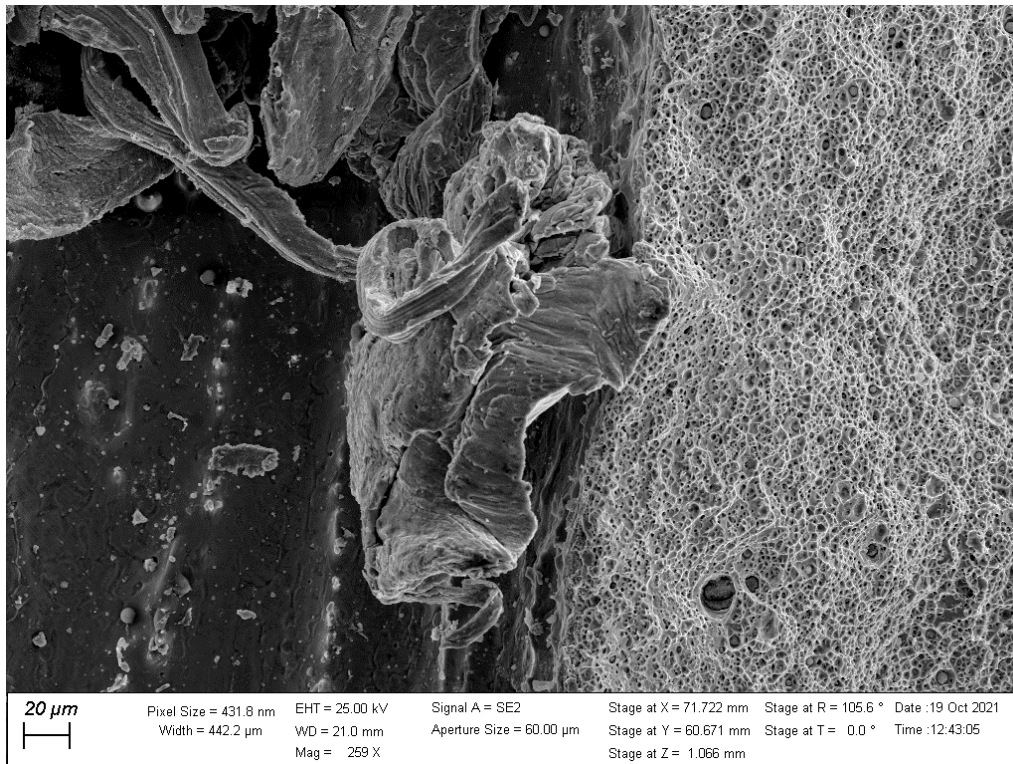
Element	Weight %	Atomic %	Net Int.	Error %
C K	0.82	2.71	18.03	18.10
Si K	31.15	43.77	3910.14	2.31
P K	4.32	5.50	380.14	4.74
Mo L	0.18	0.07	8.53	68.47
S K	0.00	0.00	0.01	99.99
Sn L	1.24	0.41	44.35	21.54
Ti K	20.84	17.17	1419.77	1.67
Cr K	15.66	11.89	846.22	2.02
Mn K	23.06	16.57	1112.78	1.80
Fe K	2.18	1.54	97.14	11.75
Ni K	0.54	0.37	20.81	28.07

EDS Spot 5 - Det 1

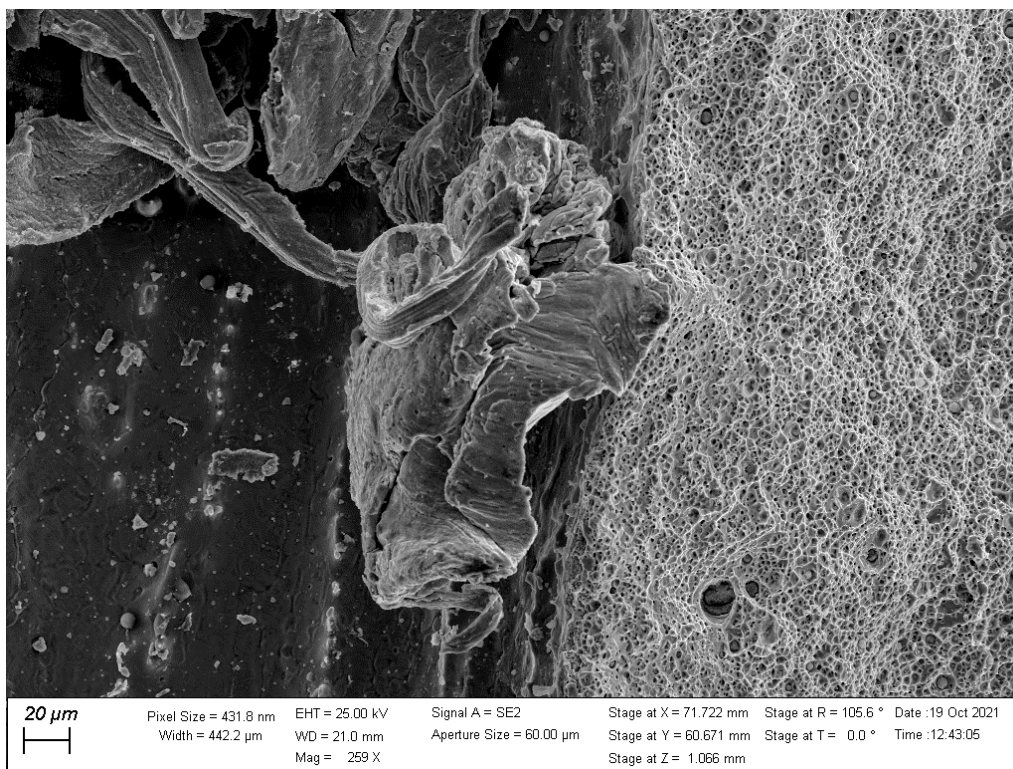


eZAF Smart Quant Results

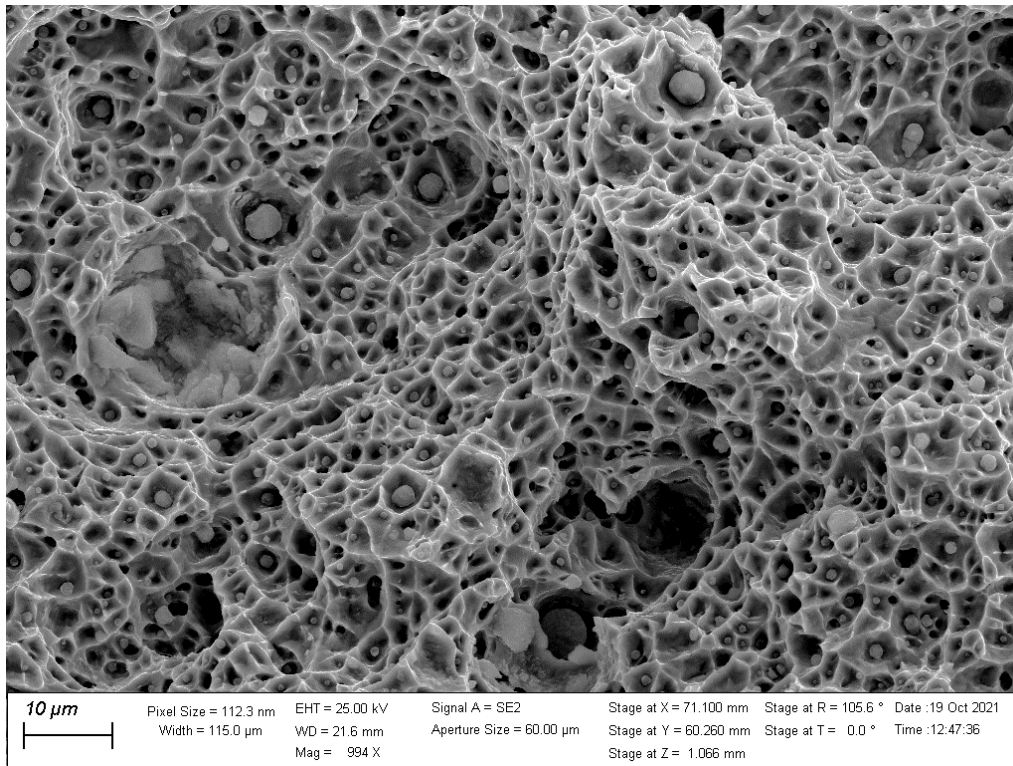
Element	Weight %	Atomic %	Net Int.	Error %
C K	0.95	4.25	57.36	8.23
SiK	0.25	0.47	48.17	12.32
P K	0.00	0.00	0.01	99.99
MoL	1.38	0.77	128.24	7.13
S K	0.00	0.00	0.01	99.99
SnL	0.63	0.29	42.20	13.30
TiK	0.41	0.46	53.90	8.28
CrK	20.87	21.57	2271.56	1.81
MnK	1.47	1.44	141.32	6.77
FeK	63.40	61.01	5338.16	1.34
NiK	10.64	9.74	733.30	2.45



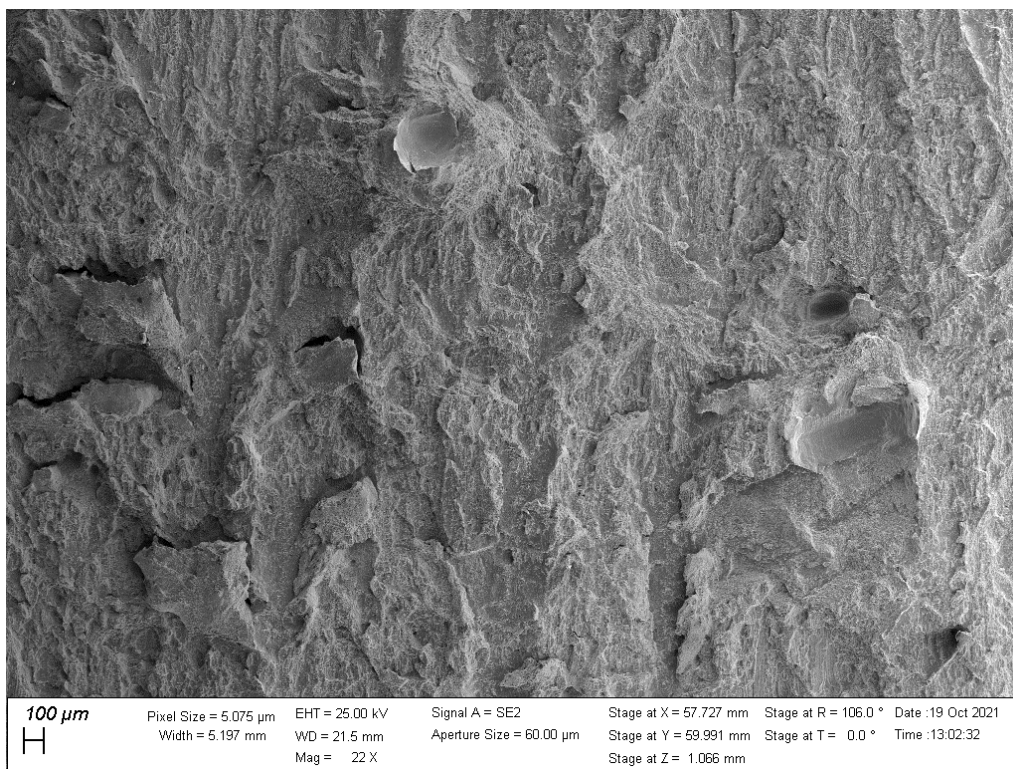
Specimen W1-C4



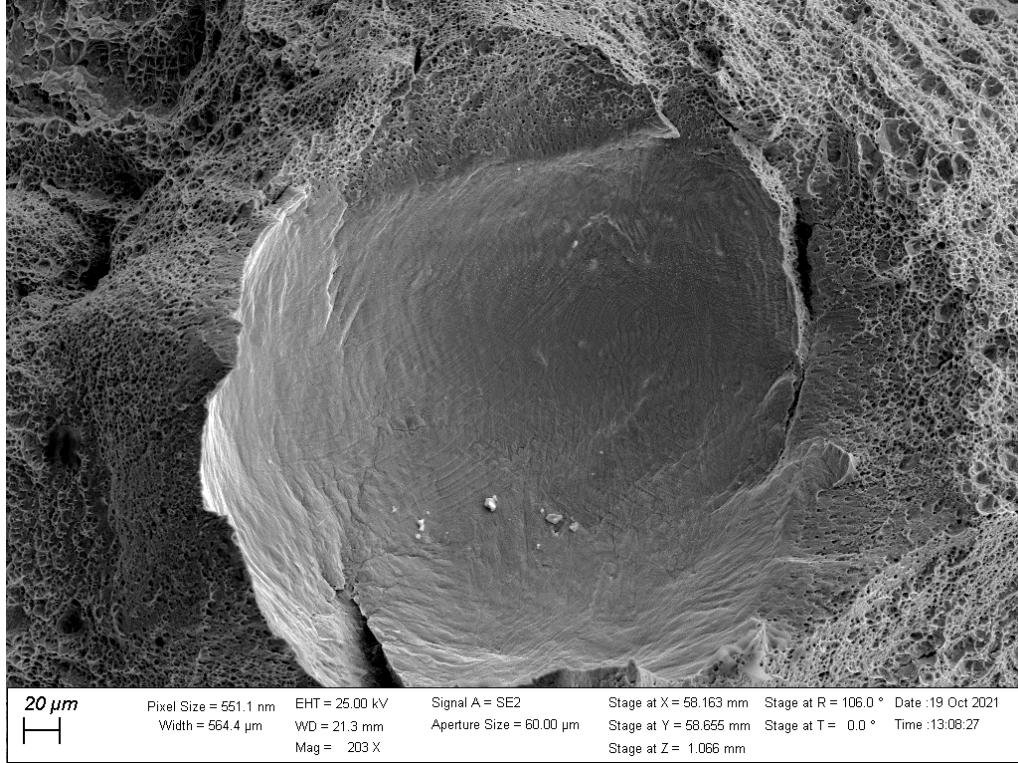
Specimen W1-C4



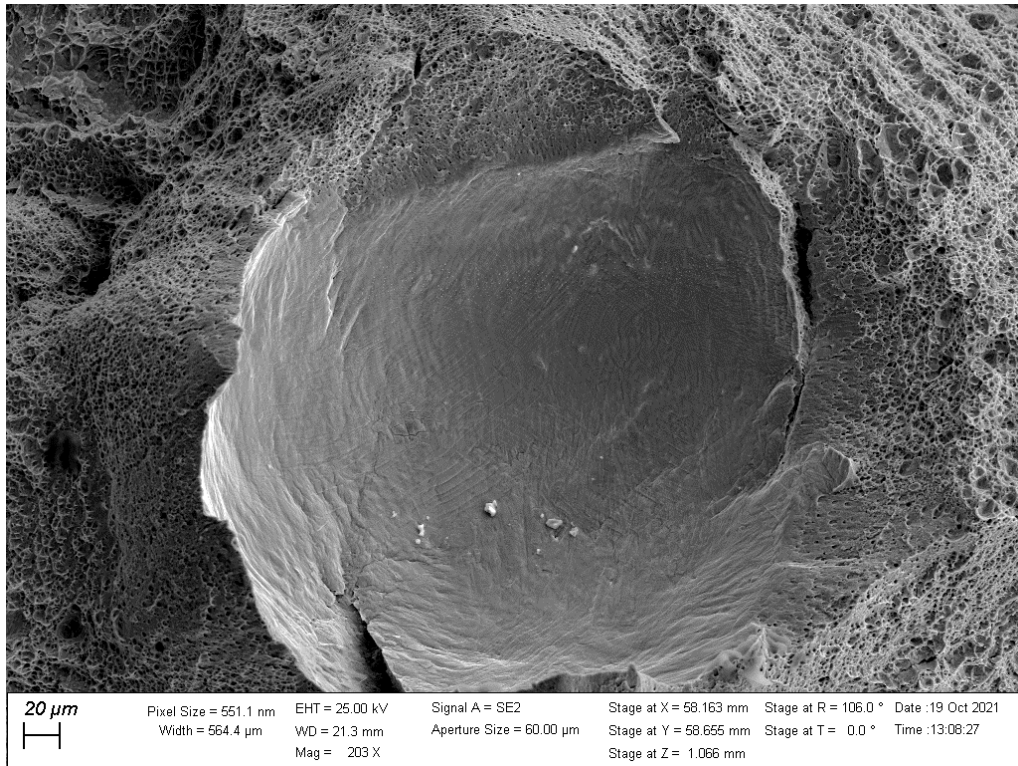
Specimen W1-C4



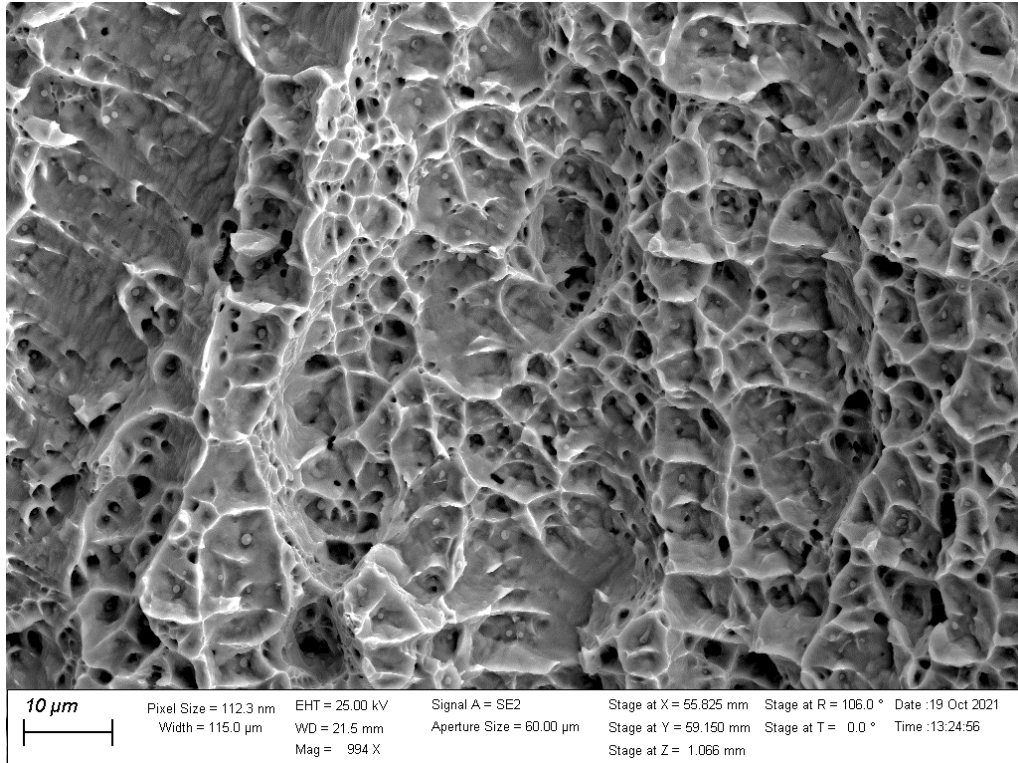
Specimen W2-C3



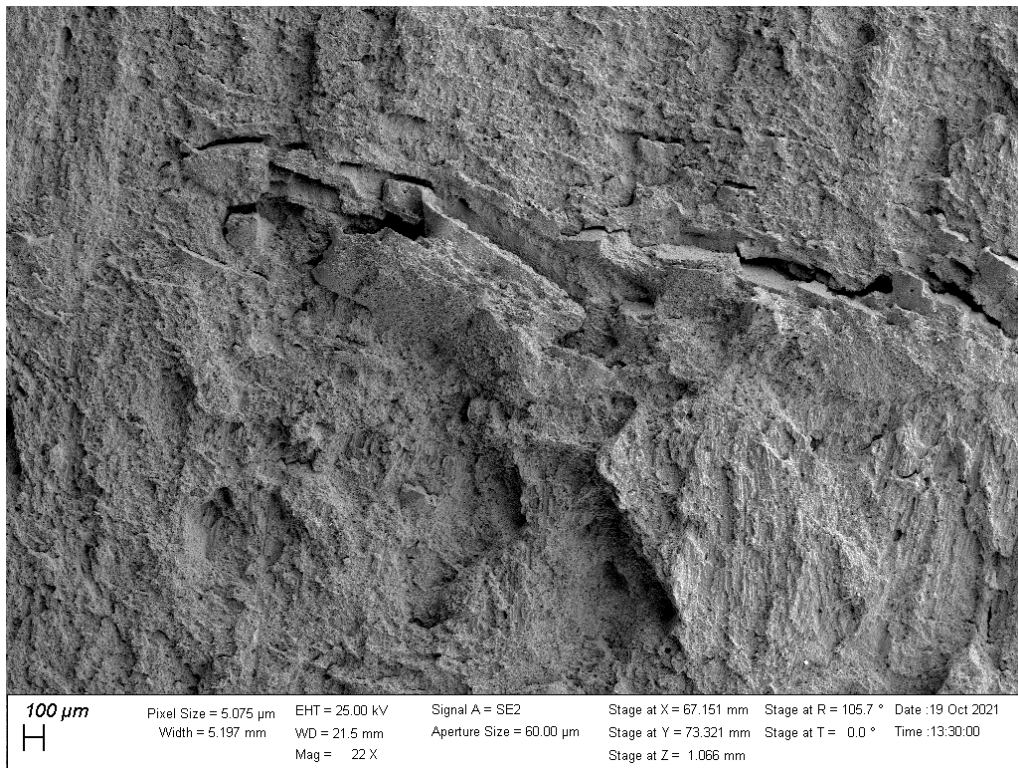
Specimen W2-C3



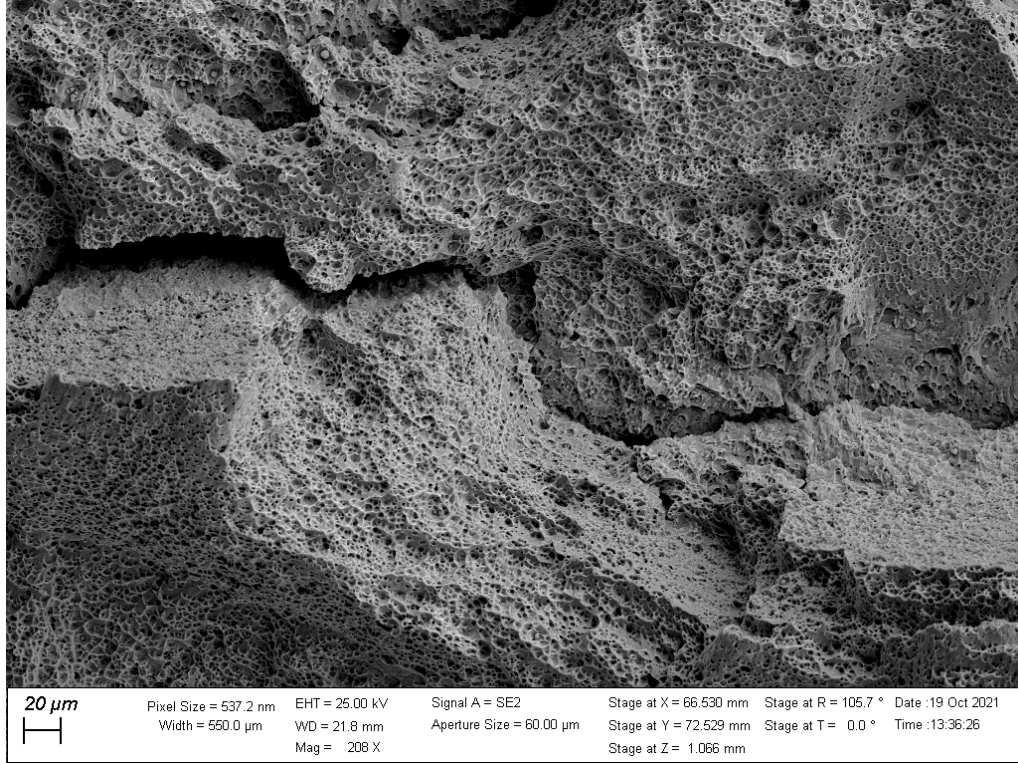
Specimen W2-C3



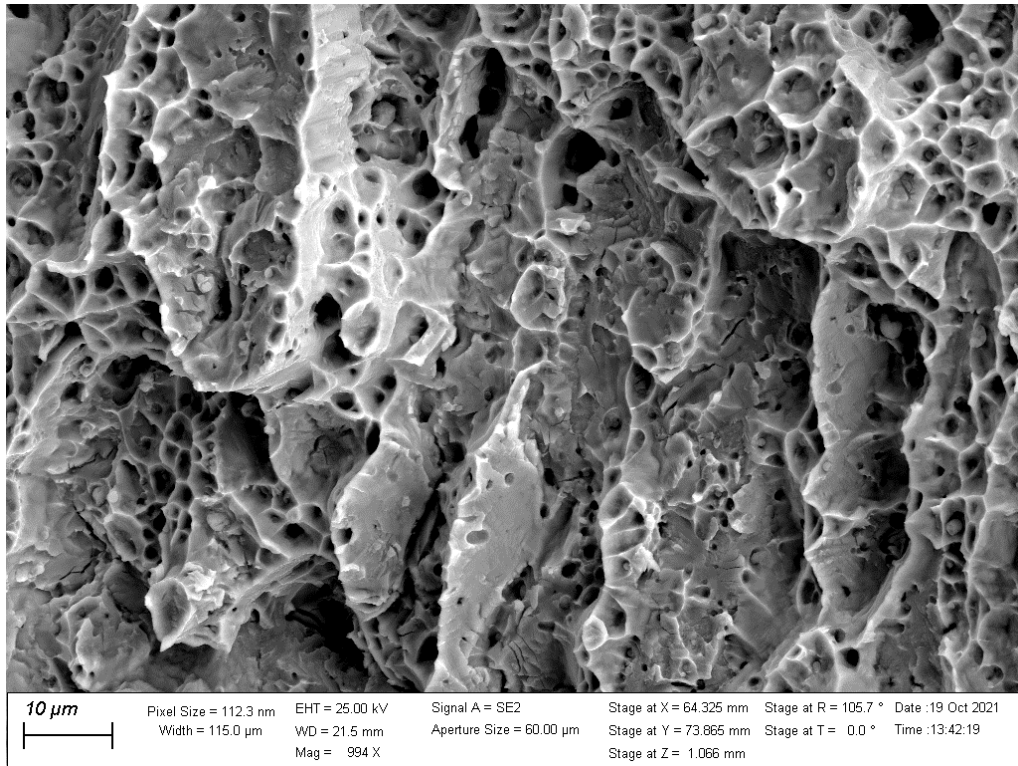
Specimen W2-C3



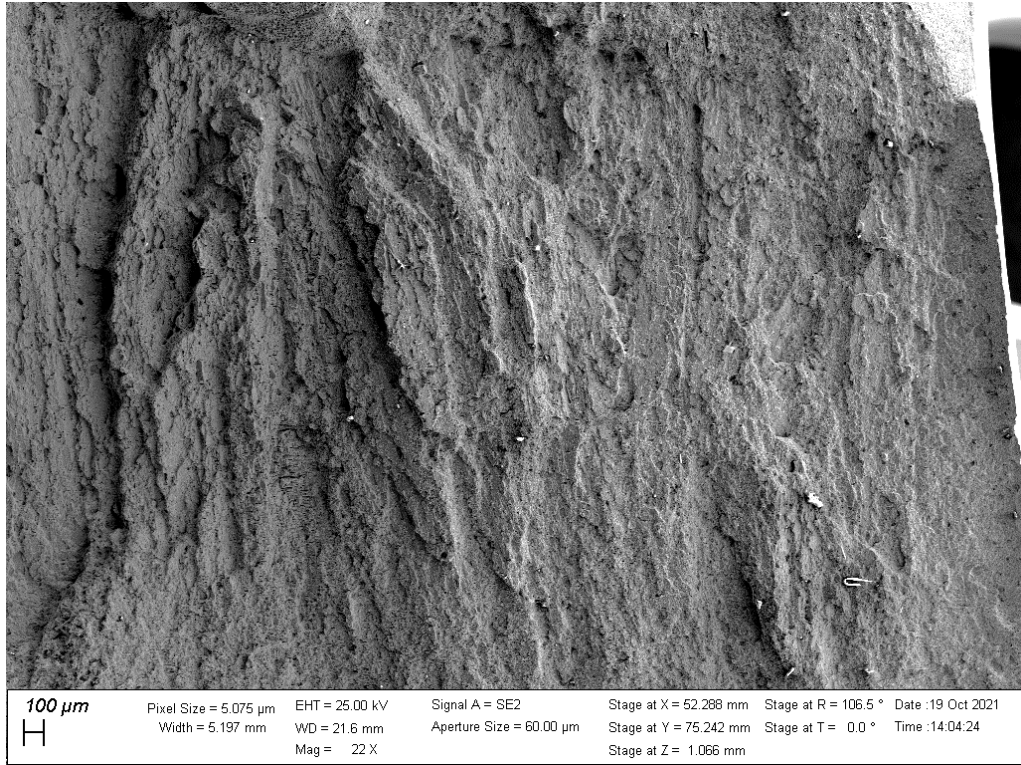
Specimen W3-C4



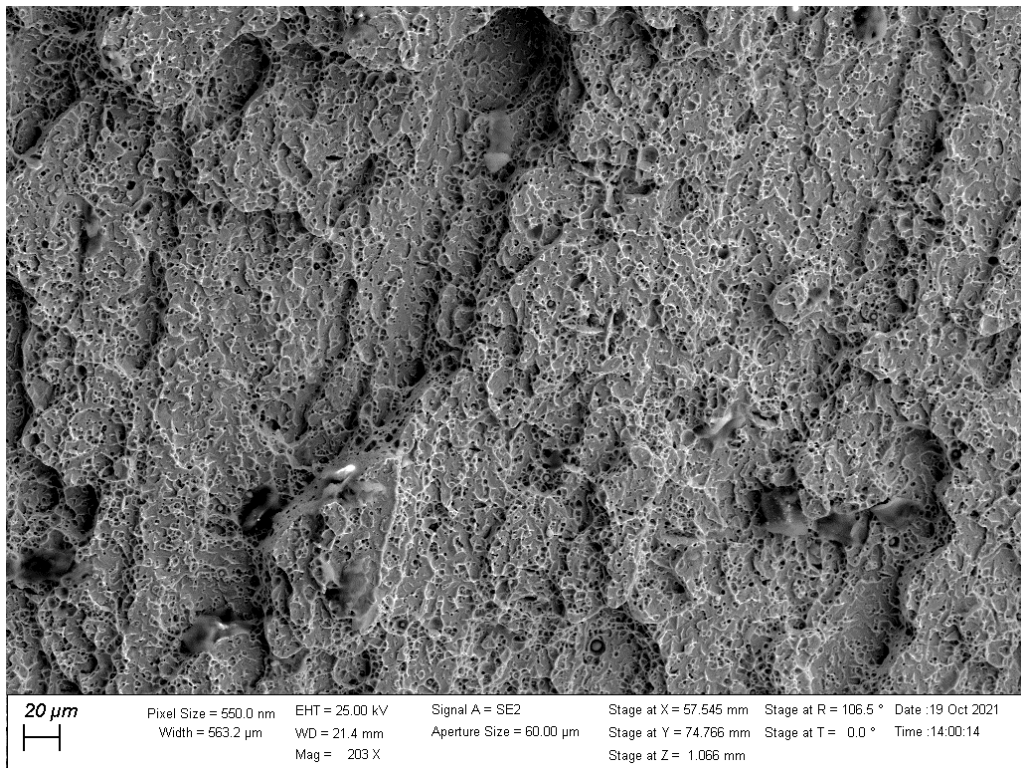
Specimen W3-C4



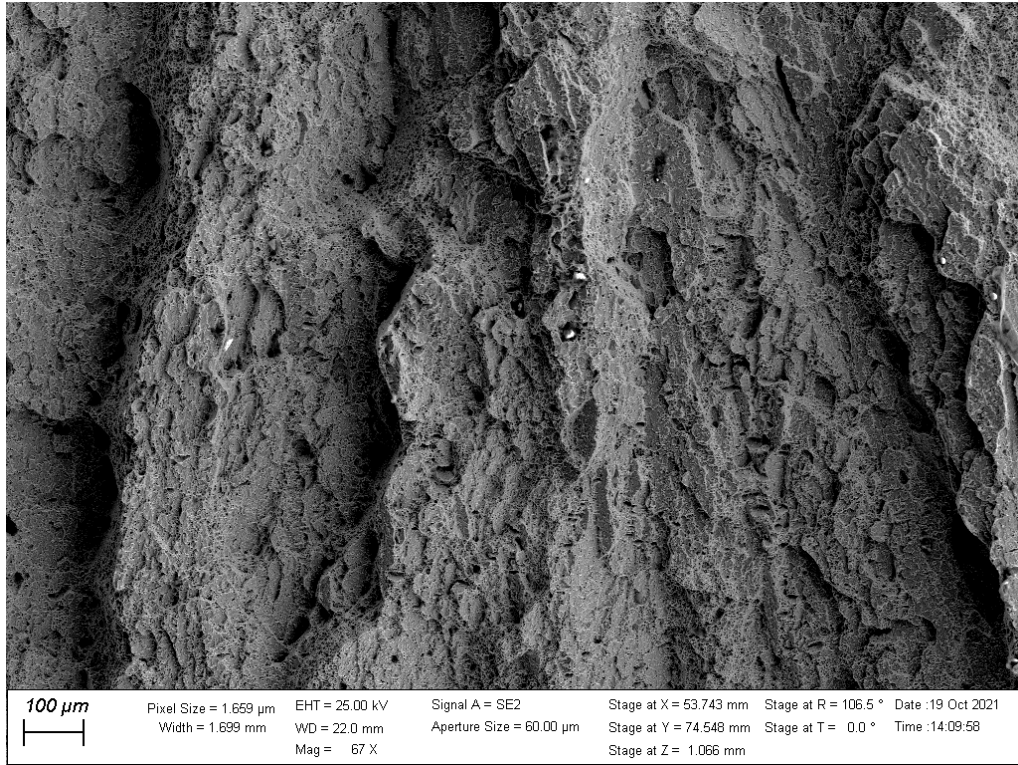
Specimen W3-C4



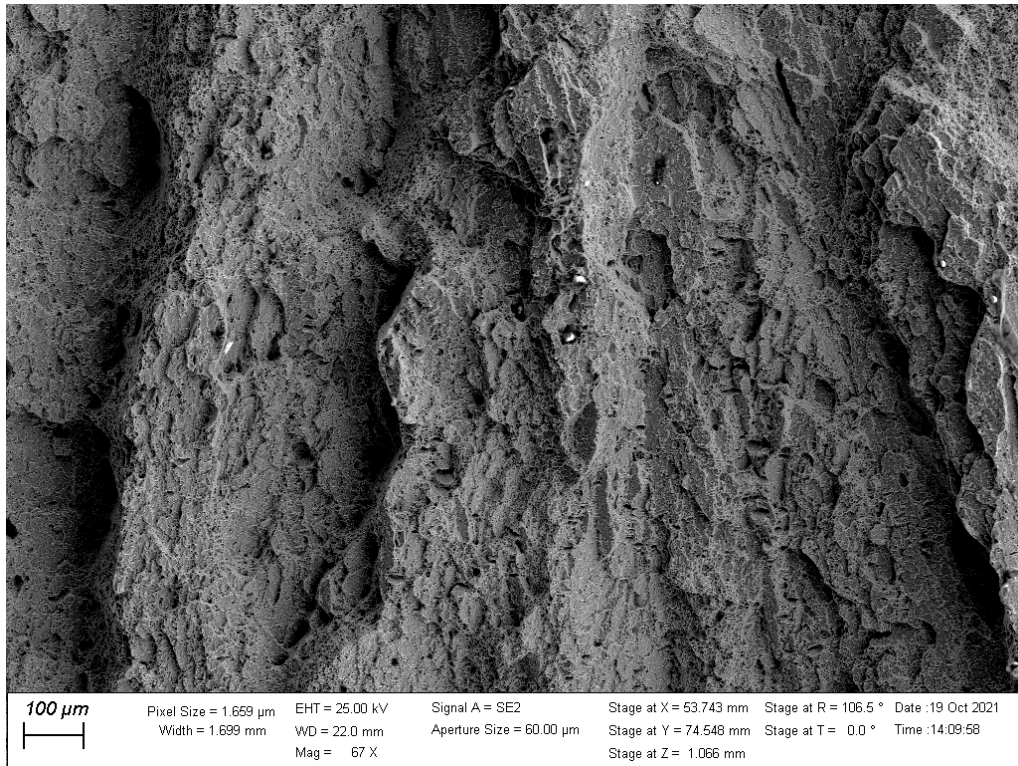
Specimen W4-C2



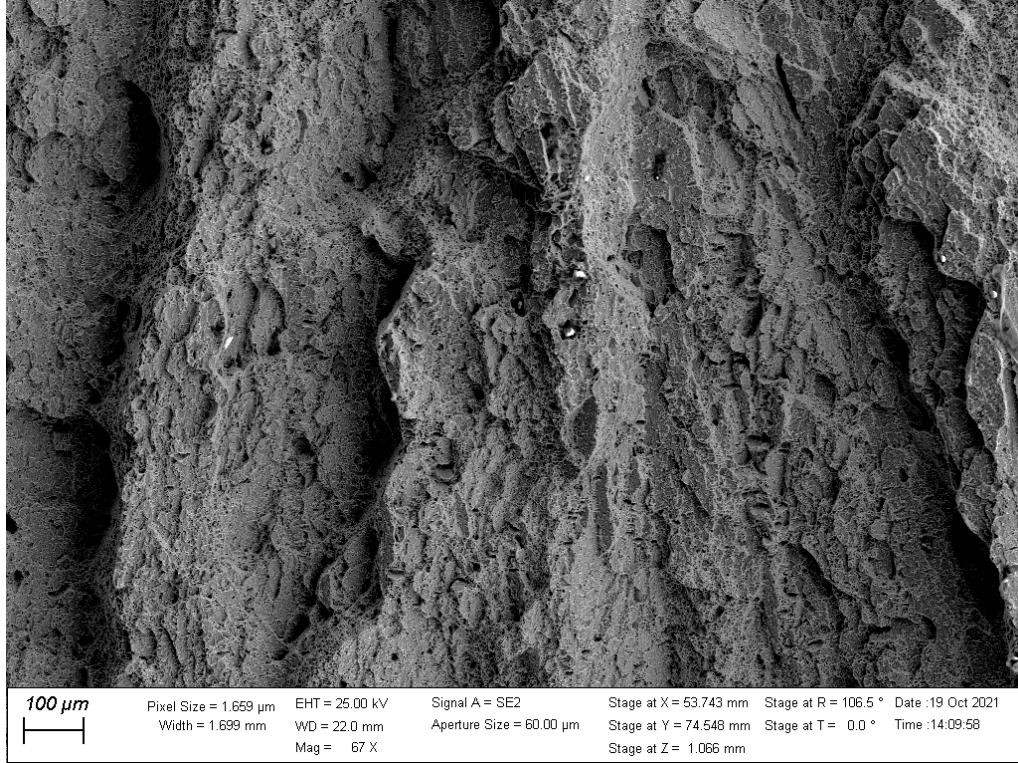
Specimen W4-C2



Specimen W4-C2



Specimen W4-C2



Specimen W4-C2